

UNIVERSITY OF SOUTHAMPTON  
DEPARTMENT OF MECHANICAL ENGINEERING

THE MEASUREMENT OF THE KINEMATICS OF THE HUMAN SPINE  
USING VIDEOfLUOROSCOPY AND IMAGE PROCESSING

BY

ALAN CLARK BREEN

A Thesis Submitted for the Degree of

DOCTOR OF PHILOSOPHY

JUNE 1991

UNIVERSITY OF SOUTHAMPTON

ABSTRACT

FACULTY OF ENGINEERING AND APPLIED SCIENCE

DOCTOR OF PHILOSOPHY

THE MEASUREMENT OF THE KINEMATICS OF THE HUMAN SPINE  
USING VIDEOFLUOROSCOPY AND IMAGE PROCESSING

by

Alan Clark Breen

The motion between the segments of the human spine intimately reflects the state of their soft-tissue linkages. Despite this, the diagnosis of mechanical disorders of the spine suffers from lack of acceptable ways of quantifying such intersegmental motion in living subjects. This thesis establishes a technique for obtaining such kinematic information by extrapolating from co-ordinates placed on digitised images from X-ray motion sequences. This provides a low radiation-dose, accurate and detailed method for the analysis of the kinematics of the lumbar spine in the coronal and sagittal planes and of the cervical spine in the sagittal plane. The technique, in addition, reduces the operator involvement with measurement and calculation traditionally associated with such issues.

The indices used in this thesis are intervertebral angles and instantaneous centres of rotation (ICRs). Using a calibration model and human volunteer subjects, the possibility for determining the former to an accuracy of 2° was established. For ICRs, provided the rotation of the segment in question exceeds 7°, the error and variation in their determination is consistently less than the range of currently accepted normality. Examples of detailed intersegmental motion patterns in asymptomatic and symptomatic human subjects are given and tentative interpretations offered. However, the clinical relevance of such findings must await the application of perhaps future generations of this system to large numbers of patients suffering from mechanical disorders of the spine.

#### ACKNOWLEDGEMENTS

I am grateful to my supervisor, Dr. Robert Allen, and to my secretary, Miss Jenny Langworthy, for their help at all stages of this work. Thanks are also due to Andrew Morris, Miles Woodford and John Detain of Odstock Hospital Spinal X-ray Department, to Bob Peach of the Engineering Workshop at Southampton University, to Tony Darwen of Kenda Electronic Systems Ltd. and to Barry Wall of the National Radiological Protection Board. I also wish to acknowledge those colleagues and undergraduates at the Chiropractic College and at Southampton University who contributed to this work. Last, but by no means least, I wish to thank the Foundation for Chiropractic Education and Research which funded my candidature and the European Chiropractors' Union which contributed considerably to the purchase of the image processor.

## CONTENTS

	PAGE
Contents of Figures	vi
1.0 INTRODUCTION	1
1.1 Objectives and Scope of the Research	2
1.2 Stages and Organisation	3
1.3 Contribution of the Research	4
2.0 EARLY STUDIES	5
3.0 LAYOUT OF THESIS	8
PART A - LITERATURE REVIEW	
4.0 CURRENT TECHNIQUES FOR JOINT KINEMATIC MEASUREMENT	12
4.1 Plane X-Ray Superimposition Studies	13
4.2 Validation of Point Selection	13
4.3 Cineradiography and Videofluoroscopy	14
4.4 Digital Radiography	18
5.0 KINEMATIC MEASUREMENT OF THE SPINE	19
5.1 Kinematic Indices	19
5.2 The Cervical Spine	24
5.3 The Thoracic Spine	26
5.4 The Lumbar Spine	27
5.5 Axial (y-axis) Vertebral Rotations	27
5.6 Coupled Motion	28
5.7 Coronal Plane (Lateral Bending) Motion Studies	28
5.8 Sagittal Plane (Flexion-Extension) Motion Studies	31
5.9 3-Dimensional Studies	31
6.0 KINEMATIC MEASUREMENT OF THE SPINE IN CLINICAL SETTINGS	33
6.1 Segmental "Instability"	33
6.2 Lumbar Surgical Fusion	35
6.3 Cervical Spine Fusion	36
6.4 Disc Degeneration	36
6.5 Retroposition - A Clinical Example	37
6.5.1 Measurement	42
6.5.2 Radiographic Findings	42
6.6 Forward Slippage (Spondylolisthesis)	45
6.7 Disc Herniation and Injury	47
7.0 IMPRESSIONS FROM THE LITERATURE	49



## PART B

### DEVELOPMENT AND ASSESSMENT OF THE DIGITAL VIDEOFLUOROSCOPIC TECHNIQUE

8.0 DESCRIPTION OF EQUIPMENT	52
8.1 X-ray Equipment	52
8.2 Image Processing Laboratory	55
8.3 Development of Procedures for Image Processing	61
8.3.1 Frame Grabbing from Videotape	61
8.3.2 Marking and Calculation of Intervertebral Angles	62
8.3.3 Marking and Calculation of ICRs	63
9.0 SUMMARY OF FEASIBILITY STUDIES	67
10.0 CALIBRATION OF SYSTEM FOR KINEMATIC MEASUREMENT	70
10.1 Development of the Calibration Model	71
10.2 Treatment of Scaling Errors	72
11.0 THE QUANTIFICATION OF SAGITTAL PLANE MOTION	78
11.1 Calibration Studies of Rotations	78
11.1.1 Undegraded Images	81
11.1.2 Degraded Images	81
11.2 Studies of Rotations In Human Volunteers	84
11.2.1 The Lumbar Spine	86
11.2.2 The Cervical Spine	88
11.3 Translations in the Sagittal Plane	91
11.3.1 Calibration Studies of Translations	91
11.3.1.1 Accuracy	93
11.3.1.2 Precision	93
11.4 Studies of Translations in Human Volunteers	96
11.4.1 The Lumbar Spine	96
11.4.2 The Cervical Spine	101
12.0 THE QUANTIFICATION OF CORONAL PLANE MOTION	103
12.1 Calibration Studies of Rotations	103
12.1.1 Undegraded Images	103
12.1.2 Degraded Images	107
12.1.3 In Vivo Simulation	107
12.2 Studies of Rotations in Human Volunteers	110
12.2.1 The Lumbar Spine	110
12.2.1.1 Absolute Lateral Flexion	110
12.2.1.2 Relative Lateral Flexion	113
12.2.1.3 Interobserver Variations	113
12.3 Translations in the Coronal Plane	116
12.3.1 Calibration Studies of Translations	119
12.3.1.1 Accuracy	119
12.3.1.2 Precision	120
12.4 Studies of Translations in Human Volunteers	128
12.4.1 The Lumbar Spine	128
12.4.2 The Cervical Spine	128

13.0 EDGE-FINDING AS AN AID TO CO-ORDINATE MARKING	130
13.1 Application of the Median Filter	130
13.2 Application of the Roberts Gradient	131
13.3 Application of the Sobel Operator	131
14.0 RADIATION DOSAGE	138
15.0 PATIENT STUDIES	143
Patient 1.	143
Patient 2.	146
Patient 3.	152
15.1 A Procedure for Processing Patient Files	163
15.2 Preprocessing Prior to Co-ordinate Marking	166
16.0 CONCLUSION, FURTHER WORK AND FUTURE TRENDS	167
16.1 Extension to 3D	170
APPENDICES	174
I Scale of the Problem of Back Pain	174
II Command Sequences for Image Processing	176
a Frame-Grabbing from Videotape	176
b Marking and Calculation of One Vertebral Angle	177
c Clear all Screens and Synchronise with Video	178
d Prepare for Second Set of 8 Images	179
e Order and Number Digitised Images	180
III ICR Programme	182
IV Glossary of terms	194
V Radiographic Data from Six Volunteer Subjects	196
VI List of Publications from this Research	197
REFERENCES	204

## CONTENTS OF FIGURES

	PAGE
Figure 1: Cable picture of Generals Pershing and Foch, transmitted by 15-tone grey level equipment from London to New York. (Reproduced by kind permission Addison-Wesley Publishing Co. Ltd.)	6
Figure 2: Stages in the investigation of the digital videofluoroscopic technique	10
Figure 3: Diagram of an X-ray machine for motion studies	16
Figure 4: Lateral X-ray of the lumbar spine showing contrast medium which has been injected into an intervertebral disc	17
Figure 5: Diagram of the three-dimensional co-ordinate system for labelling the spatial orientation of vertebrae	21
Figure 6: Diagrams of the derivation and loci of normal Instantaneous Centres of Rotation of a vertebra; a) through x-axis b) through z-axis (Reproduced by kind permission J.B. Lippincott Co.)	23
Figure 7: Diagram of the human spinal column	25
Figure 8: Diagram of "coupling" motion during coronal plane rotation in the lumbar spine	30
Figure 9: Lateral X-ray of the lumbar spine showing degenerative disc disease and retroposition of the fifth lumbar vertebra relative to the sacrum	39
Figure 10: Photograph of the Straight-Leg Raise Test (SLR)	40
Figure 11: Tracing of axial view of two lumbar vertebrae showing encroachment of nerve root when the subjacent vertebra is rotated anterior	41
Figure 12: Outline of lumbar vertebrae marked for the measurement of translation	44

Figure 13: Diagram of the lumbo-sacral spine showing forward slippage (spondylolisthesis) of the fifth lumbar vertebra relative to the sacrum	46
Figure 14: Diagram of a disc hernia showing nerve root compression	48
Figure 15: The X-ray console at Odstock Hospital	53
Figure 16: a) Wooden seat frame for stabilising lateral views b) Subject extending lumbar spine while stabilised against frame	54
Figure 17: The radiographic phantom	57
Figure 18: a) Digitised image of a wire grid obtained from a Philips intensifier b) Digitised image of same wire grid obtained using the Thompson intensifier used in these studies	58
Figure 19: Diagram of the image frame buffer	59
Figure 20: Image processing laboratory	60
Figure 21: Schematic diagram of the x-ray equipment and image processing system (Reproduced by kind permission Butterworth Scientific)	68
Figure 22: a) The calibration model set up for sagittal plane motion b) The calibration model set up for coronal plane motion	73
Figure 23: Digital X-ray image of aluminium disc for scaling	74
Figure 24: Digitised images of aluminium plates used in scaling studies	76
Figure 25: Graph depicting the best fit obtained by scaling the computer to obtain similar angles to those subtended by the sides of the aluminium blocks	77
Figure 26: Calibration model in position for fluoroscopy	79

Figure 27: Graph comparing protractor and computer estimations of flexion-extension motion in the calibration model	80
Figure 28: Contrast-expanded and magnified image of the calibration model in the lateral projection with soft tissue scatter and positional distortion, marked for determination of intervertebral angle	82
Figure 29: Graph comparing protractor and computer estimation of flexion-extension as in Figure 27 but including the influence of soft tissue scatter and positional distortion	83
Figure 30: Subject extending cervical spine when positioned beside intensifier	85
Figure 31: (a and b) Graphs of lumbar spine sagittal plane rotation at two segmental levels in a volunteer subject	87
Figure 32: Cervical spine images used for determining sagittal plane motion	89
Figure 33: Graph of cervical spine sagittal plane rotations at three segmental levels (Error bars represent $\pm 2SD$ of intra-observer variation)	90
Figure 34: a) Lateral image of lumbar spine calibration model with vertebrae marked for the calculation of ICR location b) Mean location error (cross) and inter-observer variation (circle of radius $2SD_{xy}$ ) of ICR location for a $10^\circ$ increment	92
Figure 35: Scatterplot showing the mean location errors of sagittal plane ICR locations for a variety of increment sizes	94
Figure 36: Bar graph showing the intra-observer variation of ICR locations in the calibration model in the sagittal plane for a variety of increment sizes	95

Figure 37: a) Lateral image of the lumbar spine in a human volunteer (Subject 1) marked for the calculation of ICR location at L4-5 b) Scatterplot of observer variations of ICR locations for a variety of increment sizes for Subject 1	97
Figure 38: a) Lateral image of the lumbar spine in a human volunteer (Subject 2) marked for the calculation of ICR location at L4-5 b) Scatterplot of observer variations of ICR location for a variety of increment sizes for Subject 2	99
Figure 39: Locus of ICR locations (A to E) from flexion to extension at L4-5 in Subject 2	100
Figure 40: a) Unenlarged lateral cervical spine image with mean ICR location and 2SDx and y ellipse of intra-observer variability for 10 ICR observations at C3-4 b) As 40a but using a 2x enlarged image	102
Figure 41: Calibration model (undegraded) marked for the determination of coronal plane rotations	105
Figure 42: Graph comparing protractor and computer estimations of lateral bending in the calibration model	106
Figure 43: Graph comparing protractor and computer estimation of lateral bending as in 41 but including the influence of soft tissue scatter and positional distortion	108
Figure 44: Graph comparing protractor settings and computed angles of coronal plane rotation through 30° with coupled motion and soft tissue scatter	109
Figure 45: a) Subject in lumbar lateral bending in position beside intensifier b) Computer image of human lumbar spine in the anterior/posterior projection, contrast enhanced and marked for the estimation of intervertebral angles	111
Figure 46: Graph showing increments of coronal plane motion for L2-5 relative to the x-axis of the computer monitor	112

Figure 47: (a-c) Relative coronal plane motion in asymptomatic subject at L2-3, L3-4 and L4-5 (Error bars=2SD of mean calibration error)	114
Figure 48: Relative coronal plane rotation at the L4-5 level by four observers illustrating range and mean measures	115
Figure 49: Variation (SD) in measurement of intervertebral angles by angle size	118
Figure 50: Undegraded calibration model image marked for the calculation of ICR in the coronal plane	121
Figure 51: Scatterplot showing the mean ICR location errors of coronal plane ICR locations for a variety of increment sizes	122
Figure 52: Bar graph showing the intra-observer variation of ICR locations in the calibration model in the coronal plane for a variety of increment sizes	123
Figure 53: a to d) Ellipses of inter-observer repeatability (2SDx and y) and mean locations of ICRs for increments of 5°, 10°, 20° and 30°.	124-127
Figure 54: Locus of ICRs for left to right sidebending at the L3-4 level in a volunteer subject	129
Figure 55: Unprocessed digital images of a) anterior-posterior and b) lateral projections of the lumbar spine in a volunteer subject	133
Figure 56: Dispersion of values for L3-4 intervertebral angles using 3 image processing techniques	135
Figure 57: Image as 55a after adding median and Roberts filtration with marking of L3 and L4 vertebral bodies	136
Figure 58: Image as 55b after adding median and sobel filtration	137
Figure 59: Radiation dosage (effective dose equivalents) for males and females for lumbar spine screening times of 1 minute and 15 seconds	140

Figure 60: ICR locations for four motion increments at the C4-5 and C5-6 levels in Patient 1 (circles have centres at overall ICR locations - radii represent intra-observer variations (2SDxy) at each level	145
Figure 61: Digitised lateral lumbar image of Patient 2 showing disc degeneration at the L4-5 level	148
Figure 62: (a-d) Graphs of 28 increments of sidebending for L2-5 in Patient 2	149
Figure 63: Locus of ICRs for coronal plane motion at L2-3 in Patient 2	150
Figure 64: (a-b) Incremental motion in flexion-extension of Patient 2 at the L3-4 and L4-5 levels	151
Figure 65: (a-d) Images of the extremes of sidebending (a and b) and flexion-extension (c and d) motion in Patient 3	153-156
Figure 66: (a-d) Graphs showing 12 increments of sidebending for L2-5 in Patient 3	157
Figure 67: (a-b) Graphs showing 16 increments of flexion-extension at L3-4 and L4-5 in Patient 3	158
Figure 68: ICRs for sagittal plane motion at L2-3 in Patient 3. (A = flexion phase, B = extension phase, C = overall motion)	161
Figure 69: Track of ICRs for coronal plane rotations at L3-4 and L4-5 in Patient 3	162



## 1.0 INTRODUCTION

The functional integrity of the spine as a dynamic loadbearing column is vital to the degree of biological independence enjoyed by man. In humans, the pentadactyl limbs, upright stance and highly developed intellect require a versatile support system. The mechanical demands on the spinal column increase in complexity with the sophistication of daily living. These demands relate particularly to the ligaments and intervertebral discs.

The scale of the problem of spinal pain is a vast one (see Appendix I), and the bulk of it depends on the mechanical behaviour of the spinal holding elements. These structures exhibit viscoelastic behaviour under load and this must be considered in the context of common life situations. Examples would include vibration in transport systems, prolonged sitting postures and specialised and repeated movements for industrial manufacture and assembly.

Although basic concepts in mechanics can be utilised to analyse motion and forces in the human body in various activities (1), theoretical considerations often fall far short of satisfying the need to understand what happens in life. The pain and disability of spinal dysfunction and injury does not always relate to the degree of apparent damage. There are few accurate predictors of mechanical disadvantage and clinicians are led to the conclusion that the scope

for measurement is not generally satisfied by the technology available.

Of the dichotomy of motion and forces in the spine, the greatest progress has been made in researching the latter. Here cadaveric specimens often provide satisfactory facsimilies of in vivo features with respect to intradiscal pressure (2), connective tissue strength (3) and cellular biophysics (4). In living subjects, however, the features of the soft tissues as holding elements are not amenable to scrutiny. Nevertheless, the relative motions of the vertebrae reflect these features, as cadaveric studies show. Research into intervertebral motion in vivo has therefore been widely regarded as an essential prerequisite to knowledge of mechanical disorders of the spine.

The understanding of motion, and in particular the motion between individual segments of bone in the living is largely confined to normal ranges (5) and large increments (6,7). The task of relating these to specific disease states is in its infancy. The reason for this lies in the insufficient accuracy, unacceptable radiation dosage, laborious data processing and overall expense of the systems currently available for clinical use. The clinician is therefore constrained to subjective techniques with low predictive value.

### 1.1 Objectives and Scope of the Research

This thesis propounds the viability and usefulness of digital videofluoroscopy (DVF): the digital processing of videofluoroscopic

images of the spine as a technique for overcoming the above problems. The studies presented here were, of necessity, of two dimensional motion. Such have been the doubts expressed about the feasibility of obtaining useful geometric measurements from conventional X-ray images that the validity of doing this with a digitised videofluoroscopic image of the spine was initially open to question. For example, fluoroscopic images have traditionally been less well resolved and the digitisation of such images may have created an additional degrading influence. Extension to 3-D, therefore, would be dependent on the validation of a 2-D system.

## 1.2 Stages and Organisation

The main stages of the work were:

- (i) a review of the scientific literature to identify previous work and issues in spine kinematics
- (ii) identification of suitable radiographic and computing hardware and software
- (iii) preliminary testing of a prototype system
- (iv) obtaining a system for the development of the technique
- (v) development of a calibration model
- (vi) development of programs for manipulation and quantification of kinematic indices
- (vii) calibration of this system in terms of radiographic dosage, precision and accuracy in respect of measurement indices sought in previous studies
- (viii) assessment of the technique in human volunteer subjects

- (ix) exploration of the prospects for exploiting the potential of image processing for further improving accuracy.
- (x) application of the system in patients

In view of the progress in developing both computers and image intensifiers over the past 30 years or so, and the importance of spinal mechanics in modern occupational medicine, any first system of this nature could be rapidly improved in terms of its operating efficiency.

### 1.3 Contribution of the Research

Emphasis has been placed on establishing the likely tolerance of such a system to those errors which may be imposed during clinical use. Obviously it would be impossible to conduct exhaustive error studies in the context of all the possible clinical and radiographic scenarios. Instead, extreme cases of such procedures in terms of radiography, which would challenge the tolerance of the system, have been evaluated in terms of accuracy. Seen in this light, the work represents the first known calibration for in vivo measurement of the entire range of intervertebral motion. By contrast, observer agreement has mainly been applied to those situations which are likely to arise in clinical practice. The latter have shown the tolerance to observer variation of the main indices of measurement under conditions of use which have been described by other workers who employed more conventional imaging systems (eg ultrasound and plain X-ray). In this

way, the validity of the system has been assessed, leaving its use in more esoteric situations for future study.

The importance of this work thus lies in bringing the technology to bear on the problem under conditions of some scientific rigour. The technique provides digitisation of motion X-ray images, landmark labelling on a computer monitor and on-line calculation of intervertebral angles and ICRs from these recorded co-ordinates. These data can reveal the presence or absence of known pathological joint movement patterns and shed further light on their relevance in living subjects. This thesis demonstrates that such a system, which has not previously been suggested or developed, can satisfy these requirements.

## 2.0 EARLY STUDIES

Many of the components of an image processing system for spinal kinematic measurement have been in use for a considerable time in both research and clinical settings. Digital picture processing itself was seen after World War I in the form of the transatlantic telephone transmission of a picture of the French Marshal Foch with the American General Pershing (Figure 1). The use of spinal images for kinematic assessment was first reported by Todd and Pyle in 1928 (8) and subsequently by Gianturco in 1944 (9) and Hasner in 1952 (10). Tanz (11) was the first to exploit X-rays fully for measuring the ranges of movement in the spines of symptomatic and asymptomatic subjects although some previous observations had been made by Gianturco (9). A number of papers were published which reported observations about

FIGURE 1



CABLE PICTURE OF GENERALS PERSHING AND FOCH, TRANSMITTED BY 15-TONE  
GREY LEVEL EQUIPMENT FROM LONDON TO NEW YORK. (REPRODUCED BY  
KIND PERMISSION ADDISON-WESLEY PUBLISHING CO. LTD).

spinal movements from unquantified observations (12-20). The ensuing appreciation and criticism of this work brought attention to the practical issues of balancing accuracy of measurement and radiation dosage against the necessity for objective information at the spinal segmental level. This balance was seen against the background of greater public interest in research into spinal injuries, scoliosis and other mechanical disorders of joints which have been rising in prevalence throughout the latter half of the present century (21).

The possibility of using non-invasive methods such as flexible rulers, inclinometers and goniometers has been considered (22-26) and some of these methods recommend themselves where information about the movement of a section of spine, rather than individual segments is required (27-29). In ankylosing spondylitis, for example, when gross limitations of movement of the spine as a whole are found, these methods have considerable usefulness. However, none of them can shed any light on specific sites of mechanical disruption.

The issue of the minimum accuracy which co-ordinates obtained from X-ray images can offer for vertebral kinematic analysis has been controversial. Coyle (30) suggests that propagation of errors theory makes a dispersion of 2 standard deviations less than  $2^\circ$  in the estimation of the angular position of a vertebra unlikely. Nevertheless, Triano (31), superimposed successive X-rays in a motion sequence taken of a calibration model to determine the movement of segments in terms of their angles. The accuracy of this was not stated, however a strong correlation ( $r > 0.9$ ) was shown between the

model settings and the X-ray measurements. Pearcy, however, (24) suggested that biplanar (3-D) radiographic methods will probably be required for any degree of faithful representation of the positions of vertebrae when the major axes of the object are not in plane with the primary ray.

### 3.0 LAYOUT OF THESIS

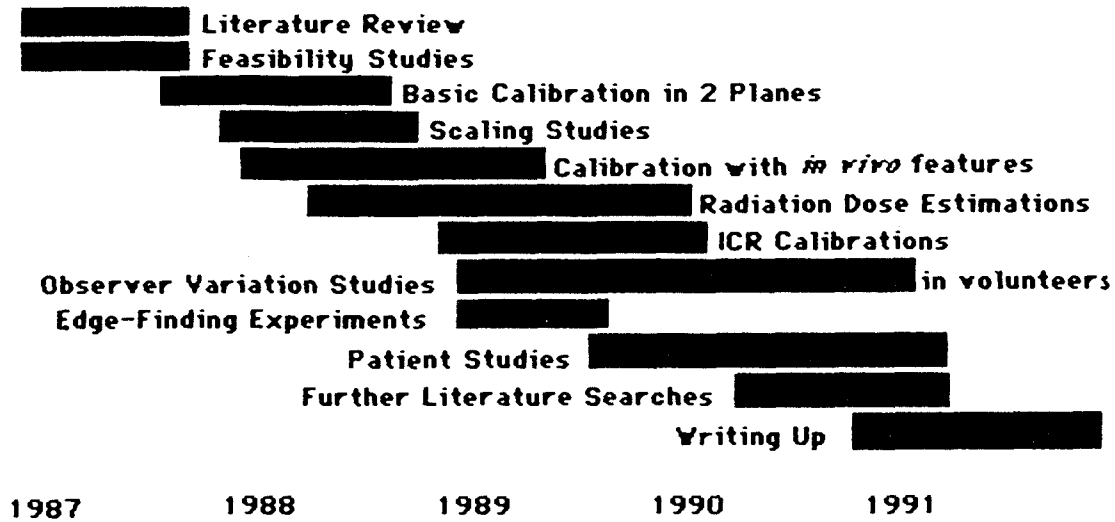
This thesis follows the traditional proforma of literature review, followed by experimental studies and conclusion. After describing the system which was assembled, Section 9.0 takes stock of the lessons learned from the preliminary experiments which were carried out. After this, the field of investigation divides to consider sagittal and coronal plane motion as two major sections. (Quantification of axial rotations (twisting) is not amenable to this technique, which is its main limitation pending extension into 3-D.)

Sagittal plane (flexion/extension, or forward/backward bending) motion is considered first, (Section 11.0) because it is relatively uncomplicated by concurrent motion in the other two planes. This is followed by the other major experimental section; coronal plane (lateral or sidebending) motion. Both of these sections involve both calibration against a realistic model and measurements using the cervical and lumbar spines of human subjects. Each section also addresses the problem of measuring both rotations and translations between vertebrae. The latter are examined in terms of instantaneous centres of rotation (ICRs), for reasons which will be apparent from the literature review. In both sections, the use of the calibration



model allows estimations of accuracy, whereas by using live subjects, observer variation in a realistic clinical setting can be studied. Examples of kinematic features in symptomatic patients in each of the two planes are given and the radiation dosage associated with the examinations is quantified. An indication of the calendar of the research can be found in Figure 2.

FIGURE 2



STAGES IN THE INVESTIGATION OF THE DIGITAL  
VIDEOFLUOROSCOPIC TECHNIQUE

In the literature review which now follows, techniques generally for kinematic measurement are considered first, in order to reveal more about why a digital videofluoroscopic technique would be desirable. The subsequent chapter considers the kinematic measurement of the spine, mainly to illustrate previous efforts in establishing baseline values and standard techniques, and to show the difficulties encountered in attempting to do this. Lastly, clinical measurement is considered. This addresses the relevance of various indices and techniques in common clinical situations. In the light of the clear division between review of previous techniques and our experimentation with a somewhat different approach, the body of the thesis is divided into two parts; 'A' and 'B'.

PART A  
LITERATURE REVIEW

4.0 CURRENT TECHNIQUES FOR JOINT KINEMATIC MEASUREMENT

Kinematic measurement of the spine has been of interest for the light it may shed on specific relationships between spinal mechanics and disabilities. Many such relationships have seemed plausible to clinicians, but very few have been proven. Of those which have, the relationships, such as that between overall spinal stiffness and ankylosing spondylitis, (32,33) tends to be an obvious one, revealing little of essential diagnostic or therapeutic value. Pearcy (34), who reviewed the literature relating to the measurement of back and spinal mobility was led to conclude that "It perhaps needs to be recognised that if measurement is part of the clinical assessment of a patient then simple techniques may not be sufficient...." "There is tantalising evidence...that the position of vertebrae at the extremes of movements are specific to certain pathologies, but there is little information on the patterns of movement by which these positions are reached."

In the light of this need for detailed information about movement in individual vertebrae in contrast to gross spinal movements and the contribution which this research makes to meeting that need, the following literature review will deal primarily with the measurement of the former.

#### 4.1 Plane X-Ray Superimposition Studies

In this method, tracings of the images with the subject in different positions are superimposed. A bony segment is fitted exactly over its counterpart on another tracing or X-ray film and the displacements of adjacent segments are measured. The technique has been popular in much of the previous research (35-39). Although suggestions have been made about movement in various clinical and pathological circumstances, the method itself has not been as rigorously validated with respect to out-of-plane images in three-dimensional terms as biplanar and other stereoroentgenographic methods (40-42). Nevertheless, it has been used in clinical assessment.

#### 4.2 Validation of Point Selection

Research into the verification of anatomical landmarks recorded from X-rays has not been plentiful. Rab (43), however, using frozen cadaver trunks and biplanar roentgenography showed that, for the lumbar spine, it is possible to obtain differences between anatomical and biplanar roentgenogram locations of as little as 3.2mm. Pearcy (44) reduced this error considerably and used the biplanar method to re-investigate both the angular and linear movements between lumbar vertebrae during voluntary movements in live subjects. He established that few normal relative translations exceed 2mm and went on to investigate the variations which occur both in non-operated low back pain patients and those who had undergone surgical fusion in the lower spine (45).

The main problem with vertebral landmark verification for kinematic purposes is recognition of the same landmark after a displacement. Improvements in the accuracy and/or precision of locating these landmarks have been achieved by using the rigid body condition for each bone (46-48), the largest possible distance between landmarks on the same bone (49) and by averaging from repeated measurements (50-52). There is general agreement that the error to be expected in measuring vertebral movements from anatomical landmarks on radiographs under standardised conditions would be of the order of 2° for rotations and 1mm for translations. It has also been shown to be extremely difficult to measure very small movements (less than 1° of rotation) in this way (47,51,52).

#### 4.3 Cineradiography and Videofluoroscopy

The Philips Company of Holland developed a type of X-ray image intensifier in the 1950s (53) using a triode valve for intensification and a system of mirrors and lenses for focusing and directing the display to a cine camera (54). Although radiologists were slow to adopt this method, a number of authors (55-61), used it in normal and traumatized living subjects for the subjective assessment of joint motion in the cervical spine. Many of these authors called for further development of the technique while others were dismissive of its possible use for objective measurement.

Lumbar spine imaging was still generally beyond the reach of this generation of intensifiers by reason of the dosage involved. This limitation prevailed despite the advent of TV cameras as the recording

medium (Figure 3) and resulted from the dependence on light quanta from the fluorescent screen for the activation of the output phosphor. Improvements in image resolution were made possible by the use of caesium iodide coatings as the scintillation layer (62) in place of the thicker sedimented zinc cadmium sulphide used previously. But the most substantial dosage reductions were not achieved until photocathodes were placed alongside the input phosphor in order that the light photons could trigger electron emissions under the influence of an electrical field. This enhancement, together with the replacement of thick glass with a thin metal input window meant reductions in settings for lumbar screening to a few milliamperes. In this way an appreciable amount of lumbar spine screening, for example for discography, (Figure 4) can be done and results in absorbed radiation dosages to the patient comparable with that required to produce one conventional X-ray plate (63).

The prospects for even greater refinements in videofluoroscopic systems are high. Automatic dosage control is already standard in many machines as is image enlargement. A variety of input window sizes are now available and developments in iris, lens control and rectification are being directed towards the reduction of intensifier flare (the tendency to uncontrolled photoelectric emission near the circumference of the input phosphor). Most importantly for patient dosage, unwanted frames within a video sequence can be dispensed with during the examination by pulsing the X-ray beam in synchrony with the camera.

FIGURE 3

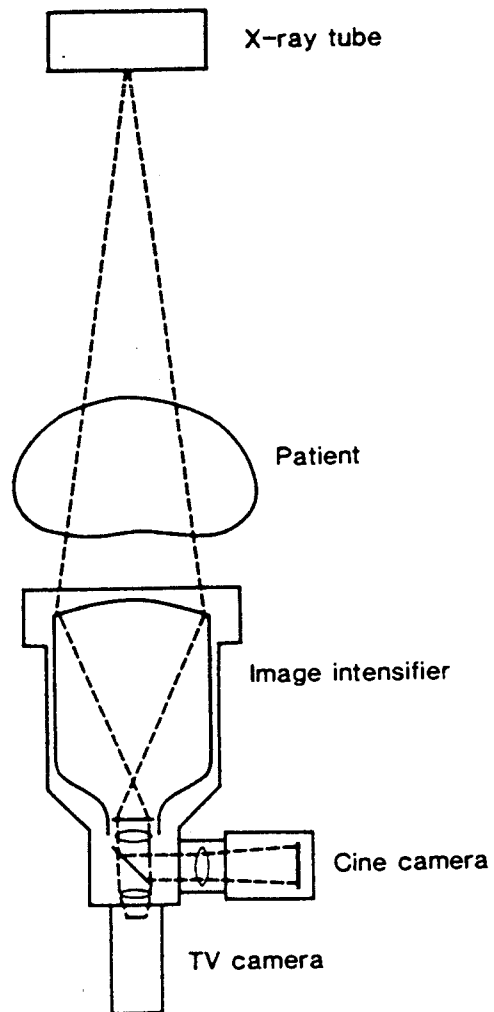
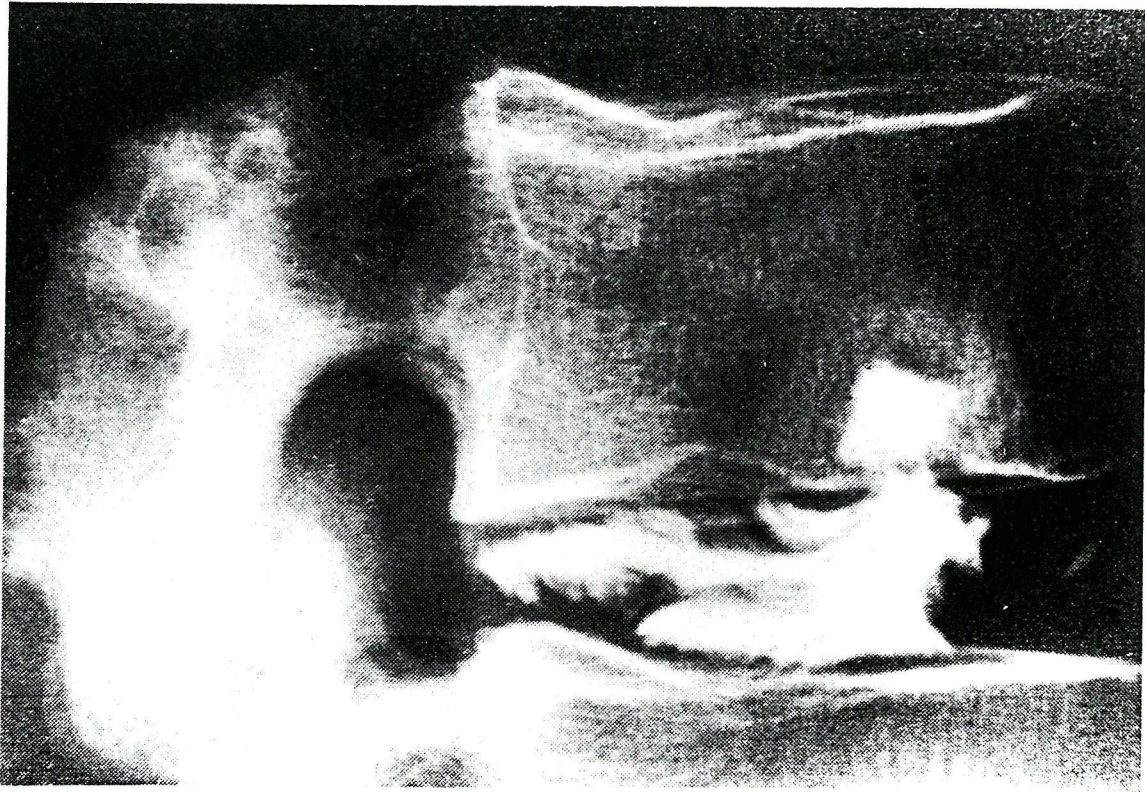


DIAGRAM OF AN X-RAY MACHINE FOR MOTION STUDIES



FIGURE 4



LATERAL X-RAY OF THE LUMBAR SPINE SHOWING CONTRAST MEDIUM WHICH  
HAS BEEN INJECTED INTO AN INTERVERTEBRAL DISC

#### 4.4 Digital Radiography

As Leung in her review of cineradiographic studies of the spine (64) points out, such assessments were subjective and meant to convey clinical impressions. Videotaped images of the cervical spine have also been used in this way (65). A more objective treatment of the spatial orientation of body segments depends on the validation of marking and data processing techniques as outlined above. This clearly calls for a computer-based solution.

The processing techniques associated with digitised images are in a state of development which has recently accelerated with the improvements in computing technology (66). Digital subtraction radiography as applied to contrast studies of blood vessels has been a major advance in medical imaging along with computed tomography and ultrasound scanning. The quality of biomedical images has also benefitted, particularly that of X-rays, by linear contrast stretching, filtering and edge finding (67). These methods may ultimately improve accuracy in recording the positions of anatomical landmarks.

Moore (68) makes a strong case for digital X-ray imaging from a number of viewpoints including storage, display, and processing. From the viewpoint of joint kinematics it is the scale of the processing opportunities which appeal. Considering image quality, any improvement in resolution which may be offered by improvements in intensifier design can be taken up by an image processor of sufficient storage capacity. In terms of enhancement for human appreciation, the

manipulation and on-line quantification of grey levels, noise reduction by filtration and edge-finding algorithms all offer the opportunity for more accurate anatomical co-ordinate marking. Any geometric distortion brought about either from patient placement, intensifier/camera or computer configuration should be amenable to forms of corrective transformation (69). The prospects for both rapid and versatile calculation and display of spatial parameters have been proven in many existing graphical programs, including some capable of 3-dimensional extrapolations (see Section 5.9). Artificial vision techniques might be applied to tracking anatomical landmarks throughout a motion sequence. These prospects are, however, far ahead of the current state-of-the-art in spine kinematics.

## 5.0 KINEMATIC MEASUREMENT OF THE SPINE

### 5.1 Kinematic Indices

The main indices of spinal segmental kinematics were reviewed by White and Panjabi in 1978 (5) and by Frymoyer the following year (70). The indices can be roughly divided into three groups; those which describe rotations, those which describe translations and those which are made up of both components. The complexity of the subject becomes felt when all the possible relative motions between selected vertebrae are considered in 3 dimensions. Not all combinations have practical use however, and, with this in mind, Hoag (71) offered a pragmatic classification of vertebral motion for kinematic purposes. In addition, and in response to the conflicting terminologies which began to appear, Panjabi Krag and Goel (72) drew attention to a three-

dimensional co-ordinate system for labelling the spatial orientations of bones (Figure 5).

Taking two-dimensional issues first, the predominant kinematic index has been the angle of rotation, either of a section of the human body, or at intervertebral level. The main reason for its use has been to establish range of motion, with little or no attention given to features of motion within this range. Methods of measurement and the application of this index are discussed throughout this review. For the three-dimensional measurement of rotations, methods employing either Euler's angles or centroids predominate.

The concern of clinicians for the stability of spinal segments has focused attention on the measurement of linear displacements, or translations, especially in the sagittal plane. Measurement of this was generally from X-rays and is usually done by various forms of direct measurement. The accuracy of these techniques has been investigated by Schaffer et al (73).

FIGURE 5

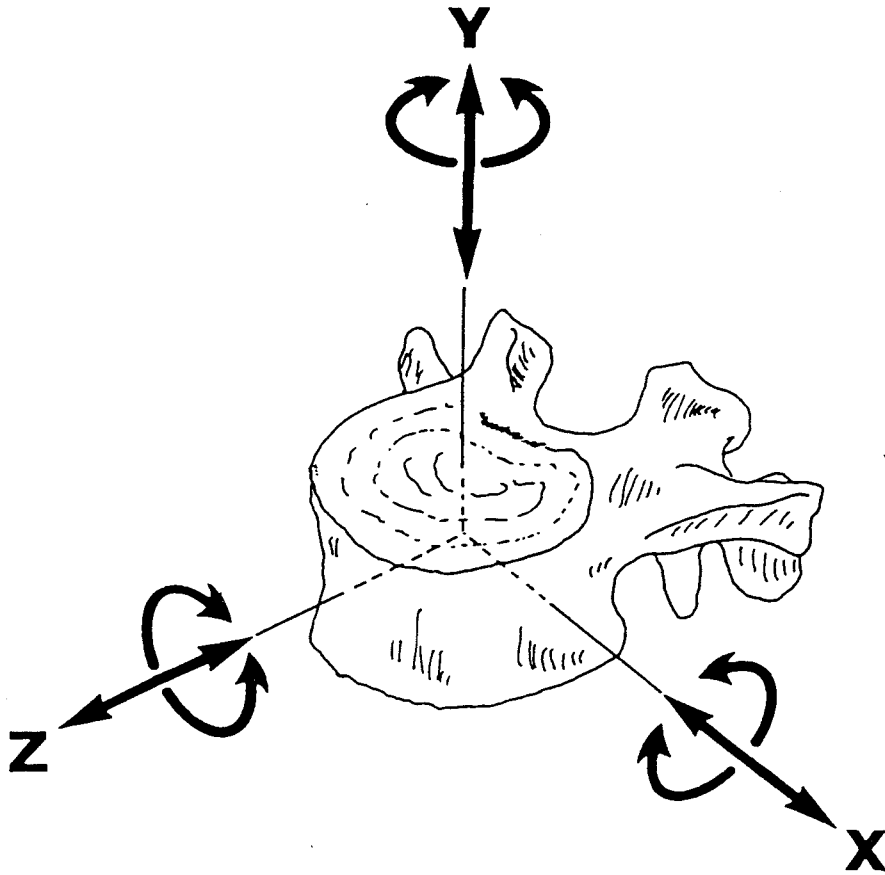
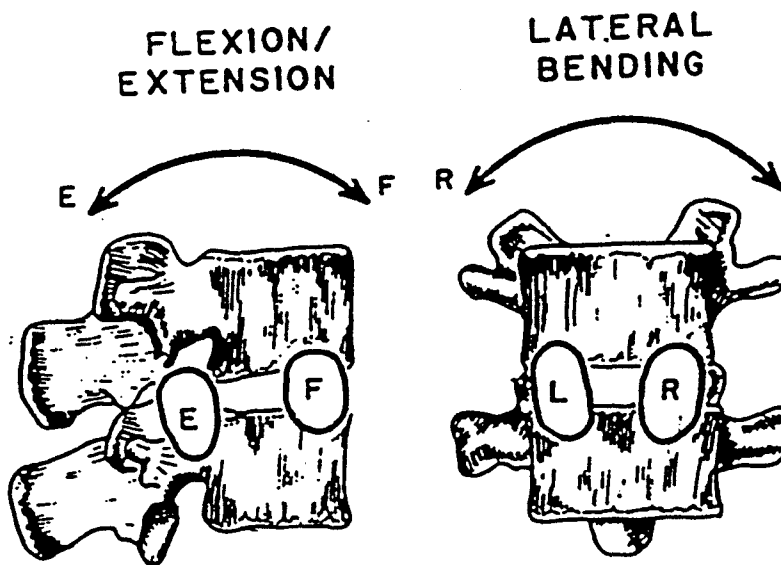
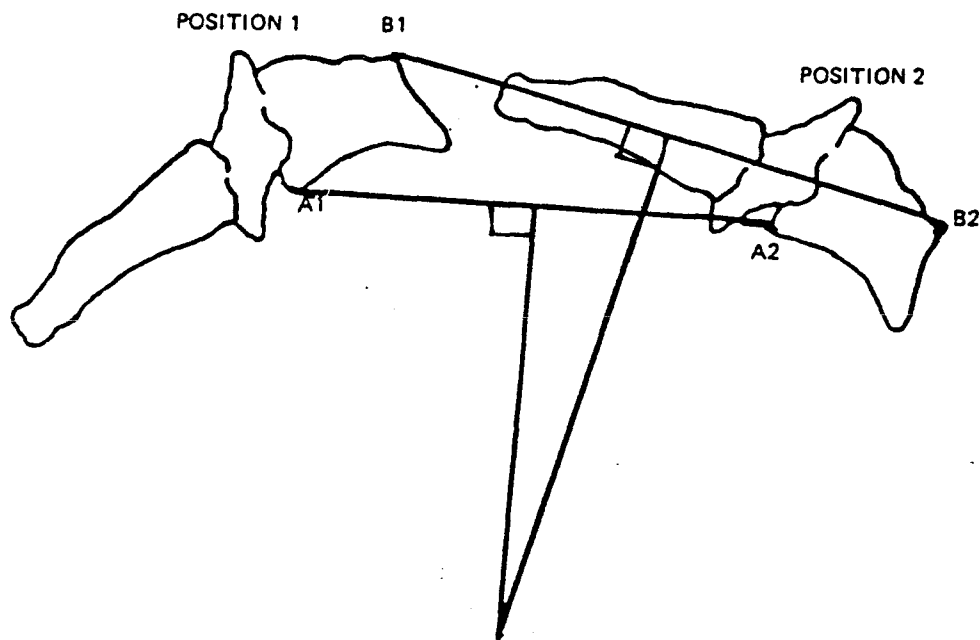


DIAGRAM OF THE THREE-DIMENSIONAL CO-ORDINATE SYSTEM FOR  
LABELLING THE SPATIAL ORIENTATION OF VERTEBRAE

Despite their usefulness and apparent accuracy in assessing the overall ranges of joint movement, these studies did not answer the need made apparent by the growing volume of evidence linking spinal injury and early pathology of the intervertebral disc with aberrations of incremental motion. To date, incremental translation along the x and z axes has been most successfully described in terms of the movement of the instantaneous centre of rotation (ICR) of one bony segment about an adjacent one (Figure 6). The technique, first described by Rosenberg (74), evolved from the application of joint centre analysis to the problem of vertebral motion. This locus, or centrode, of serial increments over the range of intervertebral rotation is normally confined to an area of about 2cm diameter within or near the disc space for most spinal levels (75,76). The variation occurs mainly because of the small amount of translation which accompanies the rotation.

The number of radiographs and co-ordinates necessary for the assessment of incremental motion, and in particular ICR, led to new considerations for improving the accuracy of point selection and the preferred use of computer analysis (77-78). Studies such as these established clear relationships between the dispersion of ICRs beyond normal anatomical confines in disc degeneration (79), disc injury (80), abnormal vertebral angulation (80) and in back pain syndromes generally (81) and revealed some differences between the in vivo and in vitro situations.

FIGURE 6



DIAGRAMS OF THE DERIVATION AND LOCI OF NORMAL INSTANTANEOUS  
CENTRES OF ROTATION OF A VERTEBRA;

a) THROUGH X-AXIS

b) THROUGH Z-AXIS

(REPRODUCED BY KIND PERMISSION J.B. LIPPINCOTT CO).

Finally, the 3-dimensional extension of the ICR is the helical axis of rotation. This index requires stereo imaging and derives from screw-axis analysis. It has been widely used in joint motion research. However, with regard to the spine, its relevance will remain obscure until a sufficient number of typical patterns have been observed.

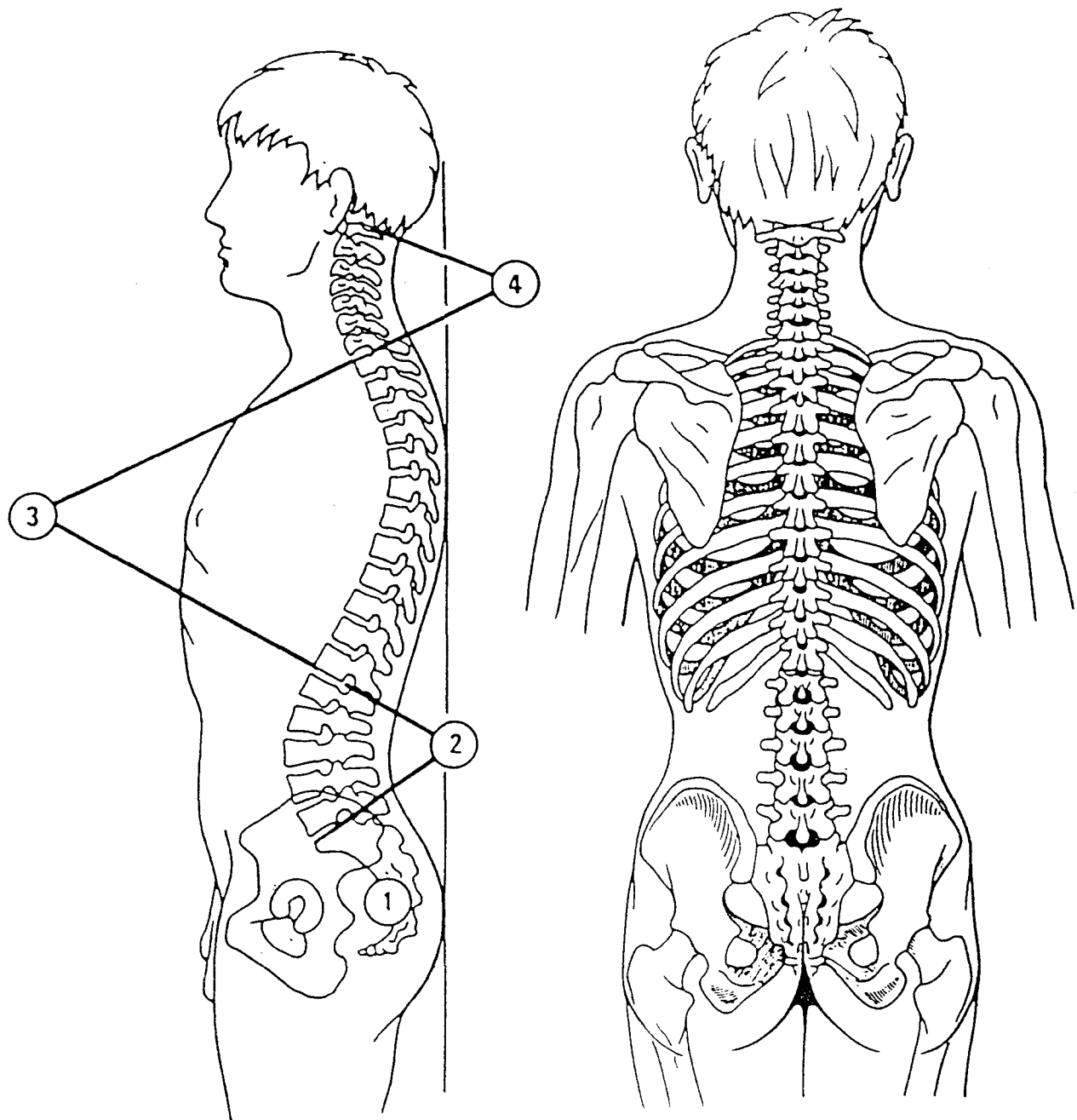
X-ray joint motion research has not been restricted to the spine. Kammerer (82) studied the prospects for the analysis of rapid joint motion using external markers and a microcomputer - a development which follows from the calibration and use of minicomputers with similar markers in the analysis of gait (83-85). The extra-spinal joints investigated include the hip (86), wrist (87) and shoulder (88,89); all by use of external markers or electrogoniometers. Langrana's method (89) was biplanar and used videotaped movements of subjects which were analysed for 3-dimensional orientations by digitising co-ordinates from videotape frames frozen on a television screen. This produced errors of a few centimeters when compared to a known reference frame which were, nonetheless, acceptable in estimating gross arm movements.

## 5.2 The Cervical Spine

The motion of the segments of the neck (Figure 7) has been investigated both qualitatively (14-17,19,20) and quantitatively (7,90-93). The focus of interest has been on traumatic rather than degenerative processes and the estimation of the extent to which a given segment is sufficiently stable to protect the spinal cord after injury has been the paramount concern. White and co-workers (94)



FIGURE 7



- |                |                  |
|----------------|------------------|
| 1 Sacrum       | 3 Thoracic Spine |
| 2 Lumbar Spine | 4 Cervical Spine |

DIAGRAM OF THE HUMAN SPINAL COLUMN

analysed the clinical stability of the cervical spine. The effects of disc injury on this was investigated by Panjabi, Krag and Chung (80), and subsequent studies showed the effects of surgical stabilisation (95) and investigated the use of methacrylate as a cement for providing this (96).

### 5.3 The Thoracic Spine

The studies of Gregersen and Lucas (97), who inserted metal pins into the spinous processes of the thoraco-lumbar spines of medical students, illustrates not only a close correspondence with the data obtained from the cadaveric work of White and Panjabi (5), but also illuminates the issue of invasiveness of procedures thought to be justified in establishing in vivo norms. The upper thoracic spine is much less mobile than the lower (3-5 degrees x and z-axis rotation at T2-3 compared with 5-20 degrees at T11-12 (5)). The mobility of the area is important in the evaluation of the stability of scoliotic spines (98) and in the assessment of the respiratory function of patients suffering from ankylosing spondylitis. Yet with such small normal movement ranges there is a considerable problem of noise in attempts to evaluate the segmental kinematics by imaging. This is compounded by the anatomical superimposition of the ribs, especially in the lateral view. Nevertheless, cadaveric work has established the normal ranges (99) and ICRs (75) and the stiffness and load-displacement properties have been researched (100) to the point of establishing the changes which occur when selected connective tissues are removed.

#### 5.4 The Lumbar Spine

Its accessibility to imaging techniques and the prevalence of back pain in the population has made the kinematics of the lumbar spine the most thoroughly investigated of all - sometimes without apparent regard to the hazards of ionising radiation to normal volunteer subjects who underwent extensive serial X-ray studies to establish the ranges of movement. Surface measurements are tantalising from this viewpoint, (101,102) but too inaccurate to obtain segmental kinematic information (25,103). For these reasons, and apart from the sources listed above, few in vivo studies of normal segmental kinematics have been undertaken, most researchers following the example of Hilton, Ball and Benn (104) in using cadaveric lumbar spines. Exceptions are the work of Porter et al (105) and Hibbert et al (106) who used ultrasound to scan the lumbar spine, mainly for canal diameter but also for canal encroachments caused by spondylolisthesis. This method did not give reliable anatomical landmarks for motion analysis but did have the advantage of safety. Much work has been done in connection with specific clinical issues related to spine kinematics.

#### 5.5 Axial (y-axis) Vertebral Rotations

In order to study the rotation of a vertebra through imaging the issue of out-of-plane distortion must be resolved. Benson et al (107) cast doubt on the accuracy of the traditional method of doing this by measuring the offset of X-ray shadows of the pedicles between successive films. Drerup (108,109) and Mehta (110) presented data, however, which support the method. Undeniably greater assurance can be obtained from biplanar studies where much of the calibration work

has been done with cadaveric specimens (111). Pearcy (44) demonstrated a relationship between pain and reduced movement using this technique. To do this requires a high degree of accuracy which has so far only been possible for overall ranges of movement and with appreciable radiation dosage.

## 5.6 Coupled Motion

As mentioned above, the description of three-dimensional segmental motion has been simplified by the introduction of the three-dimensional co-ordinate system (72) which is convenient in relation to the axes of the human body. Part of the difficulty in assessing twisting of vertebrae (y-axis rotation using this system), is the tendency, observed throughout the human spine, for this to be combined with sidebending (z-axis rotation). This is a natural consequence of the geometry of the spine (112) which was recognised from anatomical studies as early as 1903 (113). This simultaneous occurrence of motion in two planes applies not only to rotations but also to translations. The translational element is thought to be important when assessing the stability of the spine, because this is thought normally to be small. Large amounts of translation cause wide variations in the location of the ICRs over the motion sequence (114) representing a disruption of the normal pattern.

## 5.7 Coronal Plane (Lateral Bending) Motion Studies

While the rotational ranges of gross lateral flexion were investigated from X-rays by Tanz (11), Miles and Sullivan (115) reported discrepancies in some movements. These were movements contralateral

to the side of bending in individual vertebrae which were difficult to explain. However, these authors made little attempt to validate the accuracy of their method of measurement beyond stating that they related "each vertebra to the horizontal and compared the data for the lateral bending with that for the neutral position". Further radiographic studies of lateral flexion in the lumbar spine were undertaken by Dimnet et al (6) using digitised anatomical co-ordinates from serial radiographs. These confirmed the previous observation of paradoxical movement and related it to dispersion in the loci of ICRs.

In the human spine, lateral flexion is associated with the greatest amount of coupled motion (see Section 5.6) between the principal rotation about the z-axis and associated rotation about the y-axis (44). This is easily seen in the lumbar spine (Figure 8). Lack of confidence in the ability of observers to label anatomical landmarks accurately on images of vertebrae under these conditions was reflected in the small number of lateral flexion studies published in the 1980's.

FIGURE 8

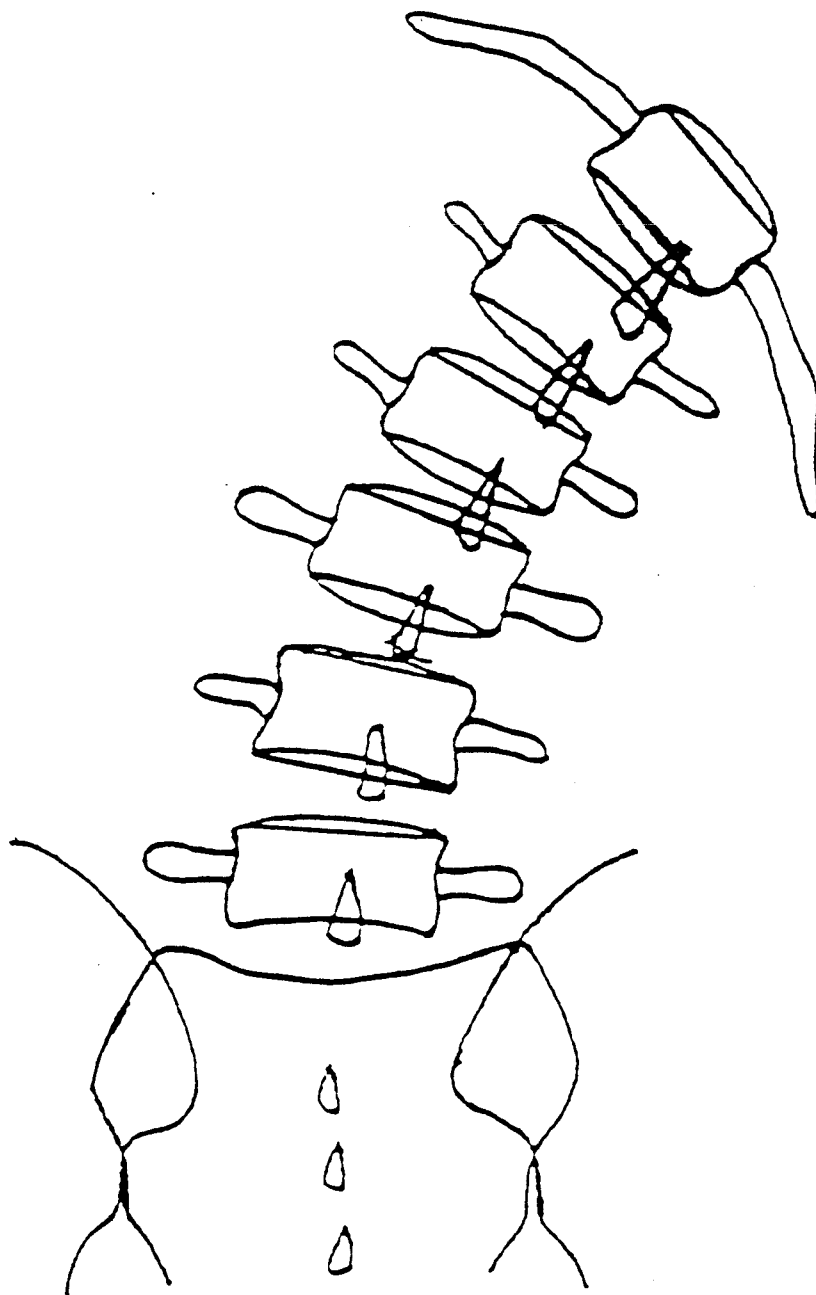


DIAGRAM OF "COUPLING" MOTION DURING CORONAL PLANE  
ROTATION IN THE LUMBAR SPINE

### 5.8 Sagittal Plane (Flexion-Extension) Motion Studies

The association between bending and back pain has made the study of this plane of motion attractive (116). The issue of stability (see Section 6.1) and the possibility of damage to discs and posterior joints during flexion led investigators to seek relationships between these problems and this type of motion (117-119). The work tended to concentrate on translations with and without loading, either by direct measurement (117) which is exceedingly error prone, or by determination of centre lengths (79,81,114,120,121). The latter, based on small samples of live and cadaveric spines, generally suggest that centre lengths equal to or less than the anterior-posterior dimension of the intervertebral disc (approximately 30mm in the lumbar spine) are consistent with either normal or very degenerate discs, both of which have inherent stability. Early disc degeneration, however, has been associated with larger centre lengths (over 50mm) and with suspected vertebral instability. Generally speaking, the laboriousness and radiation-intensiveness of performing these measurements in living patients has not allowed sufficient data to be gathered to support clinically useful conclusions.

### 5.9 Three-Dimensional Studies

Undoubtedly, a more complete quantification of vertebral kinematics requires the measurement of 3-dimensional displacements. While this may be more difficult to visualize for clinical purposes, it surmounts the problems of coupled motion and out-of-plane X-ray images. The basic requirements for such analyses from spinal X-rays has been outlined by White and Panjabi (5), Suh (48) and Chasles (122).

Traditionally, the data used are co-ordinates derived from anatomical landmarks, and the validity of doing this has been verified in cadaveric specimens by Rab (43) and by Adams (123). The latter compared the position obtained from stereo X-ray studies with those obtained using a reflex microscope. An analysis of the errors to which such stereo systems are susceptible has been investigated by Spiegelman and Woo (124), as has the mathematical treatment likely to minimize them (125).

Like the simpler 2-D studies, 3-D analysis of spinal motion has been done for gross movements, most recently using an electromagnetic transmitter/sensor system (126), as well as for segmental motion in cadaveric (100,111) and living spines (44,49). Some have verified measurements against a calibration model (44,127). The conclusions obtained from applying 3-D X-ray analysis to patients with low back pain (128), disc hernia (42) and surgical fusion (45,129) have been tentative in clinical terms, mainly because of the paucity of analyses in relation to the variety of syndromes. Nevertheless, at best an accuracy of 1mm in the measurement of translations has been claimed in spite of the difficulties involved. These include the expense, laboriousness and dosage involved in using twin X-ray tube systems and the analysis of multiple co-ordinates in sequence.



## 6.0 KINEMATIC MEASUREMENT OF THE SPINE IN CLINICAL SETTINGS

The relationships between painful and disabling conditions of the spine and the mechanical features of vertebral linkages are obscure. However, common sense has led clinicians to postulate that certain such relationships should, indeed, exist and to seek ways of testing their impressions. What tends to thwart any productive outcome of such attempts is the inaccuracy and invasiveness of the measurement systems available as well as the coherent identification of painful syndromes. What follows in this chapter is a review, in terms of kinematics, of what might be considered to be the main mechanical conditions of the spine in terms of prevalence and from the viewpoint of those who deal with them in patients.

### 6.1 Segmental "Instability"

Clinicians have found it reasonable to assume that deformation of the connective tissues of the spine beyond their elastic limits should cause pain (130), not least because most of them are richly supplied with sensory nerve endings (131). The concept of instability arises "when this deformation extends beyond the limits of normal restraint" (132). Symptoms and signs thought to indicate this have been described by Howes and Isdale (133) Hirsch, Jonsson and Lewin (134), Morgan and King (135) and MacNab (136), while other authors have warned of obscurities in the use of this term (137,138). The latter have called for improvements in the use of dynamic radiography.

In engineering terms, a mechanical system may be said to be in a state of either stable or unstable equilibrium (139). Bodies which are unstable are merely moving towards stable equilibrium at a given rate and will not, therefore, return to their original positions when any load is removed. The practical usefulness of knowing how "stable" vertebral segments are has been addressed in terms of the forces involved (140-143), ranges of motion (81,117), disc degeneration (144,145), spondylolisthesis (44) (see section 6.6) and disc hernia (118,119). Stokes and Frymoyer (116), measuring the ranges of flexion-extension and anterior-posterior translation from X-rays of 78 patients thought to have clinical signs of instability, found that the suspect segmental levels had ranges greater than the accepted norms. The mechanisms of ligamentous disruption which might account for such patterns have been investigated in cadavers by Van Akkerveeken (146).

Because ranges of movement between vertebrae are generally small, and the errors involved in measurement relatively large, there are problems in establishing, from X-rays, whether a segment is disposed towards stable or unstable equilibrium (141). Furthermore, the wide variation in ranges of rotation, as compared with translation, has made the latter more promising in relation to stability (146). The ICRs of vertebral segments are sensitive to such changes (75,79), but in view of current X-ray dosage, repeated studies of the same living individual have not been done to establish the dispersion of their locations at different points in time.

## 6.2 Lumbar Surgical Fusion

Lumbar instability has been inferred and acted upon surgically by Knutsson (147) on the basis of subjective observation of increased translation seen on X-rays at the extremes of range where disc degeneration was evident. Lettin (148) described similar criteria for undertaking surgical fusion in spondylolisthesis. Fusion of the spine does not, however, always abolish spine motion (149), and Frymoyer et al (150) found, in comparing fusion and non-fusion patients ten or more years after lumbar disc surgery, an association between increased range of movement and pain. Olsson, Selvik and Willner (129) developed an elegant roentgen stereophotogrammetric method for measuring translational and rotational movements in the lumbar spine. This method claimed an accuracy of  $0.3^\circ$  in measuring the rotations of the lumbosacral spine and utilised a 3-dimensional reference frame and implanted metal shot as reference markers in the vertebrae of the living subjects. Using 3-dimensional screw-axis analysis (122), the method was applied to patients who had undergone surgical fusion and revealed considerable movement in many of them. Pearcy and Burrough (45) used the biplanar radiographic technique referred to above to obtain similar 3-dimensional information without the necessity of metal implants. It was found that immobilisation was possible but sometimes resulted in increased motion above the fused level. Sometimes, however, motion at the fused levels did occur which was paradoxical to the direction of the lumbar spine as a whole. Lumbar fusion survives as a technique despite this, albeit under more stringent criteria and was justified by Rolander (151), who showed

that fused cadaveric spines are marginally better able to bear compression loads.

### 6.3 Cervical Spine Fusion

Neck injuries are potentially more disabling than those of the lower spine and surgical stabilisation techniques have seen considerable advances in recent years, particularly with the increasing use of the anterior approach. The kinematics of the normal, injured and stabilised cervical spine was investigated by Goel et al (152) in an effort to identify the main dynamic stabilisers. White et al (94) defined cervical spine instability as a range of translation in the z-axis of more than 3.5mm and a range of rotation of more than 11° about the x-axis as measured on a standard lateral cervical X-ray and later reviewed the concepts of lower cervical spine stability (153). Instability of the upper cervical spine, associated with stroke, has been usefully investigated using computed tomography (CT) by Dvorak and his colleagues using cadavers (154) and live subjects (155).

The techniques and role of surgical stabilisation have also been examined by White and Panjabi (95). Understandably, testing of cervical spine stability in vivo is difficult to justify ethically; and the ranges of movement cited as abnormal have also been observed in asymptomatic, uninjured subjects. This suggests that other indices of the problem need to be sought, perhaps within the range of motion.

### 6.4 Disc Degeneration

Disc degeneration is not necessarily a problematic process in terms of

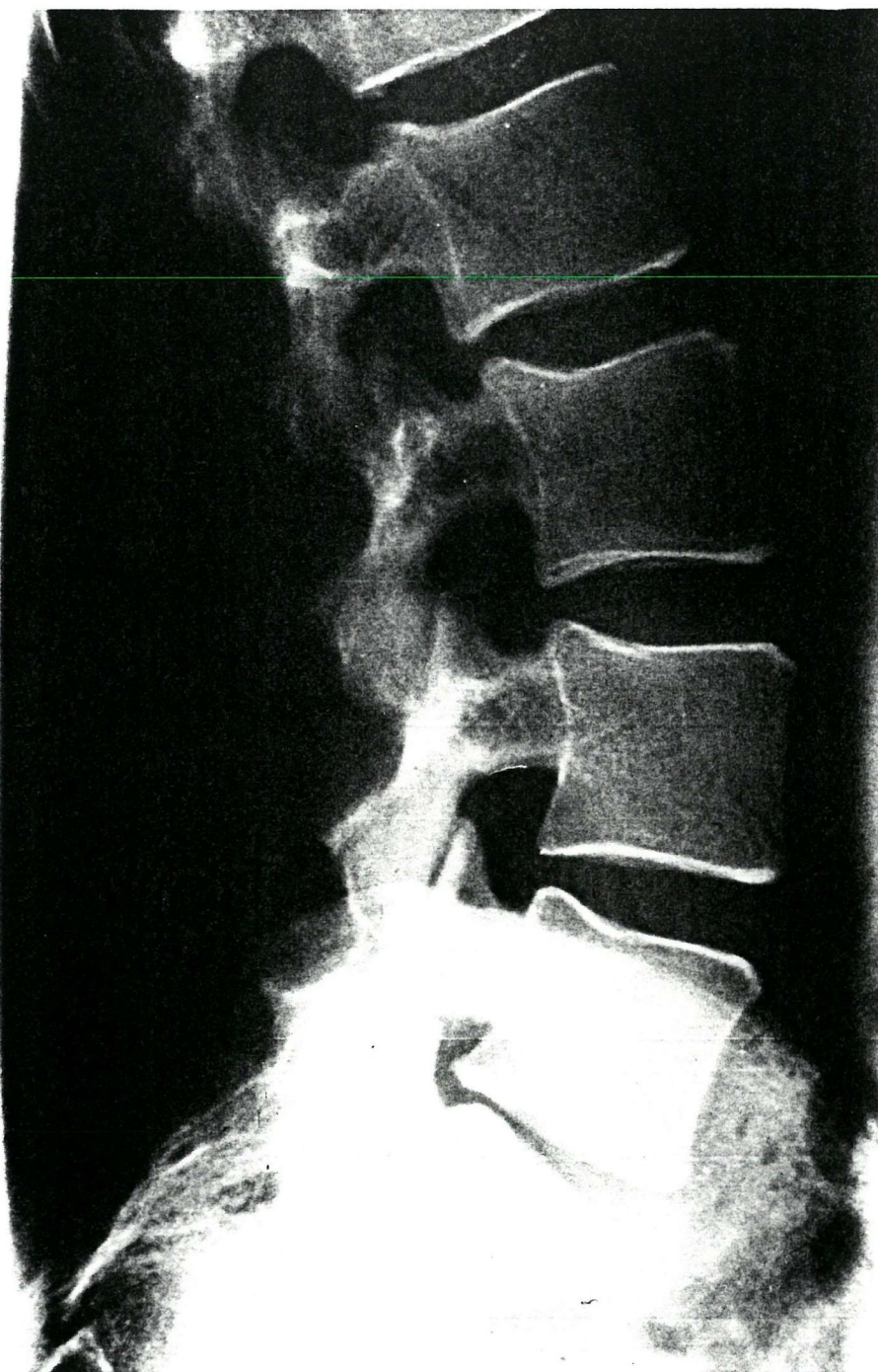
the comfort and independence of the individual. Lawrence (156) showed that pathology of this nature and symptoms are not necessarily concomitants. Seligman et al (81) and Gertzbein et al (79), in computer studies of cadaveric spines, found that the dispersion of ICRs is small and uniform in normal and severely degenerated discs but large and erratic in early and moderate lumbar disc disease, where symptoms are more prevalent (156) but not detectable by standard investigations. This is consistent with the tendency for back troubles to concentrate in middle life (21), however, there is no ready clinical method of detecting such early mechanical changes.

#### 6.5 Retroposition - A Clinical Example

Vertebral retroposition has long been identified as a cause of nerve compression in the lateral recess of the lumbar spine (157,158). It is not the only cause however, the others being (most notably) posterolateral disc herniation and osteoarthritic outgrowth. From a management point of view, the differential diagnosis is very important, since inappropriate treatment could delay, if not completely prejudice, recovery from what is at best a disabling condition. Backward displacement of the fifth lumbar vertebra was associated with degenerative disc disease by Fletcher (159) (Figure 9) and the classification and criteria for the diagnosis of true retrodisplacement were set out by Melamed et al (160) in 1947. In clinical terms, however, its part in the production of pain has remained unclear. Gillespie (161) pointed out the prospect for false positive diagnosis when the lateral lumbar radiograph is rotated out of plane and showed that some true retrodisplacements are painless.

Attention meanwhile turned towards possible methods of measurement and the recognition of pain syndromes which incorporate this finding. A few clinical tests, such as straight-leg raise (Figure 10) are well established in the diagnosis of nerve root "entrapment", which is a clear possibility, especially if the retroposition is unilateral (Figure 11).

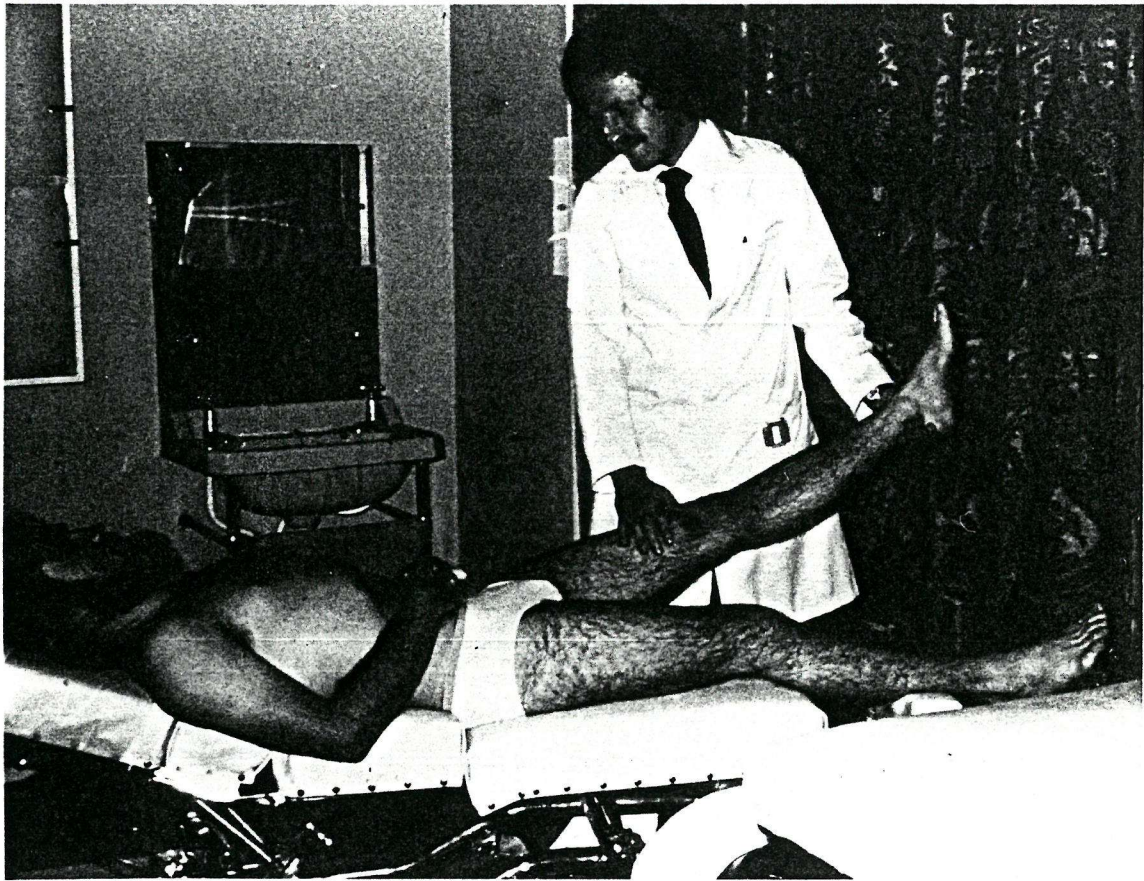
FIGURE 9



LATERAL X-RAY OF THE LUMBAR SPINE SHOWING  
DEGENERATIVE DISC DISEASE AND RETROPOSITION  
OF THE FIFTH LUMBAR VERTEBRA RELATIVE TO  
THE SACRUM



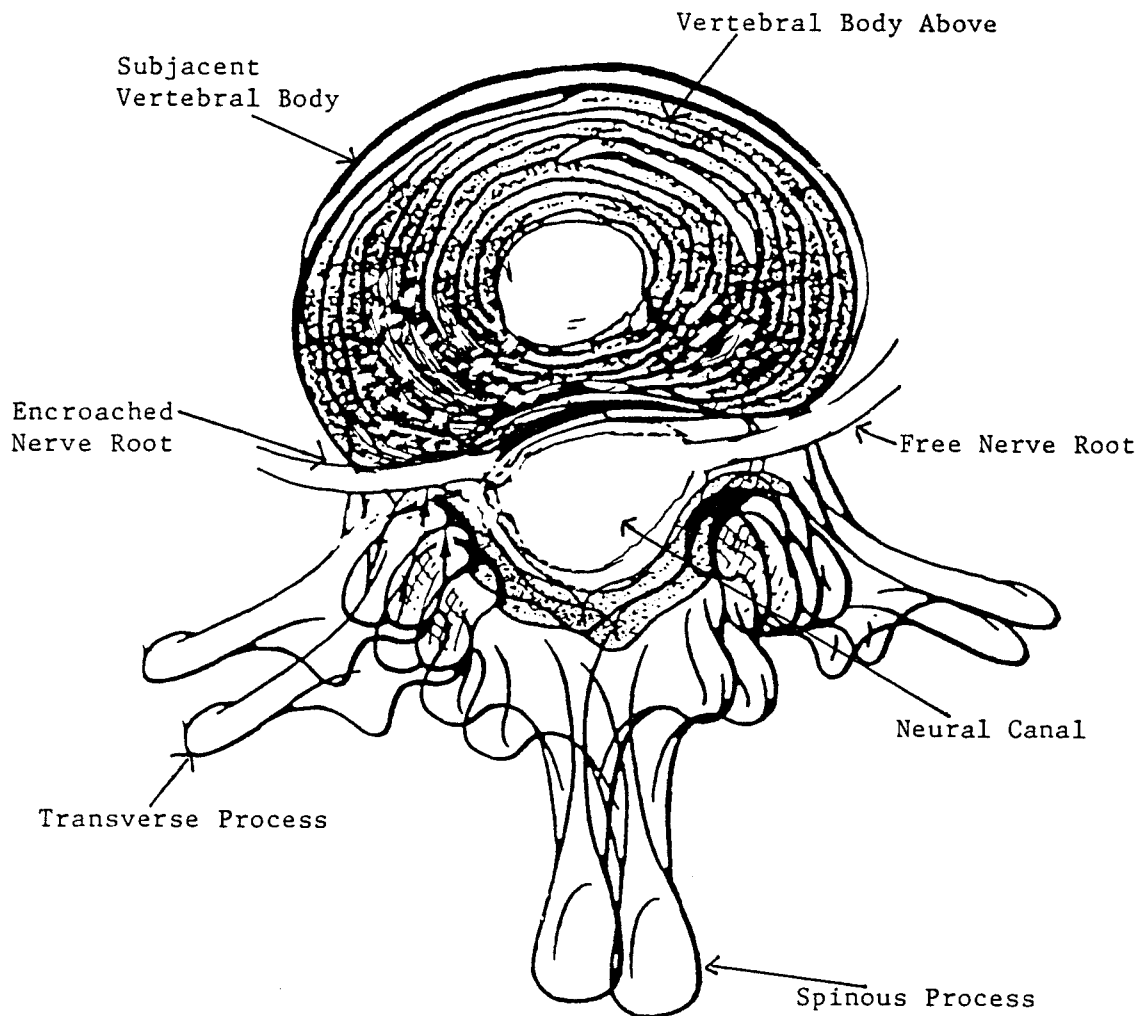
FIGURE 10



PHOTOGRAPH OF THE STRAIGHT-LEG RAISE TEST (SLR)



FIGURE 11



TRACING OF AXIAL VIEW OF TWO LUMBAR VERTEBRAE SHOWING  
ENCHROACHMENT OF NERVE ROOT WHEN THE SUBJACENT  
VERTEBRA IS ROTATED ANTERIOR

#### 6.5.1 Measurement

The simplest method of measurement is that of calculating the percentage posterior shear between the displaced vertebra and its subjacent neighbour. Alternatively, the Euler method of superimposing flexion-extension radiographs, reviewed by Ben-Eliyahu, Rutili and Przybysz (162), or the method of concentric radii (163) can be used. However, as has been pointed out by Mior and Cassidy (164), only an image in the transverse plane, such as can be obtained from computed tomography, will reveal actual canal or lateral recess encroachment and it would be useful to compare the prevalence of these in these images with that found in orthogonal radiographs of the same subjects.

Even more useful would be the ability to quantify anterior-posterior translations incrementally throughout a range of movement, for stress radiographs can only guarantee what happens at the extremes and may therefore result in false negatives. This can be done by examining the locations of the ICRs for each increment (165). Unfortunately the radiation dosage associated with serial X-rays and the necessity of sophisticated computing techniques denies this measurement to clinicians for the present.

#### 6.5.2 Radiographic Findings

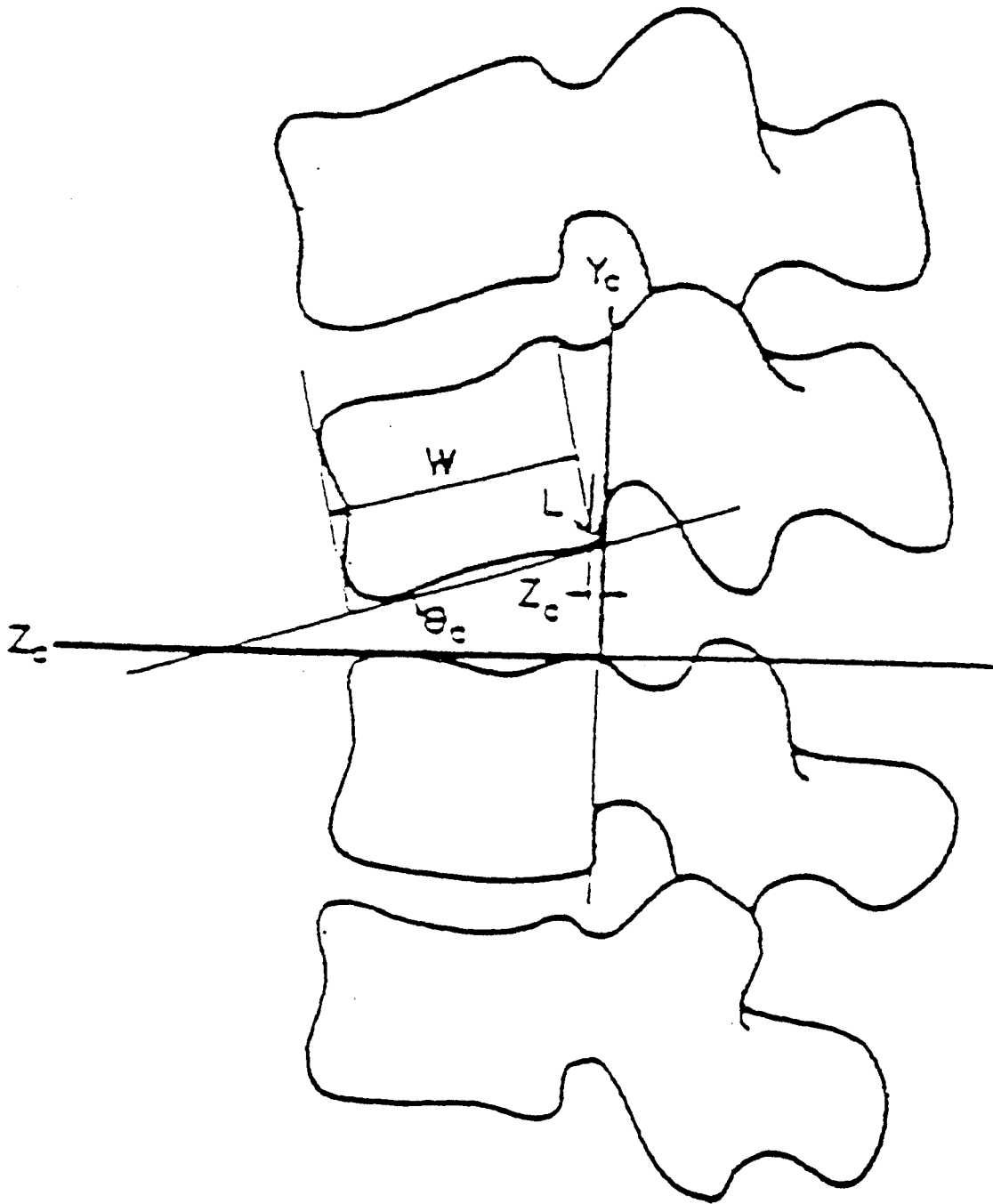
While degenerative changes are common in this condition, they are by no means the rule. Slight disc thinning, combined with a shallow lumbosacral angle (eg. below  $30^{\circ}$ ) and retrodisplacement have been observed in younger patients suspected of this syndrome. Patients with the clinical features who have advanced degenerative change

however, particularly around the posterior joints, should perhaps be seen less optimistically as candidates for trial manipulation.

Flexion-extension stress radiographs will help to highlight any anterior-posterior instability, (Figure 12) but the relationship of this to prognosis is uncertain. However, the procedure itself may decisively increase symptoms and the importance of the various permutations of anterior-posterior movement and degenerative change is also uncertain.

Vertebral retroposition as a cause of back pain and disability is a fertile area from which to begin the often uncertain process of associating clinical features which have little reliance on observer interpretation with objective kinematic measurement. What is lacking in the latter is the facility to measure incremental movement without excessive X-ray dosage in order to gain a clearer understanding of the movement patterns, if any, which are typical of the syndrome. In particular it would be useful to know whether centre patterns are always disrupted in this condition, whether of the static or dynamic type. It is hoped that this would help to predict the outcome of conservative versus surgical management.

FIGURE 12



OUTLINE OF LUMBAR VERTEBRAE MARKED  
FOR THE MEASUREMENT OF  
TRANSLATION

## 6.6 Forward Slippage (Spondylolisthesis)

Defects in the neural arches of a vertebra reduces the strength of these structures as holding elements in an anterior direction (Figure 13). The causes of spondylolisthesis have been divided into congenital, traumatic, osteolytic and degenerative (132,166). All but the latter, which results from wear on cartilage of the posterior joints, relate to such neural arch defects which leave the spinous process behind, while allowing the vertebral body and the spine above, which it supports, to slide forward. The more severe forms may threaten bladder function and lower limb strength because of the tension imposed on the lumbar nerve roots within the spinal canal; but minor displacements can be associated with disabling back pain. Inferring spondylolisthesis as a cause of back pain depends on mechanical evidence of the "instability" involved. This evidence is often hard to come by, even with the help of stress radiographs. Multiple examinations are necessary to establish the stresses.

FIGURE 13

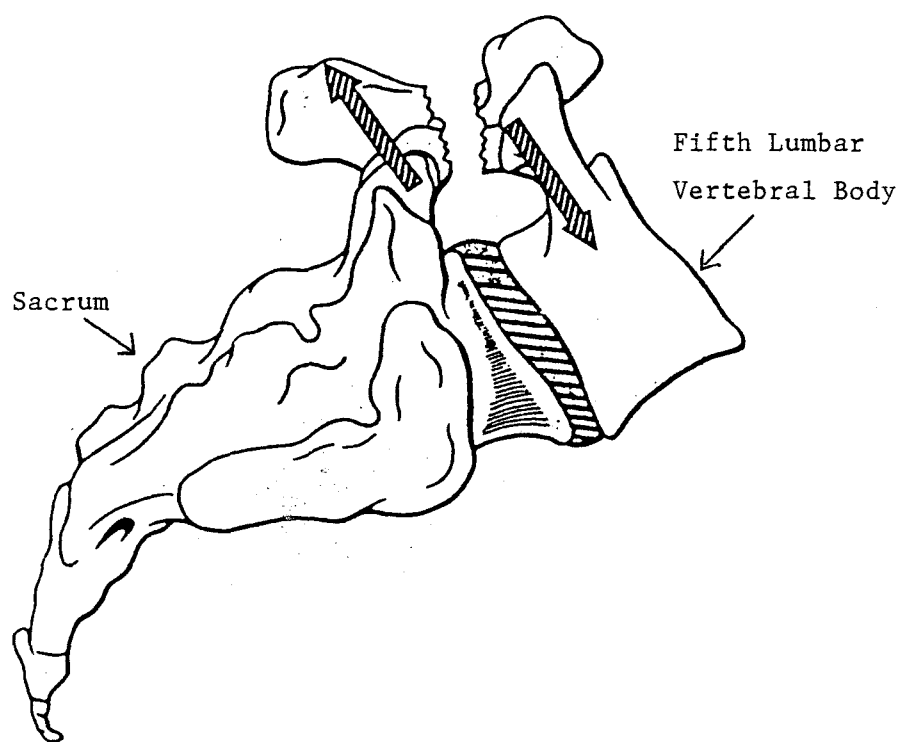


DIAGRAM OF THE LUMBO-SACRAL SPINE SHOWING FORWARD  
SLIPPAGE (SPONDYLOLISTHESIS) OF THE FIFTH  
LUMBAR VERTEBRA RELATIVE TO  
THE SACRUM

## 6.7 Disc Herniation and Injury

Rupture of the intervertebral disc as a pain-inducing pathology was first described in 1934 by Mixter and Barr (167). Since then, the successful surgical removal of herniated discs has virtually cured many people of disorders which hitherto would have rendered them lifetime cripples. Conversely, failed surgery on the spine can have disastrous consequences. Maximum benefit to patients with such conditions can, therefore, only be achieved when the mechanical derangement is fully understood and can be detected at an early stage.

Disc herniation (Figure 14) is thought to result from the degradation of type II collagen within the disc annulus in tandem with the loss of proteoglycans and, consequently, water. This causes the formation of radial cracks and fissures through which the amorphous nucleus can seep. Extrusion of the nucleus is usually in a posterior direction and in this event may compress adjacent nerve roots resulting in pain and loss of power and/or sensation in the legs. Early detection of such changes is problematical. Myelography and radiculography only reveal pathology once hernia has taken place. Discography (Figure 4), however, can detect early fissuring. The disadvantages of this technique are its invasiveness, patient distress and the danger of infective discitis. There is evidence of altered mechanical behaviour in the spine in the pre-hernia situation (114,168) as well as after extrusion (80). These changes are related to the symmetry of vertebral rotations, of coupled movements and to the dispersion of ICRs and have also been observed as a consequence of the partial surgical removal of discs (169). They have been noticed subjectively

FIGURE 14

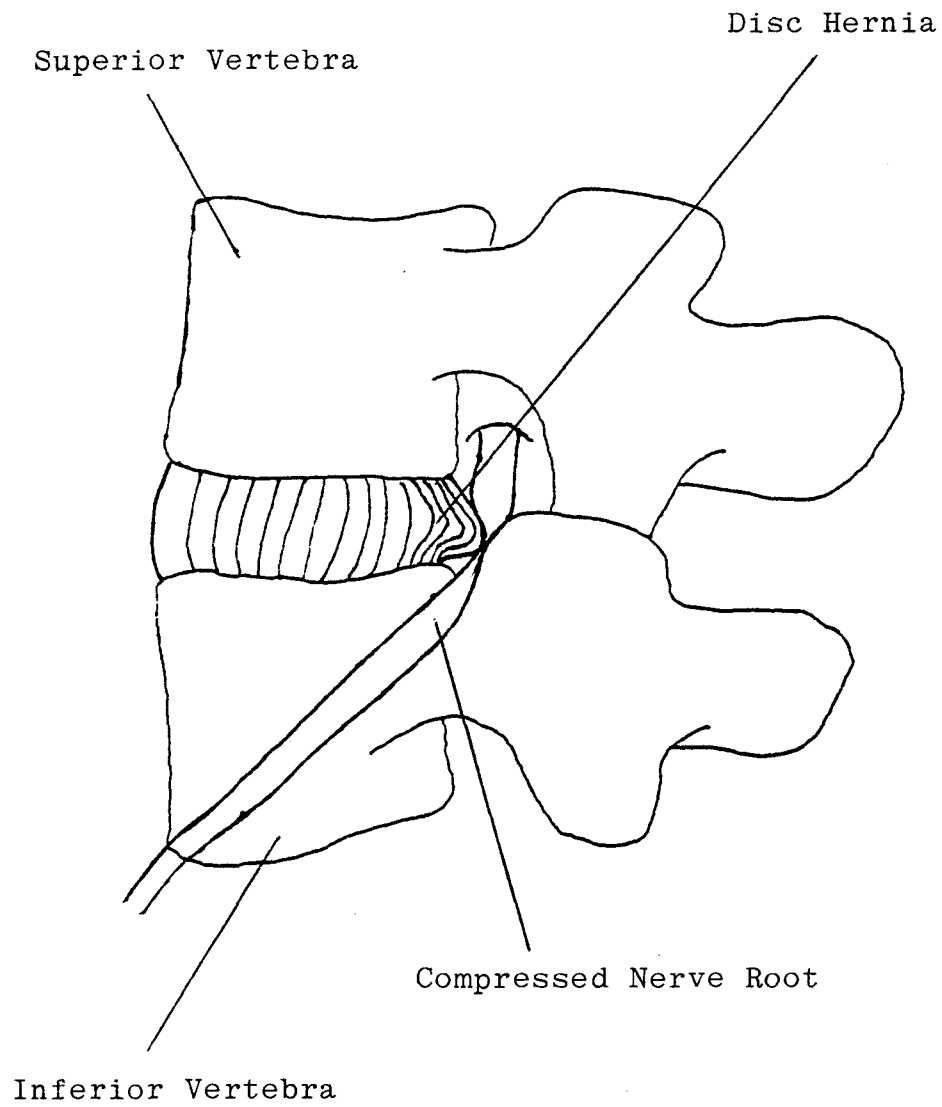


DIAGRAM OF A DISC HERNIA SHOWING NERVE  
ROOT COMPRESSION



by clinicians on palpation of the spine during movement, but owing to the necessity for serial radiographs, and the laborious and difficult nature of current measurement techniques, are not in routine use for screening.

## 7.0 IMPRESSIONS FROM THE LITERATURE

The acknowledged problems of diagnosis of spinal injuries and pain syndromes relate in a large part to the inadequacy of current techniques in determining the functional integrity of the intervertebral tissues and their response to therapeutic intervention. Of prime importance in this is the kinematics of the vertebrae which are held and stabilised by these tissues. Their mechanical status, whether advantageous or disadvantageous to the loads and stresses imposed, are difficult to assess even after damage has progressed substantially. This can result in considerable uncertainty and controversy over the correct approach to treatment.

The literature identifies the sources of the main issues in this regard. The techniques which claim the greatest accuracy tend to be those which are the most invasive, either in terms of radiation or penetration of the skin. Indeed, most investigators have resorted to cadaveric studies to obtain accurate measurements for research purposes and this has, of course, no value in patient screening. The main measurements appear to be intervertebral angles and ICRs. The former have been used to establish normal ranges and the existence of aberrant motion in serial X-rays, whereas ICR is the most popular measure of intervertebral translation, mainly in relation to early

degenerative disc disease and its relationship to spine stability. The practical use of the ICR does, however, depend on there being sufficient intervertebral rotation present (170).

In terms of radiation dosage reduction, digital videofluoroscopy must provide useful information with dosages below 20MGy, being the approximate absorbed dosage attributable to a single plain lumbar X-ray in the anterior-posterior projection. Any new technique which claims to have value for screening would have to meet this standard in order to be considered much less invasive than plain X-ray.

Many of the measurement techniques require rather a lot of meticulous operator use of pencils, rulers and digitisers. The prospect of placing co-ordinates on a digitised video image does not, so far, appear in the literature. The accuracy of doing this by digital videofluoroscopy will depend on many factors. These include the pixel density of the monitor, the size of the image, and the quality which can be obtained. The use of an image processor does not, of itself, guarantee a reduction in labour. The time taken to convert the radiographic image to digital form and the ability to hold a sufficient number of them in the computer's on-line memory is fundamental to any gain in efficiency.

All imaging methods require the plane of the image to be known. In most cases, orthogonal alignment of the object with the imaging device is mandatory. This is not always possible in the clinical situation, therefore, for purposes of the studies which follow, the effects of

such non-orthogonal presentations will be important. Three-dimensional studies have an advantage in this, and other regards. It is clear, however, that the initial questions about the validity of digital videofluoroscopy for spinal kinematic measurement will rest on two-dimensional issues. If the technique is successful, the considerable additional investment in three-dimensional X-ray hardware would then be justified.

The literature seems to fall into four categories where validation of technique is concerned: papers which describe purely visual impressions, investigations which measure uncritically with no error analysis, studies in which the error analysis consists of between and within-observer error and studies which involve calibration against a known standard. Whatever system is chosen, validation will depend on its calibration against a mechanical model which approximates the mechanical behavior of adjacent vertebrae closely. Such a device should be amenable to accurate external measurement of intervertebral angle and ICR.

Technological progress in the fields of image processing and X-ray videofluoroscopy combined with new knowledge about the kinematics of vertebral motion in health and disease suggests that early detection in this area should be possible with low invasiveness, rapid data processing and acceptable and quantifiable accuracy. This depends on the development of digital videofluoroscopy for spinal kinematic measurement.

## PART B

### DEVELOPMENT AND ASSESSMENT OF A DIGITAL VIDEOFLUOROSCOPIC TECHNIQUE

This project sought to identify and evaluate a system for investigating human intervertebral kinematics based on a combination of image processing techniques with videofluoroscopy. The progress of the work is summarised in Figure 2.

#### 8.0 DESCRIPTION OF EQUIPMENT

##### 8.1 X-Ray Equipment

A Thompson CGR X-ray machine with motorised tilt table and above-table X-ray tube was used. The equipment, located in the X-ray department of the Duke of Cornwall Spinal Treatment Centre at Odstock Hospital in Salisbury, included a modern 9" diameter image intensifier, sited under the tilt table. Both the intensifier and tube arm were equipped with remote-controlled positional adjustment. The generator and control panel (Figure 15) incorporated automatic dosage control and the system was capable of producing fluoroscopic sequences of lumbar spine motion using settings in the region of 2-3 milliamperes and 70-125 kilovolts. The equipment was operated by the hospital radiographers for all recordings and with the table in the upright position. Human subjects were X-rayed with the minimum of stabilisation, to allow natural motion. However, a wooden seat frame (Figure 16a) was constructed to stabilise the sacrum during lumbar extension (Figure 16b).

FIGURE 15



THE X-RAY CONSOLE AT ODSTOCK HOSPITAL



a)

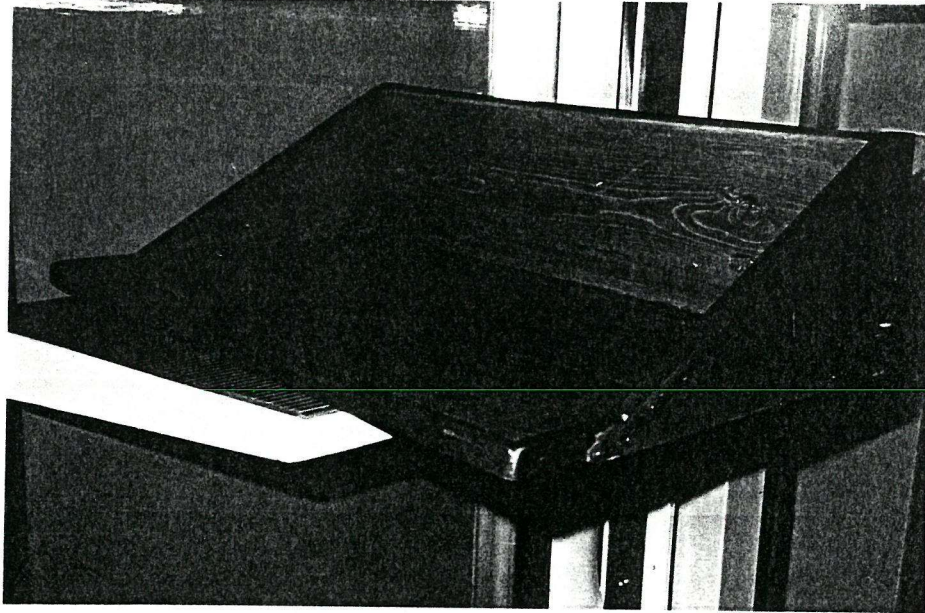
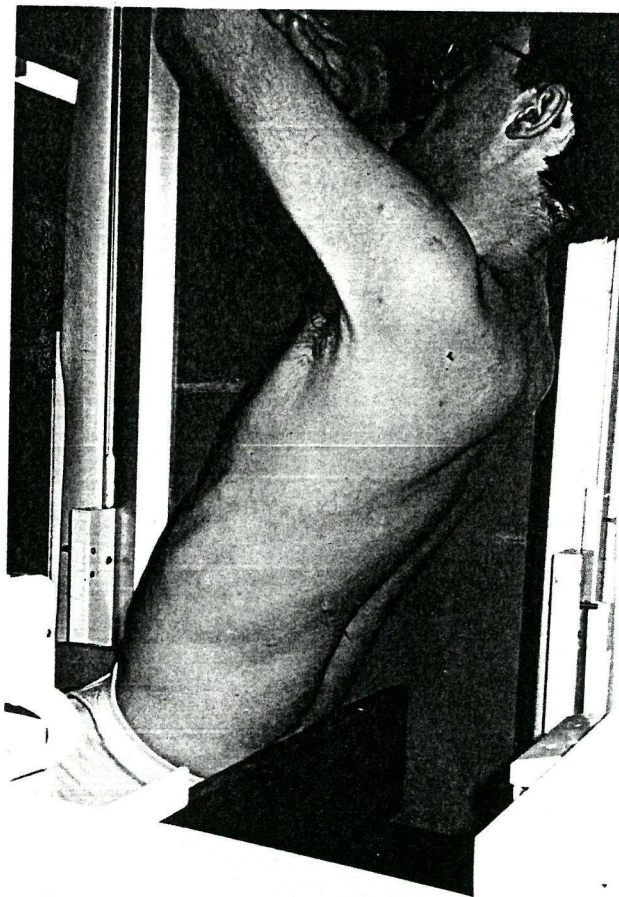


FIGURE 16

b)



- a) Wooden seat frame for stabilising lateral views  
b) Subject extending lumbar spine while stabilised  
against frame

Gonadal protection was used for all subjects and radiation dosage measurements were made using lithium borate thermoluminescent dosimeters. These were generously supplied and processed by the National Radiological Protection Board and were placed on both the torso of a human subject and on a radiographic phantom (Figure 17).

The intensifier incorporated electronic correction of pin-cushion distortion, which was confirmed by comparing the images from the Thompson machine of a wire grid with 1cm squares with those from an older Phillips intensifier (Figures 18a and b). Images were recorded onto 3/4" (U-Matic) videotape for transporting to the image processing laboratory at the Chiropractic College in Bournemouth for study (see section 8.2). The processor could, however, be interfaced directly with the intensifier as shown in Figure 15.

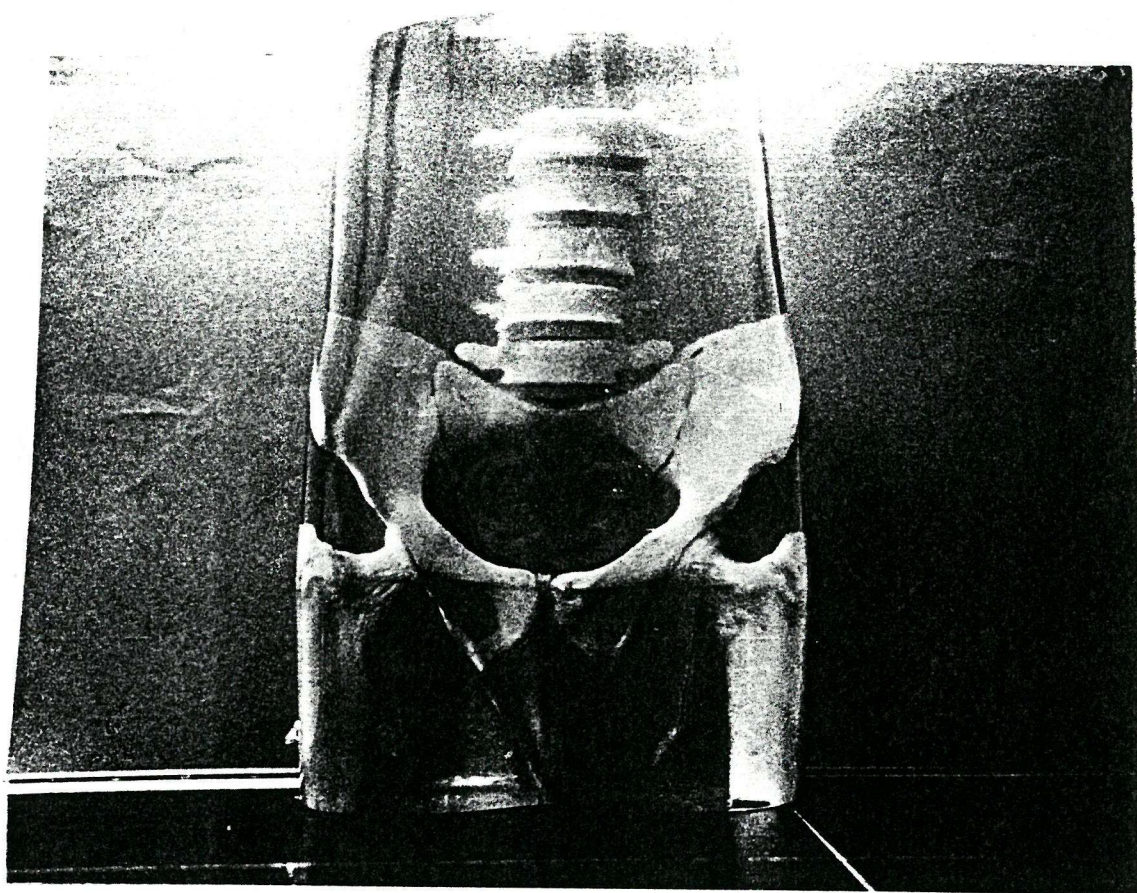
## 8.2 Image Processing Laboratory

The computing hardware comprised a PDP11-based image processor (Kenda Electronic Systems Limited). This included an 80Mb hard disc drive and a high resolution colour monitor of 512x512 pixel density with electronic cursor. The software was, for the most part, commercially bought (Signum Computer Systems), and included automatic frame-grabbing, video synchronisation, contrast stretching and edge-finding. Also included were algorithms for the geometric manipulation of screen co-ordinates and for the movement of images within the on-line memory. The latter could hold 16 256x256 pixel images on-line, of which 4 were visible at any given time (Figure 19). The computer was housed in a laboratory at the Anglo-European College of Chiropractic in

Bournemouth (Figure 20). The laboratory was equipped with a Sony 3/4" (U-Matic) videotape recorder and television monitor. A 35mm camera and a Polaroid screen camera were used to obtain slides and hard-copy prints of the images.



FIGURE 17



THE RADIOGRAPHIC PHANTOM



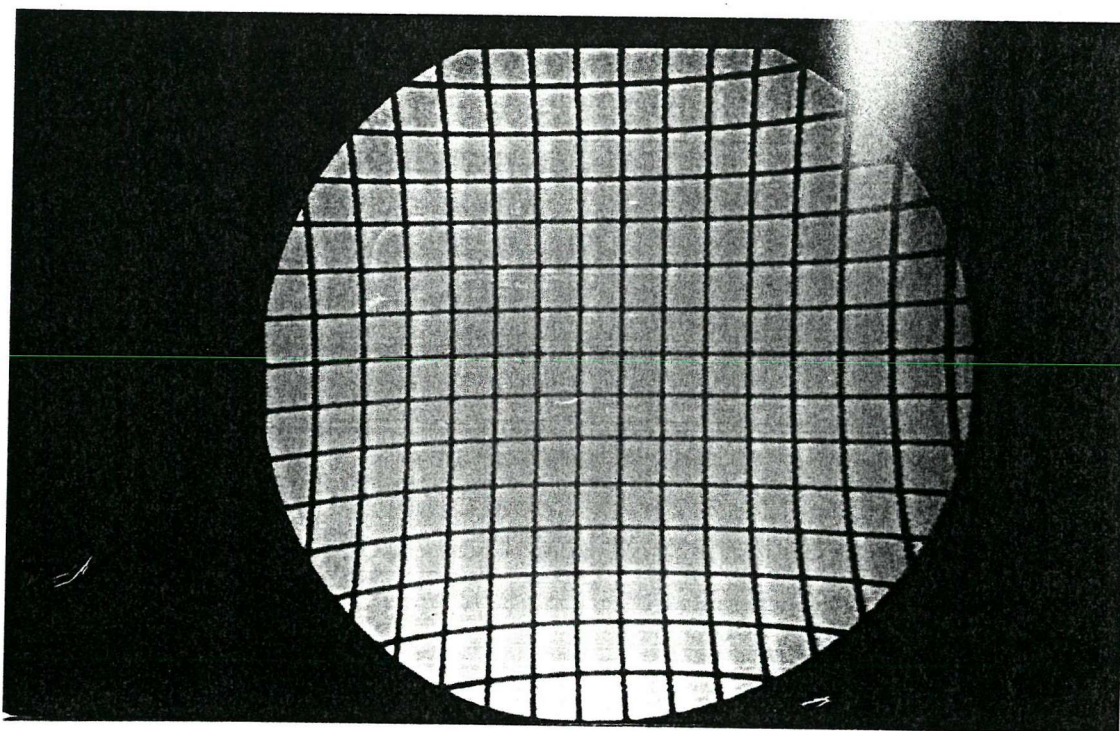


FIGURE 18a

DIGITISED IMAGE OF A WIRE GRID OBTAINED FROM A PHILIPS INTENSIFIER

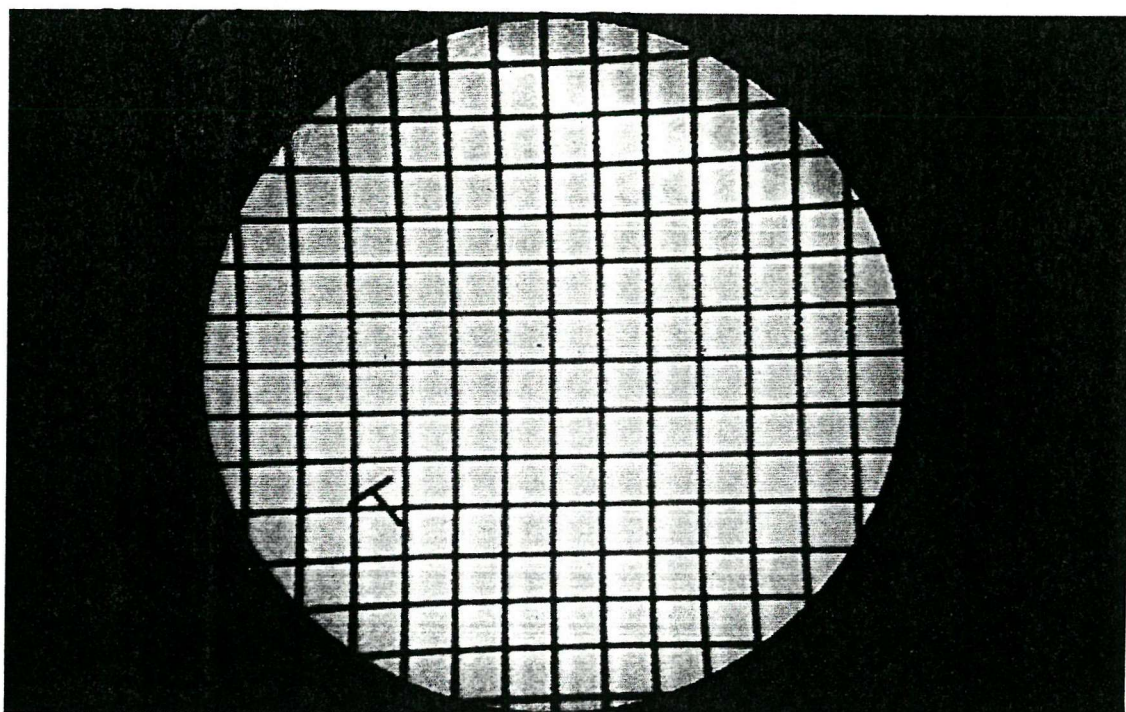
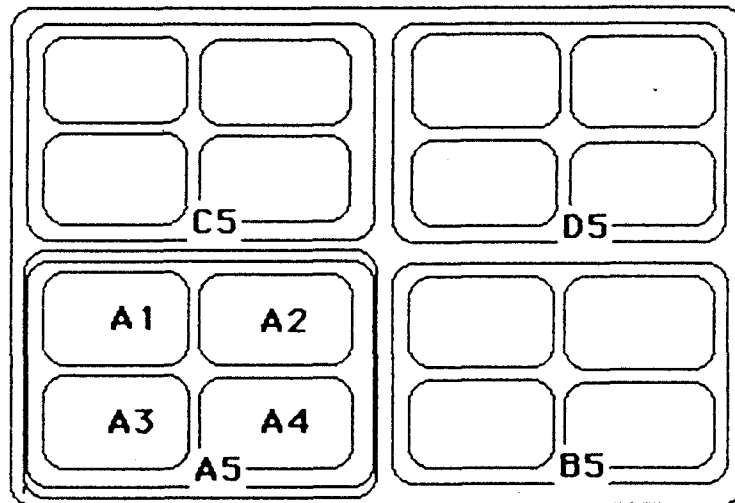


FIGURE 18b

DIGITISED IMAGE OF SAME WIRE GRID OBTAINED USING THE THOMPSON  
INTENSIFIER USED IN THESE STUDIES

FIGURE 19



**Image Frame Buffer (G)**

DIAGRAM OF THE IMAGE FRAME BUFFER



FIGURE 20



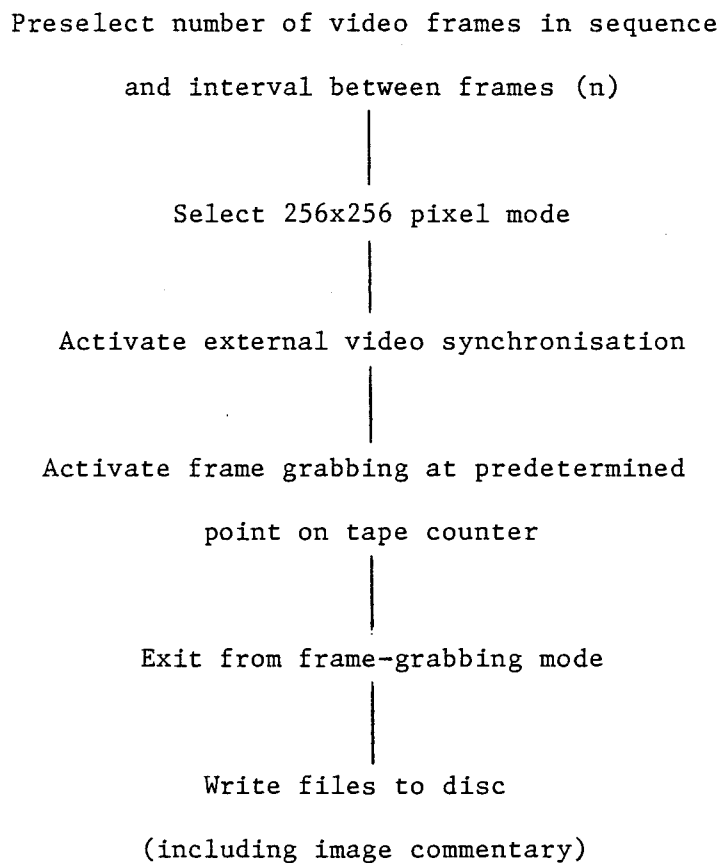
IMAGE PROCESSING LABORATORY

### 8.3 Development of Procedures for Image Processing

The basic requirement for the image processing of the motion sequences were: 1. Frame grabbing from videotape; 2. Marking and calculation of intervertebral angles; 3. Marking and calculation of ICRs

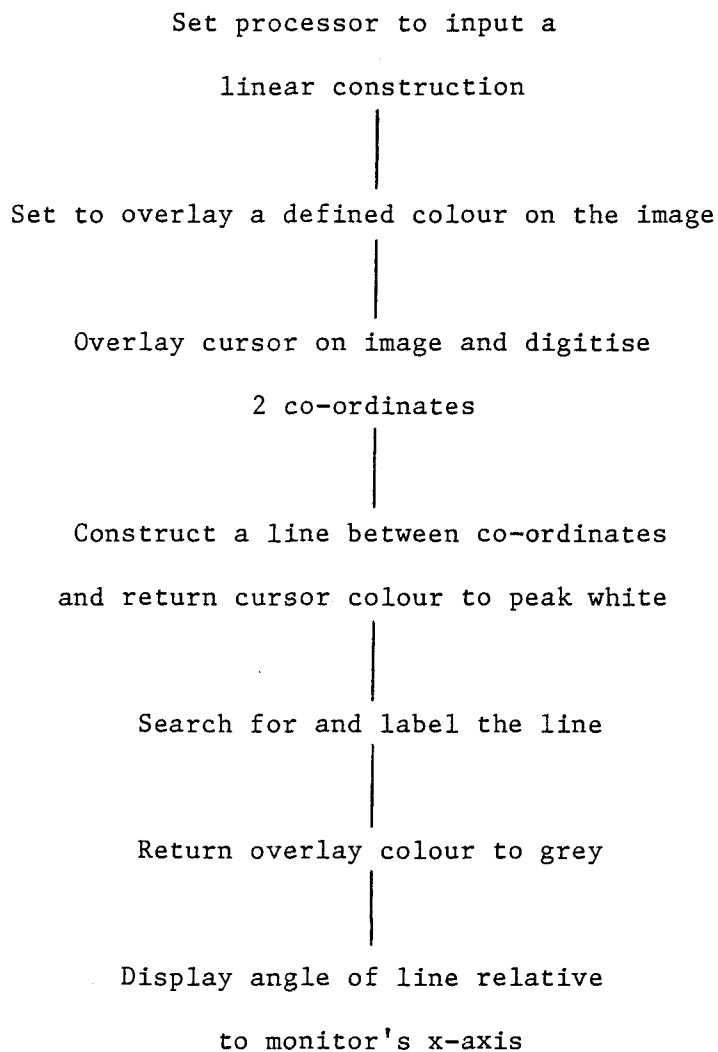
#### 8.3.1 Frame-grabbing from Videotape

The image processor was used to digitise either single frames of the calibration model and scaling devices, or motion sequences in either volunteer subjects or patients. A typical procedure for frame-grabbing from videotape is described in the following flow diagram, the command sequence for which can be seen in Appendix IIa.



### 8.3.2 Marking and Calculation of Intervertebral Angles

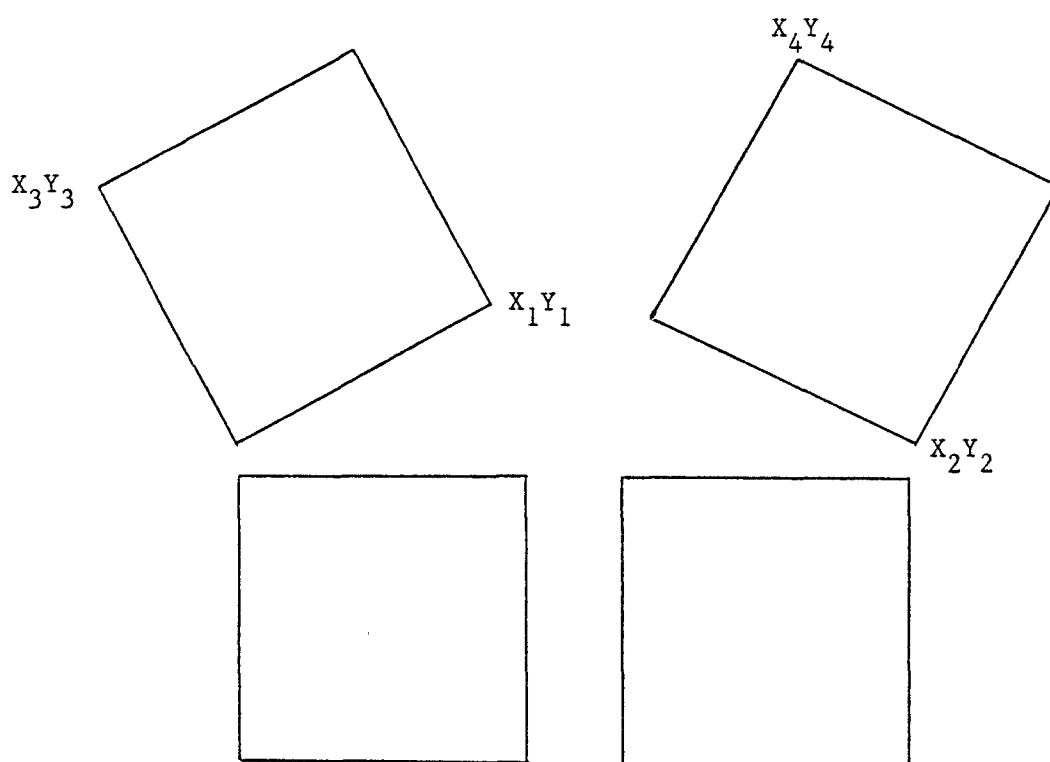
The simplest requirement in relation to vertebral angles was the calculation of the angle generated by a line joining two co-ordinates placed by the screen cursor in relation to the x-axis of the monitor. This was accomplished as follows for an image on one 256x256 screen (See Appendix IIb for command sequence).



This procedure could be expanded to measure any number of angles from sets of screen co-ordinates and the expanded version automated as a batch file which could be activated by a single command.

### 8.3.3. Marking and Calculation of ICRs

The development of this procedure required careful consideration of errors and optimisation criteria (49). The traditional algorithm uses a Pythagorean approach to the the co-ordinates marked on the vertebrae. The equations are as follows:



Where X<sub>icr</sub>, Y<sub>icr</sub> = ICR co-ordinates;

Angle = angle of rotation

$$A = X_2^2 - X_1^2 + Y_2^2 - Y_1^2$$

$$B = X_4^2 - X_3^2 + Y_4^2 - Y_3^2$$

$$C = (X_2 - X_1) \times (Y_4 - Y_3) - (X_4 - X_3) \times (Y_2 - Y_1)$$

$$X_{icr} = \frac{(Y_4 - Y_3) \times A - (Y_2 - Y_1) \times B}{2 \times C}$$

$$Y_{icr} = \frac{(X_2 - X_1) \times B - (X_4 - X_3) \times A}{2 \times C}$$

and

$$\text{Angle} = \arctan \frac{(Y_3 - Y_1)}{(X_3 - X_1)} - \arctan \frac{(Y_4 - Y_2)}{(X_4 - X_2)}$$

The use of the squared terms, however, can have the effect of magnifying errors and an algorithm based upon the following vector-matrix description was assessed as a means of overcoming this problem.

$$\begin{pmatrix} \cos\theta & \sin\theta \\ -\sin\theta & \cos\theta \end{pmatrix} \begin{pmatrix} X_1 - X_{icr} \\ Y_1 - Y_{icr} \end{pmatrix} = \begin{pmatrix} X_2 - X_{icr} \\ Y_2 - Y_{icr} \end{pmatrix}$$



where  $\Theta$  represents the angle of rotation  
and  $X1\ Y1$  and  $X2\ Y2$  are the co-ordinates of the initial  
and final vertebral landmarks and  $Xicr$  and  $Yicr$  are  
the co-ordinates of the ICR

Caution was required in the use of this algorithm also, in that small difference in position of the vertebrae in question in either an x or y direction could result in the magnification of errors. The procedure for computing a single ICR for a rotating vertebra is shown in the flow diagram below and the complete ICR program can be found in Appendix III.

The program was developed with the assistance of D. Woolnough and R. Allen. Significant problems arose in the interface between the PASCAL system and the image processing software (INCOS2), but these were eventually overcome with the help of Kenda Electronic Systems Ltd.

```

graph TD
    USER[USER] --> ICR[ICR]
    ICR --> D1{Request number of frames}
    D1 --> D2{Request number of points  
on each vertebra}
    D2 --> D3{Request name of 1st image}
    D3 --> D4{"New position: Lower  
vertebra, Point 1"}
    D4 -- yes --> D4
    D4 -- no --> D5{"Would you like to  
change the position  
of the last point?"}
    D5 -- yes --> D4
    D5 -- no --> D6{New position next  
point (for next  
2 points)}
    D6 --> D7{"New position: Upper  
vertebra, Point 2"}
    D7 -- "(after 2nd frame)" --> D8{"Do you want to apply  
a rigid body constraint?"}
    D8 -- yes --> A1[apply  
constraint]
    D8 -- no --> A2[Calculate ICR co-ordinates  
and present to user]
    A1 --> A2
    A2 --> D4
    A2 --> D6
    A2 --> A3[after 1st  
frame,  
computer  
exchanges  
1st with  
2nd frames]
    A3 --> D4

```

In practice, the problem of small displacements in one plane was found to be more acute in the calibration studies where the rotations tended to be much more symmetrical around the universal joint. This was, therefore, more likely to leave an x co-ordinate little altered by the rotations. In studies involving human volunteers, the motion was understandably less regular, which tended to minimise this problem.

## 9.0 SUMMARY OF FEASIBILITY STUDIES

The description of the feasibility studies and preliminary experiments associated with this work can be found in a previous report (171).

These studies began as an enquiry into the practicability of digitising moving images directly from an intensifier and established the possibility of doing this for cervical and lumbar spine images. This was followed by experiments in frame-grabbing from sequences on videotape and by studies of any inherent variations in image background density. The latter were found to be negligible. These experiments established the basic system structure (Figure 21).

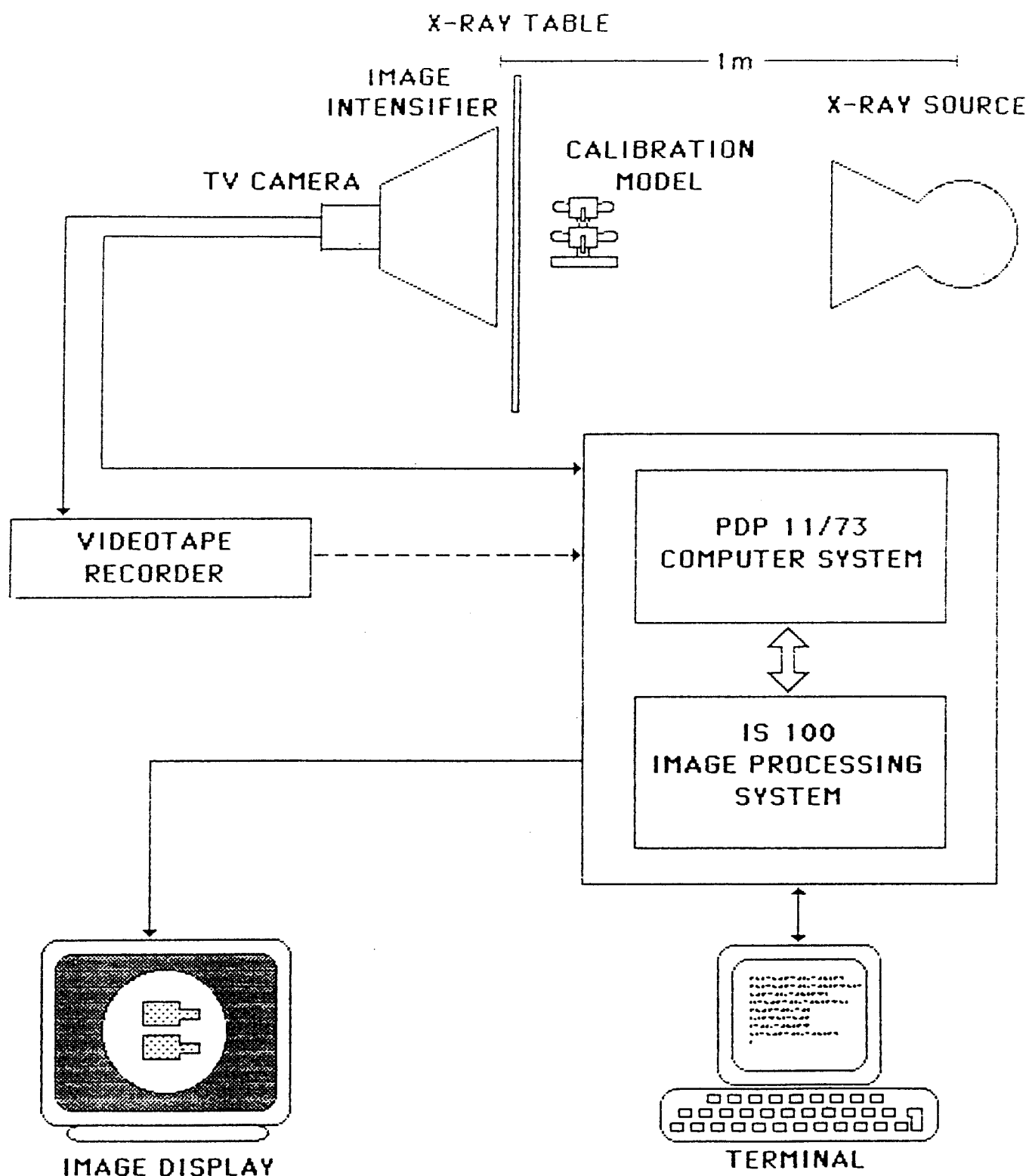


FIGURE 21

SCHEMATIC DIAGRAM OF THE X-RAY EQUIPMENT AND IMAGE PROCESSING SYSTEM.

(REPRODUCED BY KIND PERMISSION BUTTERWORTH SCIENTIFIC)

Stored images of the cervical and lumbar spines were subjected to anatomical marking using the electronic screen cursor and algorithms for determining angular positions of vertebrae were tried. Variations between observers using 10 measurements each of the angular position of a single lumbar vertebra were carried out using an image which was selected for its poor quality. The results (Table 1) suggested that the range of variation between mean measurements of the angular position of this single digitised image was 1.01 degrees across the five observers (SD 0.41).. The maximum range of variation seen was 2.14 degrees and related to one observer, whereas the minimum was 0.04 degrees.

TABLE 1

OBSERVER VARIATION IN 10 REPEATED ESTIMATIONS OF L3 ANTERIOR BODY  
ANGLE

Observer	1	2	3	4	5
Mean angle (degrees)	84.55	84.14	85.15	84.19	84.30
sd	(0.72)	(0.04)	(0.05)	(0.56)	(0.30)

#### 10.0 CALIBRATION OF SYSTEM FOR KINEMATIC MEASUREMENT

The use of a realistic calibration model was central to the rationale for this research. The previous studies which seemed most reliable were those which calibrated their measurement systems. Although comparatively few in number (31,44,49,172), they did confer credibility upon the systems in terms of their accuracy against a known standard. Essential to the testing of any system which will involve extrapolating kinematics from co-ordinates placed on images of vertebrae, is the use of reasonable representations of these from a calibration model. The use, for example, of ball bearings implanted in wood gives very clear definition in an image, but this does not represent the practical situation. If the edge of the vertebral body

is the chosen site for marking, is it more logical not to use such metal implants at all, but actual bony outlines?

If, as was done in the studies which follow, animal soft tissues are placed around the model when it is X-rayed, a close approximation to in vivo conditions in terms of image degradation should be achievable. It is also important that geometric distortion resulting from patient malpositioning can be incorporated in a realistic way. Therefore, it is necessary to obtain the true shape and radiographic consistency of vertebrae as well as universal movement between them.

#### 10.1 Development of the Calibration Model

The model used in these studies (Figures 22a and b), comprised two human lumbar vertebrae (L3 and L4) linked at the position of the centrum of the disc by means of a universal joint. Perspex pointers were fitted to the front and to one side of the body of the superior vertebra in such a way as to describe arcs whose centres corresponded to that of the universal joint. The measurement of these arcs was obtained from a protractor attached to the base of the model. This could be moved to either pointer, depending on which plane of rotation was being studied, and later included preset angles (using holes and pegs). The useful range of these protractors was 30°.

The base of the model rotated and also incorporated a protractor so that rotation about the vertical axis could be obtained. The model was thus suitable for the study of the accuracy of measuring rotation of a vertebra about its 3 axes. It was later to prove useful in the

study of translations along the x and z axes. Initially, however, the model was X-rayed in the anterior-posterior (A/P) and lateral projections using an object-to-intensifier distance of 1 metre, as would apply in the examination of patients.

## 10.2 Treatment of Scaling Error

Preliminary studies with the model (171) in determining rotations through  $20^\circ$  in the two planes also revealed a constant error of scaling. This derived from the rectangular arrangement of pixels on the computer's monitor and resulted in a uniform discrepancy which was dependent on the angle of rotation involved. This was initially resolved by using a digitised X-ray image of an aluminium disc of 10cm diameter (Figure 23). The disc was attached to the image intensifier to obtain this image and was produced with an array of slots in one quadrant at relative angles of 10 degrees.



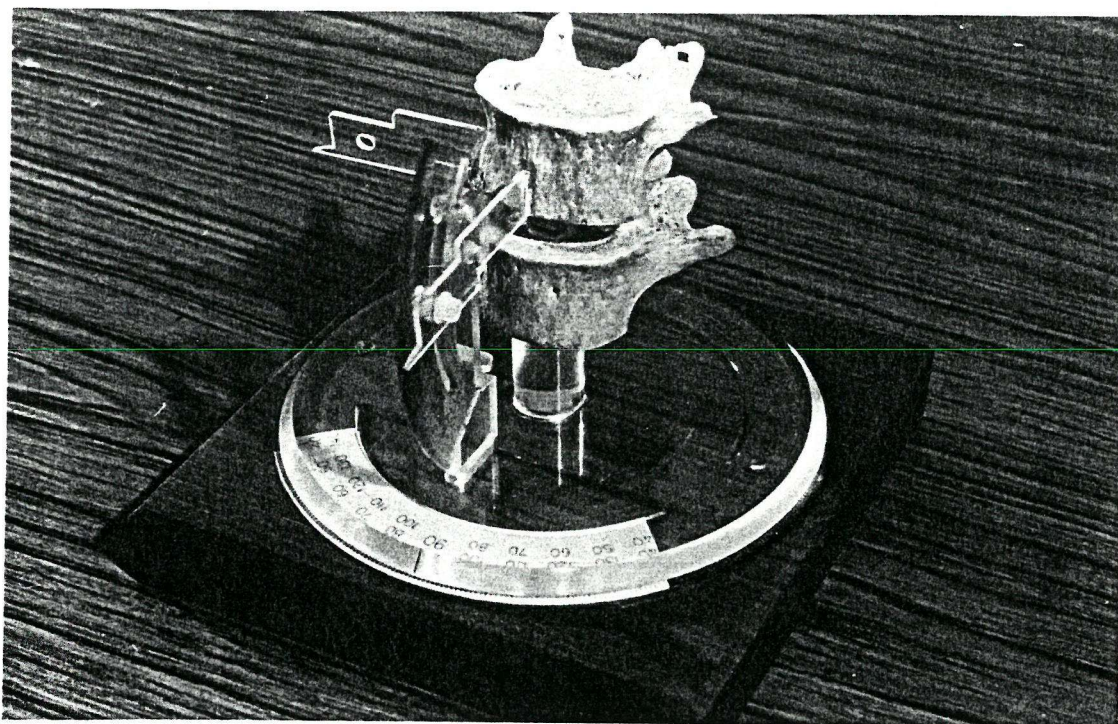


FIGURE 22a  
THE CALIBRATION MODEL SET UP FOR SAGITTAL PLANE MOTION

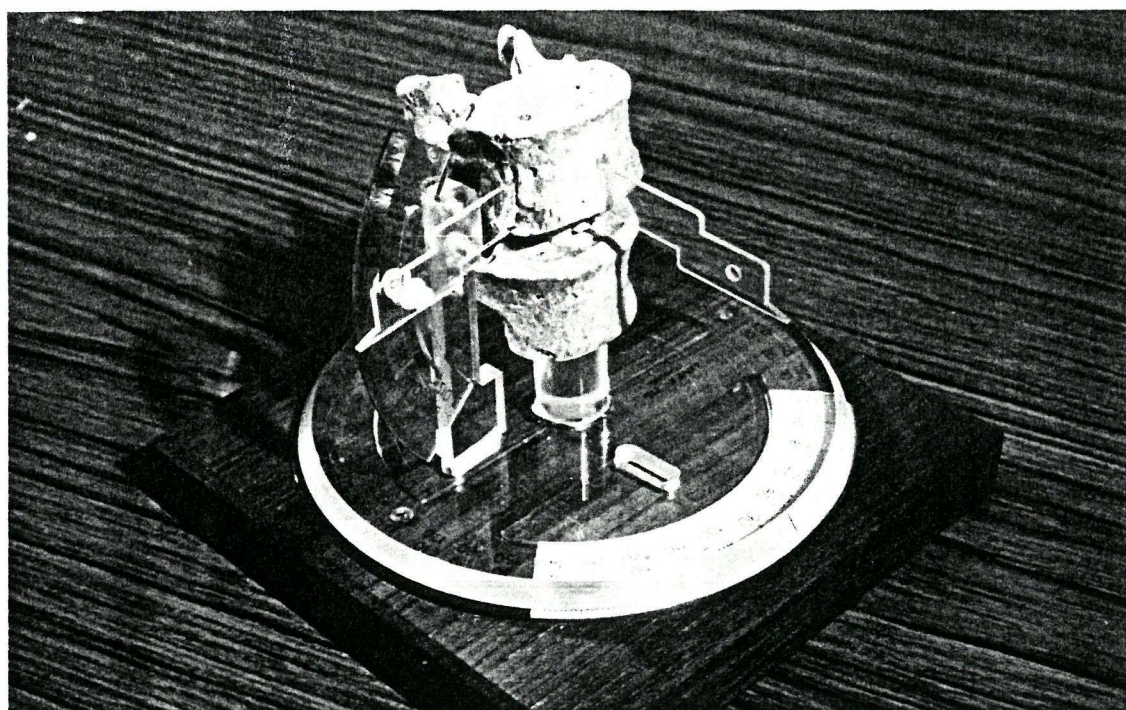
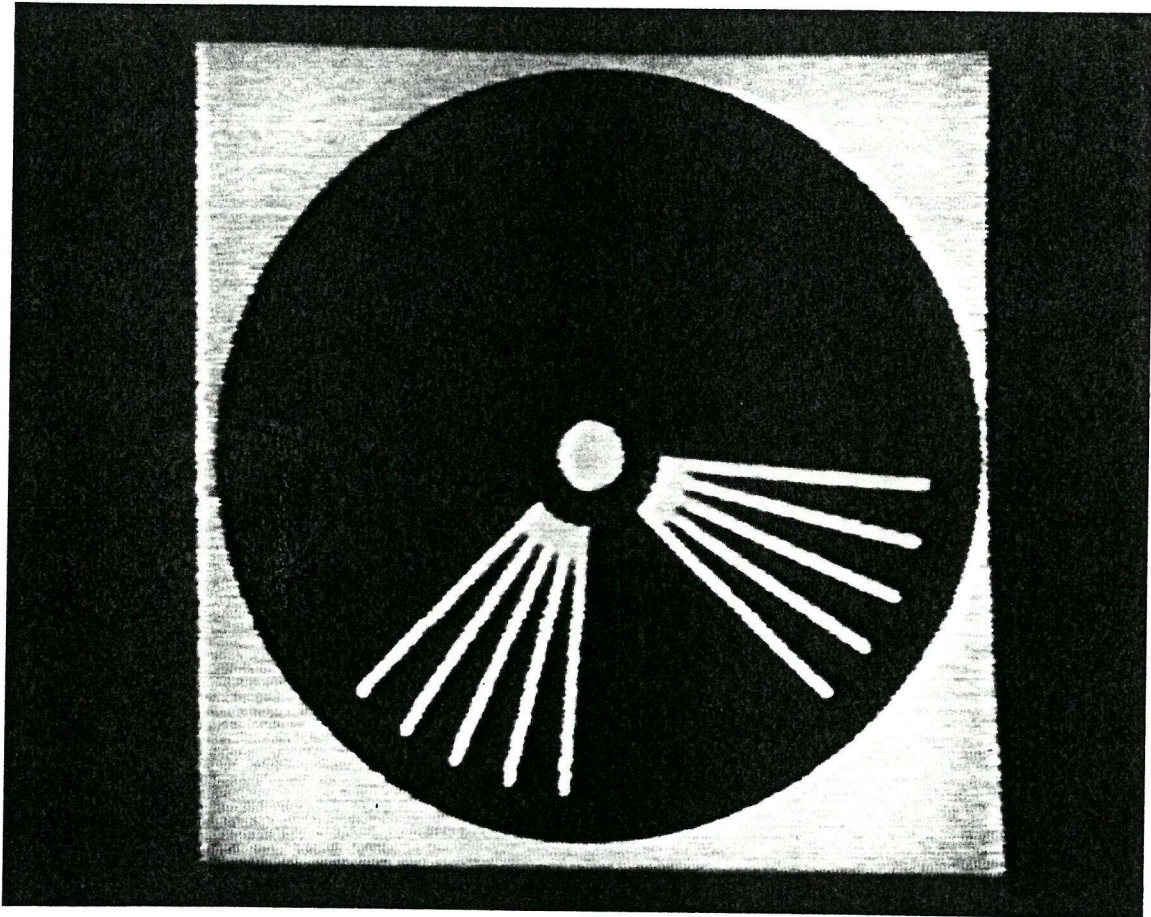


FIGURE 22b  
THE CALIBRATION MODEL SET UP FOR CORONAL PLANE MOTION



FIGURE 23

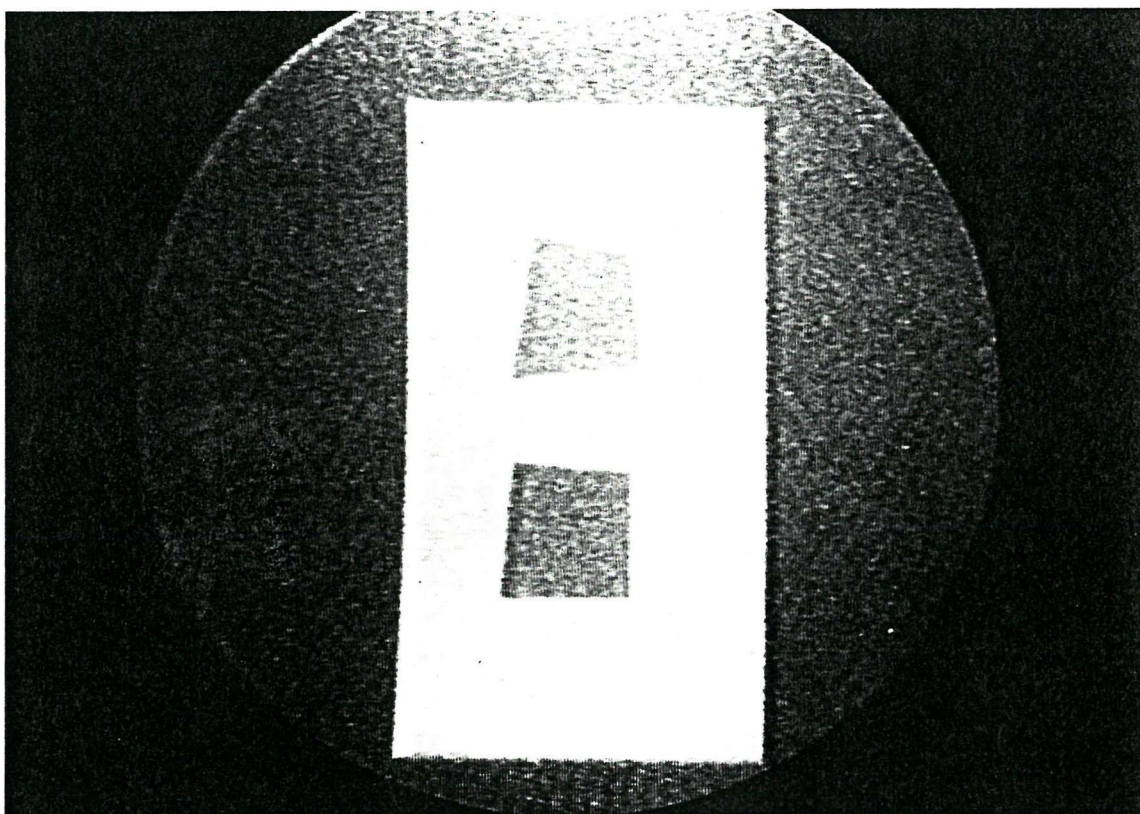


DIGITAL X-RAY IMAGE OF ALUMINIUM DISC  
FOR SCALING

When digitised, the image of the disc appeared elliptical and a scaling factor for the computer display was obtained by manipulating the image to produce the original circle. Using the aluminium disc, the distortion due to the rectangular arrangement of pixels on the computer display was calculated to be a factor of 1.48 between the horizontal and vertical axes.

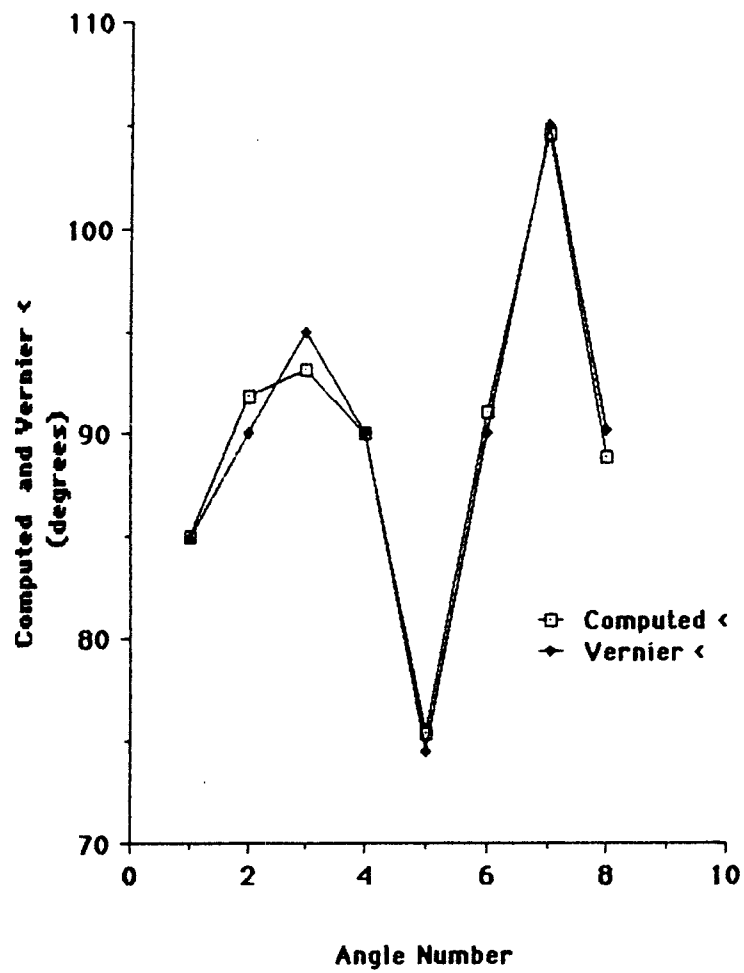
Despite satisfactory calibration for coronal and sagittal plane rotations, both with and without orthogonal alignment of the model, there was still some evidence of a slight, but persistent, scaling problem. In order to identify the scaling error more precisely, images of two aluminium plates, 5mm thick (Figure 24), were digitised. The angles subtended by their sides, as determined by the image processor from co-ordinates marked using the cursor, were compared with those obtained by vernier measurement of the plates themselves. A scaling factor was obtained from the best fit between the two sets of angles. Figure 25 illustrates the results of this procedure. This represented an adjustment of the x:y dimensions to the ratio of 1.65:1 and, for all further experiments, this scaling factor was used.

FIGURE 24



DIGITISED IMAGES OF ALUMINIUM PLATES USED  
IN SCALING STUDIES

FIGURE 25



GRAPH DEPICTING THE BEST FIT OBTAINED BY SCALING THE  
COMPUTER TO OBTAIN SIMILAR ANGLES TO THOSE  
SUBTENDED BY THE SIDES OF THE  
ALUMINIUM BLOCKS

## 11.0 THE QUANTIFICATION OF SAGITTAL PLANE MOTION

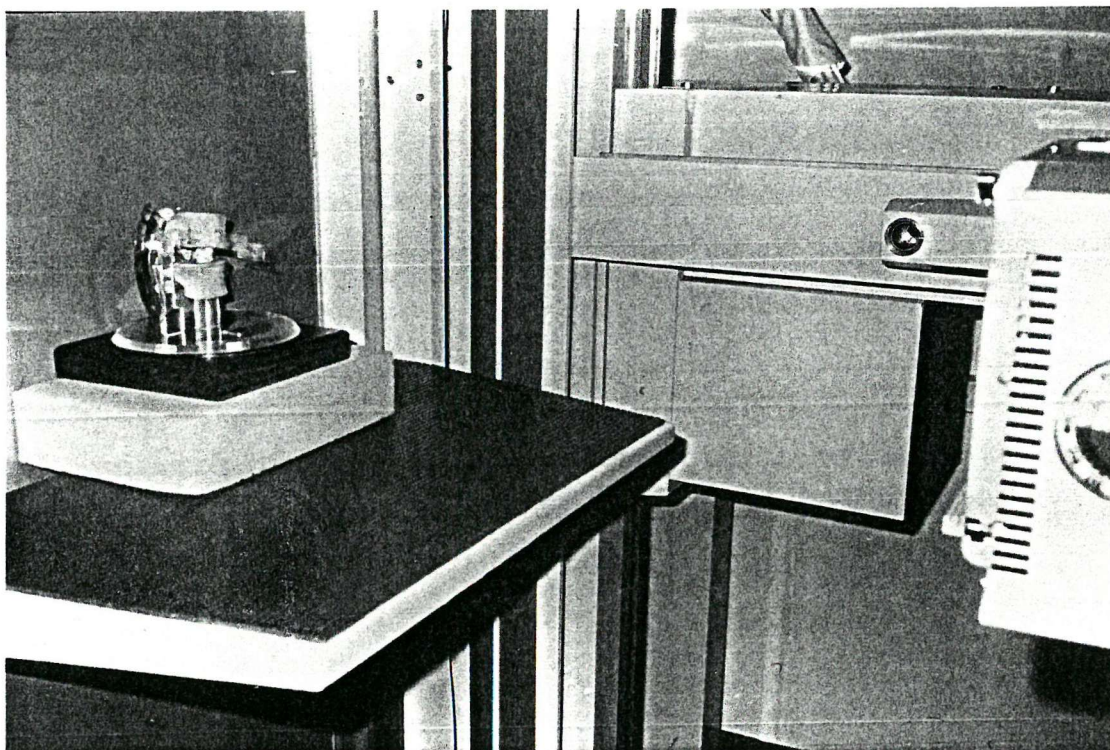
Vertebral images in this plane are obscured by fewer soft tissue shadows than those in the anterior-posterior projection where viscera are superimposed. Moreover, the effect of coupling is negligible (44). On the other hand, tissue density, being largely spinal musculature, is generally greater and this can result in poor delineation of the tissue-bone interface in obese or arthritic patients. Geometric distortion resulting from non-orthogonally aligned vertebrae is a further problem which affects all spinal X-rays. For these reasons, the choice of anatomical landmarks for co-ordinate placement has to be made in such a way as to minimise the effects of these and other sources of error.

### 11.1 Calibration Studies of Rotations

The calibration model was X-rayed in six 5-degree steps of flexion using a 1 metre focus-to-intensifier distance and a 12" object-to-intensifier distance to simulate clinical conditions (Figure 26). Recordings on to videotape were obtained for each protractor position and were digitised and marked in the image processing laboratory. The intervertebral angles obtained were compared with the protractor settings, the zero setting in the computed measurements being normalised to that of the protractor setting by the manual input of the latter.

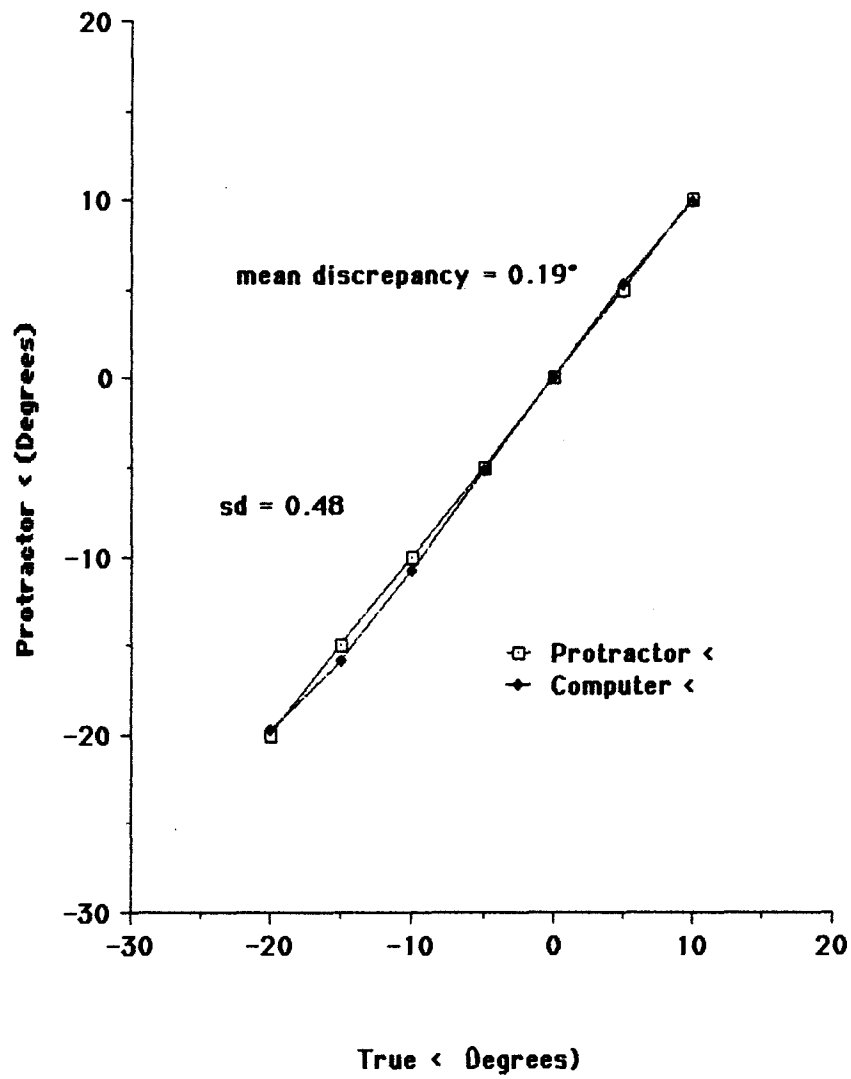


FIGURE 26



CALIBRATION MODEL IN POSITION FOR FLUOROSCOPY

FIGURE 27



GRAPH COMPARING PROTRACTOR AND COMPUTER  
ESTIMATIONS OF FLEXION-EXTENSION  
MOTION IN THE CALIBRATION  
MODEL



#### 11.1.1 Undegraded Images

The result of this experiment is shown in Figure 27. Two standard deviations of the differences between the computed and known positions over  $30^\circ$  of motion give an error of  $\pm 0.96$  (2SD). There is no apparent tendency for the lines on the graph to diverge, indicating the absence of the distortion due to scaling found in the preliminary studies.

#### 11.1.2 Degraded Images

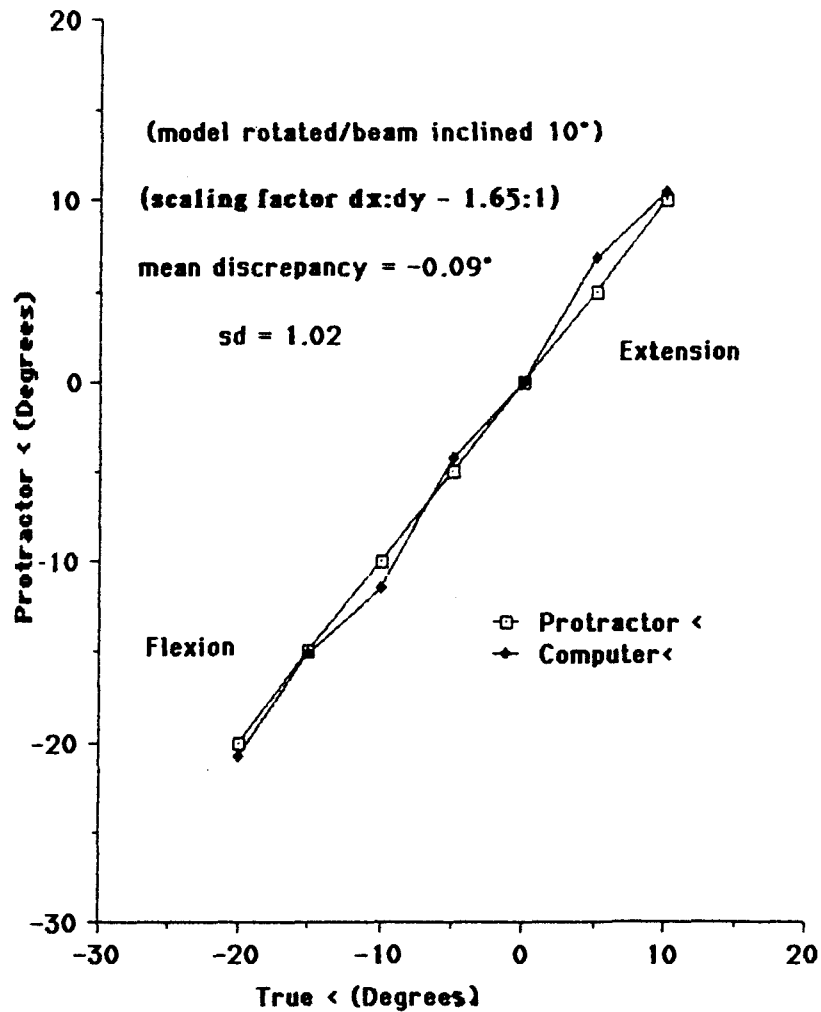
In order to simulate the effects of out-of-plane alignments, the model was rotated by  $10^\circ$  and the X-ray tube was inclined downwards by the same amount. In addition, to produce soft-tissue X-ray scatter, pieces of animal soft tissue 10cm thick, were placed immediately in front of the model. Using this arrangement, images were obtained of the seven positions as before (Figure 28). The results, seen in Figure 29, suggest that such degradation of the images does have some detrimental effects, in this case increasing the 2SD error to  $\pm 2.04$  degrees.

FIGURE 28



CONTRAST-EXPANDED AND MAGNIFIED IMAGE OF THE  
CALIBRATION MODEL IN THE LATERAL PROJECTION  
WITH SOFT TISSUE SCATTER AND POSITIONAL  
DISTORTION, MARKED FOR DETERMINATION  
OF INTERVERTEBRAL ANGLE

FIGURE 29



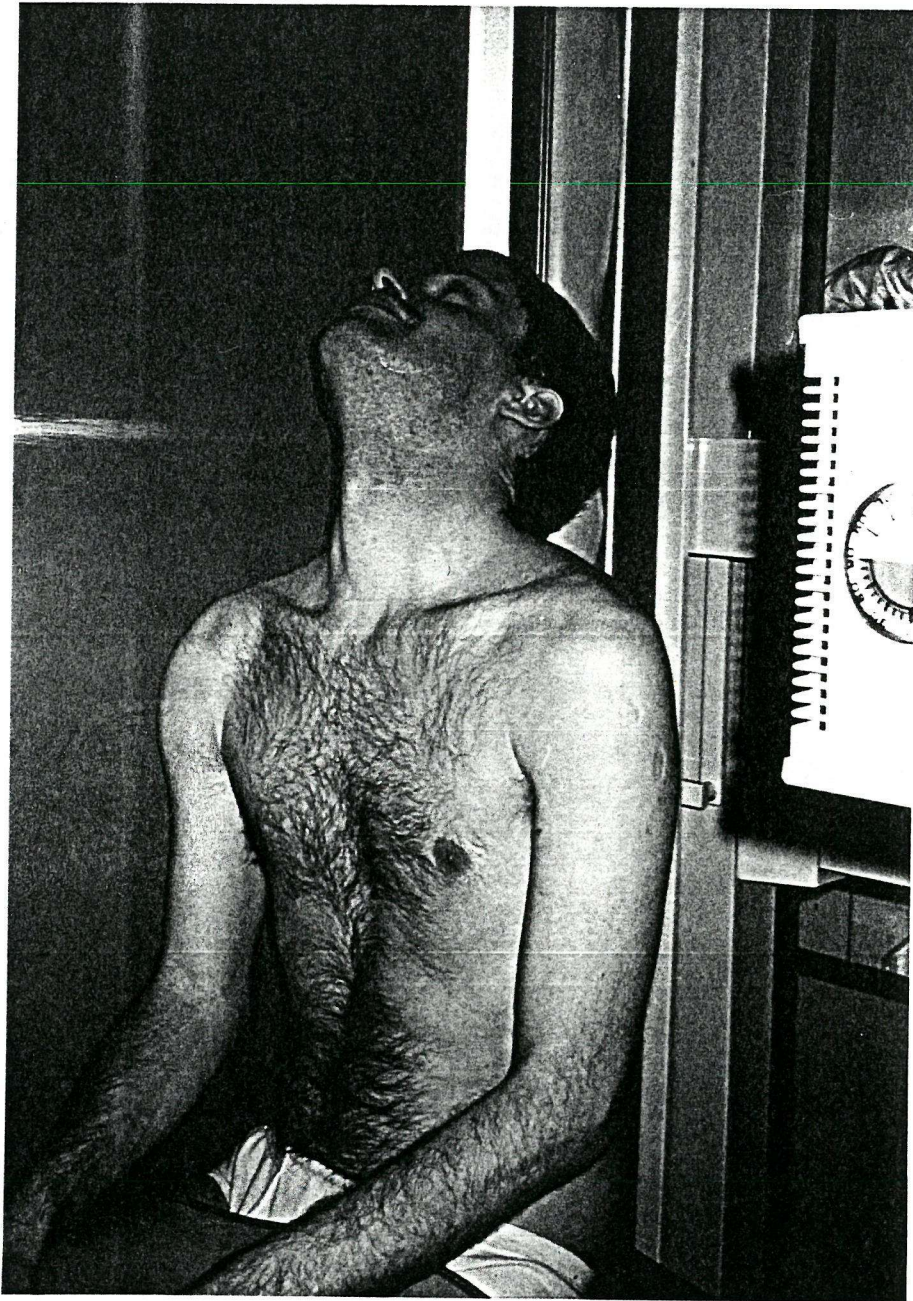
GRAPH COMPARING PROTRACTOR AND COMPUTER ESTIMATION OF FLEXION-EXTENSION AS IN FIGURE 27 BUT INCLUDING THE INFLUENCE OF SOFT TISSUE SCATTER AND POSITIONAL DISTORTION

## 11.2 Studies of Rotations in Human Volunteers

Local Medical Ethics Committee approval was obtained for the X-raying of volunteer subjects using this system. Each subject was male, aged between 24 and 54 years. Of primary concern was the acquisition of a full range of motion with the minimum of exposure time. During the preliminary studies, the radiographic procedure for doing this became established as essentially a two-stage recording. For the lumbar spine, subjects were asked to sit on the stabilising frame, as described in section 8.1, keeping their buttocks in contact with the frame. For the cervical spine, the movement was unconstrained, stabilisation being limited to an instruction to keep the shoulder in firm contact with the table (Figure 30). They then practised full forward bending over a time of approximately 6 seconds. When this could be seen to be operating comfortably in the position which would be needed for recording, a few seconds of exposure were used for alignment, followed by X-raying of the motion required. This procedure was then repeated for spinal extension. The results provided about 12 seconds of videotaped motion of an area of 9" diameter, centred around a segment of interest. In the image processing laboratory, the sequence was timed and the computer set to sample 16 frames throughout the motion sequence. This provided two files. The angles between all accessible vertebrae were measured simultaneously for each frame, using the same procedure as in the calibration studies (section 11.1). The intervertebral angles obtained for the neutral position were normalised and the results for the two files amalgamated to provide a series of angles from flexion to extension.



FIGURE 30



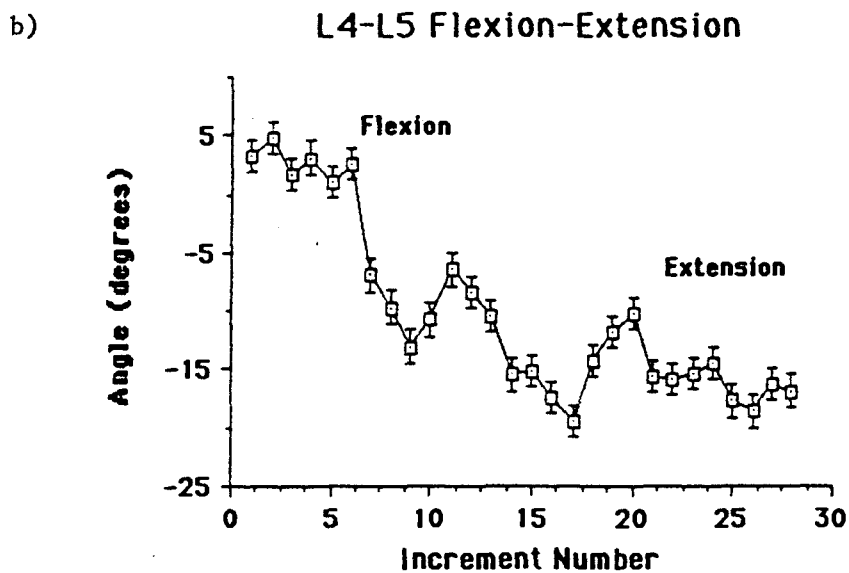
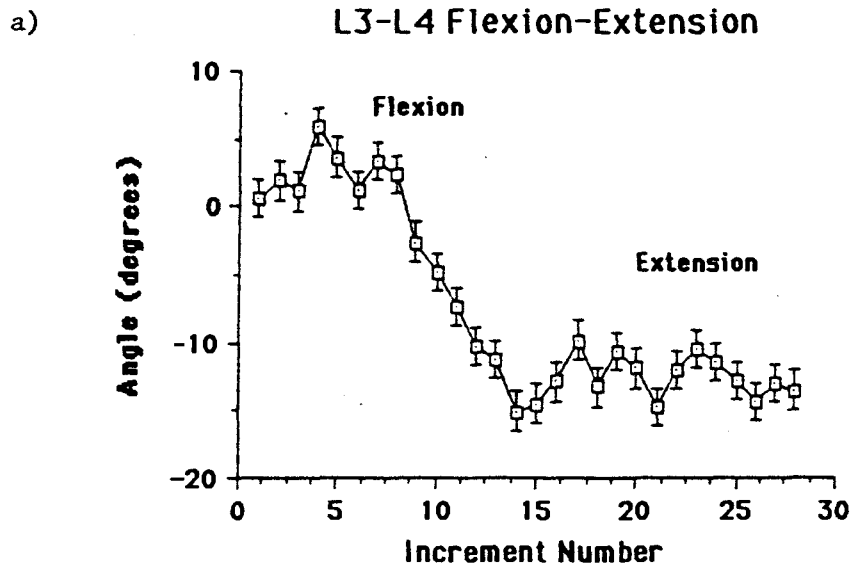
SUBJECT EXTENDING CERVICAL SPINE WHEN  
POSITIONED BESIDE INTENSIFIER

### 11.2.1 The Lumbar Spine

Examples of this description of motion in one male volunteer at L3-4 and L4-5 are shown in Figure 31 a and b. The error bars represent +/- the 2SD error found in the calibration studies of degraded and positionally distorted images.

It can be seen that the flexion component of the motion (ie from increment number 15 to 0) seems to reverse towards the extreme of this range (ie at increment numbers 4-0) for the L3-4 level (Figures 31a), but not at the L4-5 level (Figure 31b). This, at present can only be regarded as a curiosity since the sample is not representative. Nevertheless, there are possible explanations in terms of muscle and disc dynamics.

FIGURE 31



GRAPHS OF LUMBAR SPINE SAGITTAL PLANE ROTATION AT TWO SEGMENTAL LEVELS IN A VOLUNTEER SUBJECT

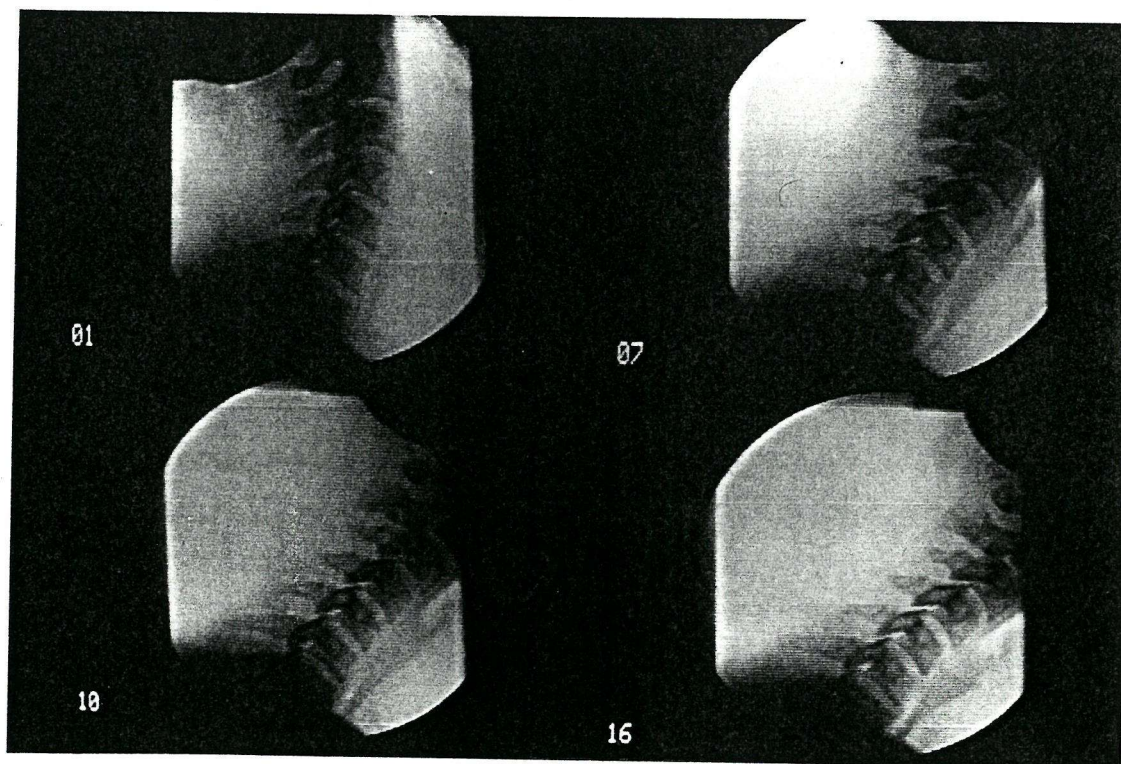
### 11.2.2 The Cervical Spine

An example of the images used for measuring sagittal plane motion in the neck can be seen in Figure 32. These images were enlarged by a factor of 2 prior to measurement, in an attempt to reduce the error to a scale obtained with the calibration model. An example of the results for a series of levels in one subject is shown in Figure 33. The interobserver variation for determining one intervertebral angle in this subject was  $\pm 1.45$  (2SD). This is greater than the calibration error for undegraded images (see section 11.1.1) and it is recommended that the greater of the two be used when reporting.

Presenting results in this way allows the clinician to compare each segmental motion sequence in terms of range, regularity and timing of the greatest and least rapid changes. Viewing videotape does not provide this; nor, in the case of suspected pathological motion, does any other current method of objective measurement.

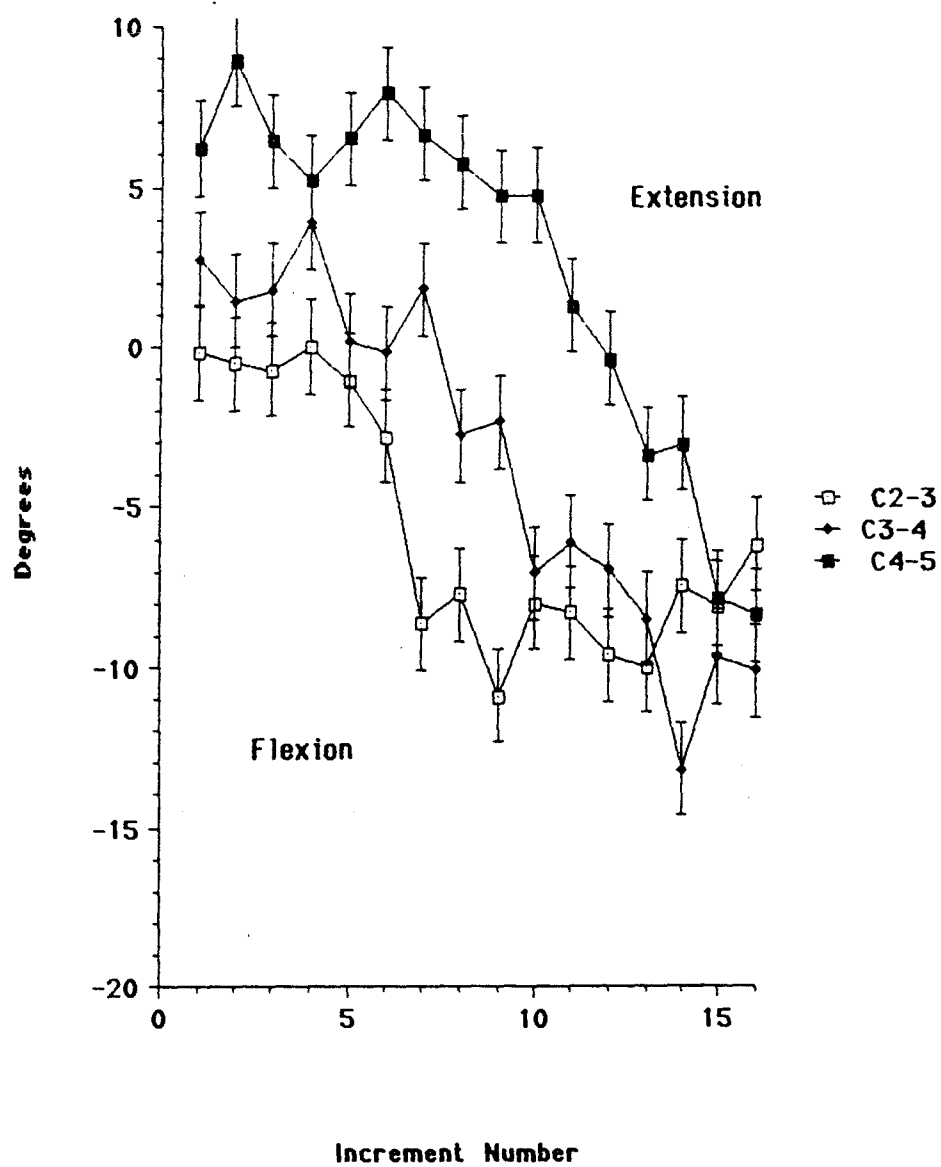


FIGURE 32



CERVICAL SPINE IMAGES USED FOR DETERMINING  
SAGITTAL PLANE MOTION

FIGURE 33



GRAPH OF CERVICAL SPINE SAGITTAL PLANE ROTATIONS  
AT THREE SEGMENTAL LEVELS (ERROR BARS  
REPRESENT +/- 2SD OF INTRA-OBSERVER  
VARIATION)

### 11.3 Translations in the Sagittal Plane

A number of methods have been used to measure sagittal plane translation in the lumbar spine by direct measurement from two plain X-rays representing the extremes of joint range. These have been evaluated by Shaffer et al (172). Essentially, the main difficulty with such evaluations is their low inter-observer reliability which results from the small range of motion involved. For this reason, direct measurement of translation using digital videofluoroscopy (DVF) was only used for comparison with the technique used in this study which was by locus of ICRs throughout the motion range, the maximum diameter of which has been reported for intact cadaveric vertebral motion segments at about 23mm (79).

#### 11.3.1 Calibration Studies of Translations

By using digitised images of the calibration model from the studies of rotations in the sagittal plane, and an algorithm devised for its calculation which incorporated a rigid-body constraint (173), the location of the ICRs in a variety of rotational increments was determined. This involved marking, by screen cursor, of the end-plates of the two vertebrae in such a way as to minimise the errors identified by Panjabi (49) (Figure 34a). The centre of the universal joint defined the actual ICR for all increments and the mean location error and intraobserver variation (based on 10 observations) could be illustrated for each increment as shown in (Figure 34b).



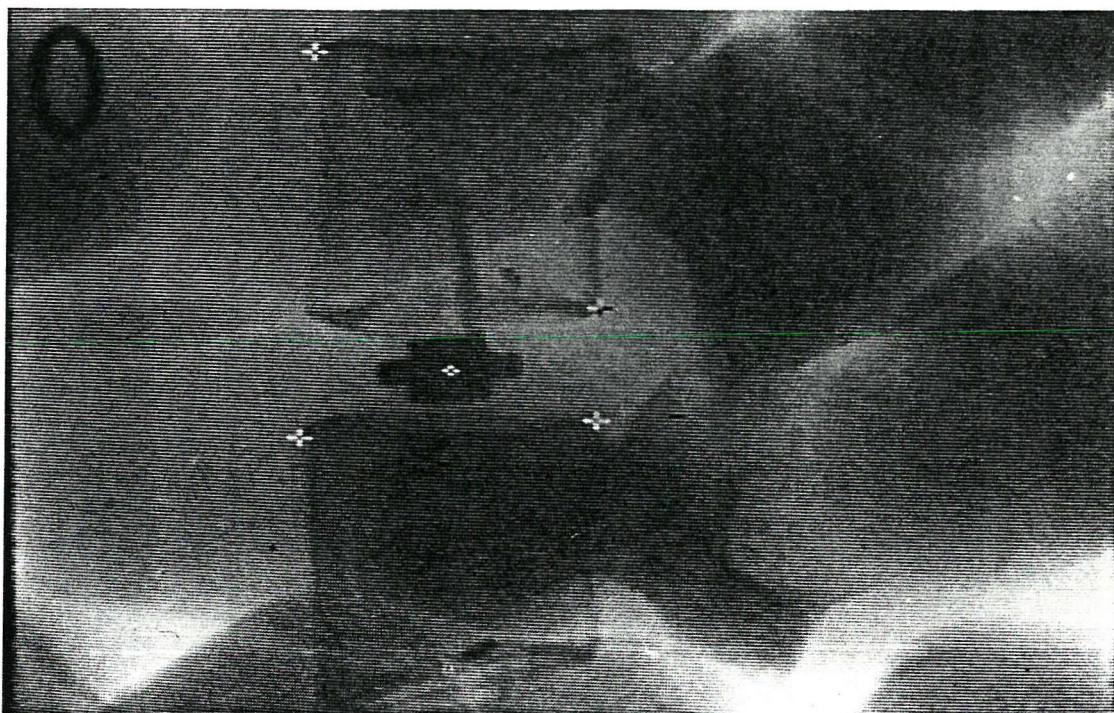


FIGURE 34a

LATERAL IMAGE OF LUMBAR SPINE CALIBRATION MODEL WITH VERTEBRAE  
MARKED FOR CALCULATION OF ICR LOCATION

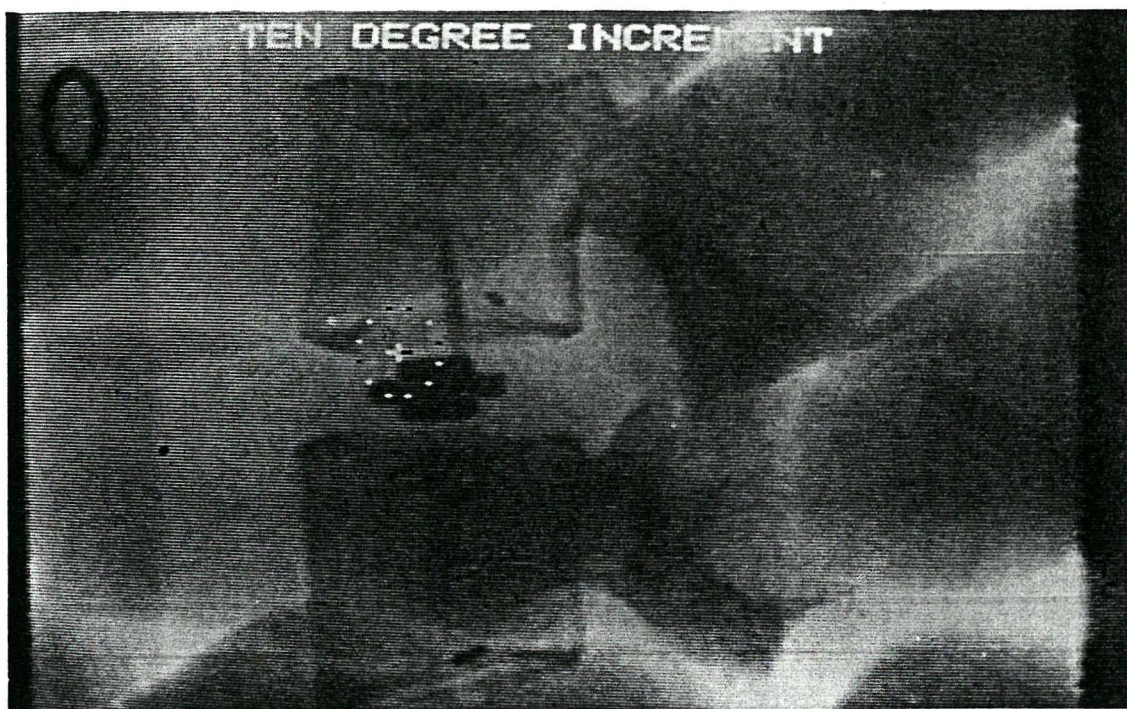


FIGURE 34b

MEAN LOCATION ERROR (CROSS) AND INTER-OBSERVER VARIATION  
(CIRCLE OF RADIUS  $2SD_{xy}$ ) OF ICR LOCATION FOR A  $10^\circ$   
INCREMENT

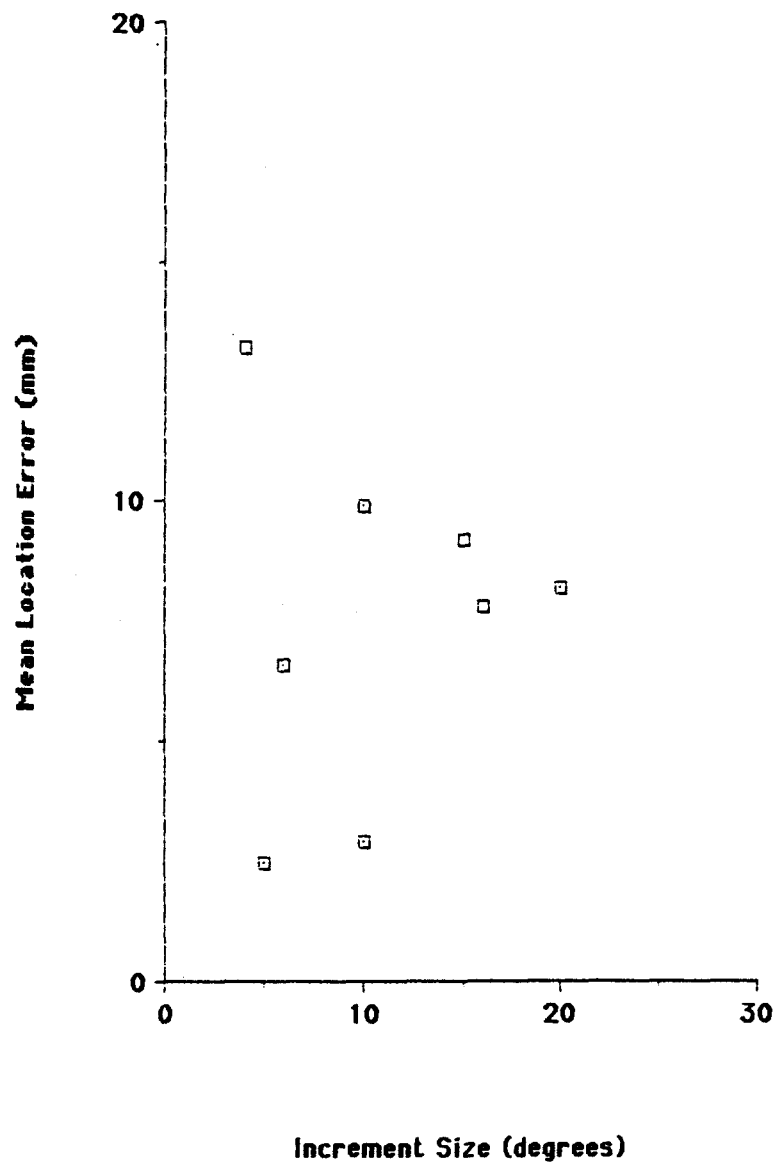
#### 11.3.1.1 Accuracy

The accuracy of the system in determining ICR locations in terms of the calibration model in the sagittal plane is summarised in Figure 35, for increments from  $4^{\circ}$  to  $20^{\circ}$ . The conversion from pixels to millimeters is to illustrate the error which could be expected in relation to the width of a vertebral body (about 30mm) and in order to illustrate a "worst case" result, the plot represents consecutive measurements by two independent observers which were not averaged. The results are the first known attempt to calibrate for ICRs in spinal joints but they do closely resemble the anticipated scatter predicted from mathematical theory by Spiegelman and Woo (124).

#### 11.3.1.2 Precision

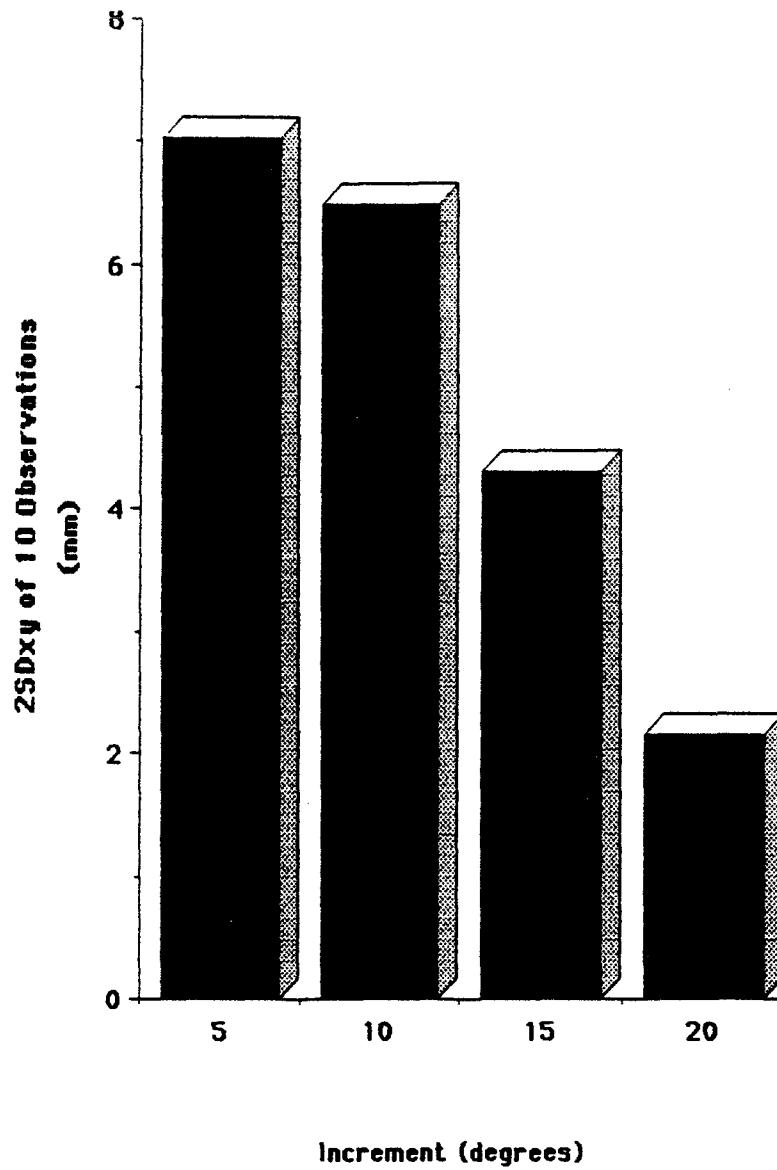
The ability to locate the ICR repeatedly in the same place is also an important feature of reliability. This has been investigated for sagittal plane lumbar spine X-rays in human subjects by Pearcy and Bogduk (170). The 2SD variation from ten consecutive observations by a single observer, again in millimetres, is shown in Figure 36. In general, therefore, to the extent that the calibration model represents what would happen in life, an increment of less than  $5^{\circ}$  could produce an error of 14mm ( $\pm 2SD$ ), which represents about 60% of the norm for centre length (about 23mm) identified from cadaveric studies. In all probability, therefore, where rotation is less than about  $5^{\circ}$ , the detection of translation using ICR is inadvisable.

FIGURE 35



SCATTERPLOT SHOWING THE MEAN LOCATION ERRORS OF  
SAGITTAL PLANE ICR LOCATIONS FOR A  
VARIETY OF INCREMENT SIZES

FIGURE 36



BAR GRAPH SHOWING THE INTRA-OBSERVER VARIATION OF  
ICR LOCATIONS IN THE CALIBRATION MODEL IN THE  
SAGITTAL PLANE FOR A VARIETY OF INCREMENT  
SIZES

#### 11.4 Studies of Translation in Human Volunteers

The repeatability of ICR location in the spines of volunteer subjects with no history of spinal troubles was investigated by performing 10 ICR estimations for a variety of rotational increments. These estimations employed samples of the digitised images used for the studies of rotations (Sections 11.2.1 and 11.2.2). This was done for both the cervical and lumbar spines in order to compare results with those found using the calibration model.

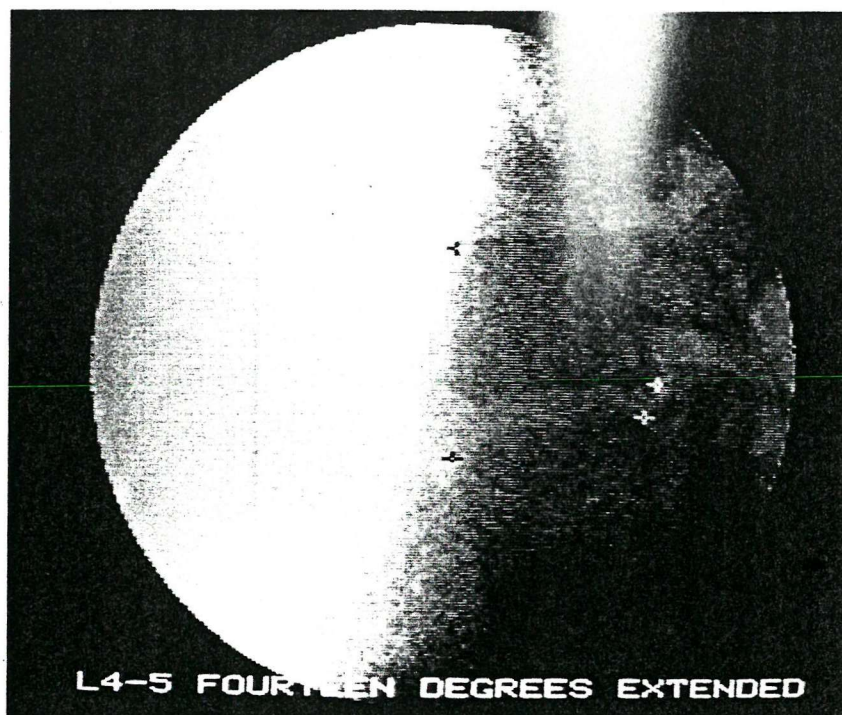
##### 11.4.1 The Lumbar Spine

Subject 1.

Figure 37a shows an image of one of the subjects with cursor marks for the determination of ICR between the 4th and 5th lumbar vertebrae. Figure 37b shows the scatter of observer variations (2SD in x and y) according to the size of increment used. This example was of a young male subject whose rotational range at this level and in this plane was high ( $26^\circ$ ). The scatter plot displays the same features for repeatability as was found in the calibration studies and suggests that this was not an unreasonable estimate of the in vivo situation. Despite this, the magnitude of the variation for small angles of rotation is greater, suggesting that  $7^\circ$  would be a more realistic minimum rotation to be aimed for.



a)



b)

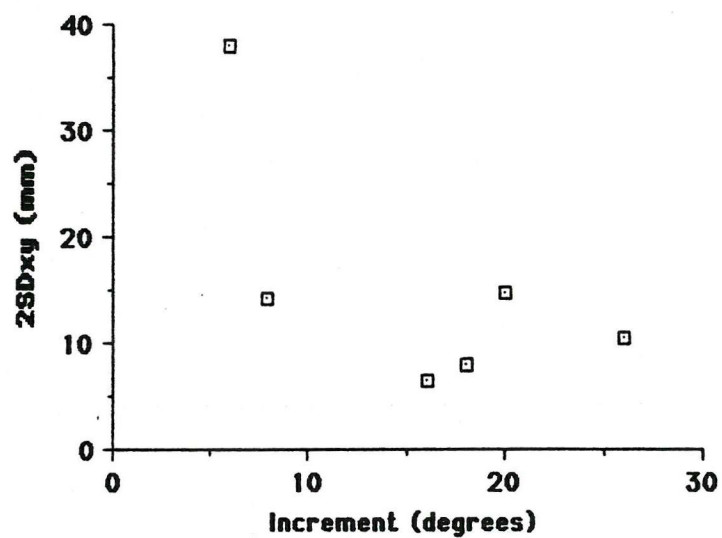


FIGURE 37

a) LATERAL IMAGE OF THE LUMBAR SPINE IN A HUMAN VOLUNTEER (SUBJECT 1)  
MARKED FOR THE CALCULATION OF ICR LOCATION AT L4-5

b) SCATTERPLOT OF OBSERVER VARIATIONS OF ICR LOCATIONS FOR A VARIETY  
OF INCREMENT SIZES FOR SUBJECT 1

Subject 2.

A similar experiment was performed with a second asymptomatic subject who had a more typical range of motion at the same vertebral level. The results of this can be seen in Figure 38a and b. Despite the differences (albeit subtle) in the images, the relationship between observer variation and increment size remains consistent.

Using the same subject and vertebral level, a plot of ICRs was obtained using 5 increments, each of  $7^\circ$  or greater, throughout the motion sequence from flexion to extension (ie clockwise rotation of L4). The motion increments overlapped so that some represented part of flexion, some the transition through the neutral position and some the extension component of the motion. The results, shown in Figure 39, reveal that the positions of the ICRs, from A to E, throughout the motion, descend as extension progresses. ('O' represents the overall motion). This is consistent with some translation during extension which, measured on the screen by direct methods, was about 4mm. This can presumably be regarded as a "normal" mechanical situation since the ICR locus is similar to that found in intact cadaveric spines investigated using Moire fringes attached to the vertebrae (Gertzbein et al (121)).

a)



b)

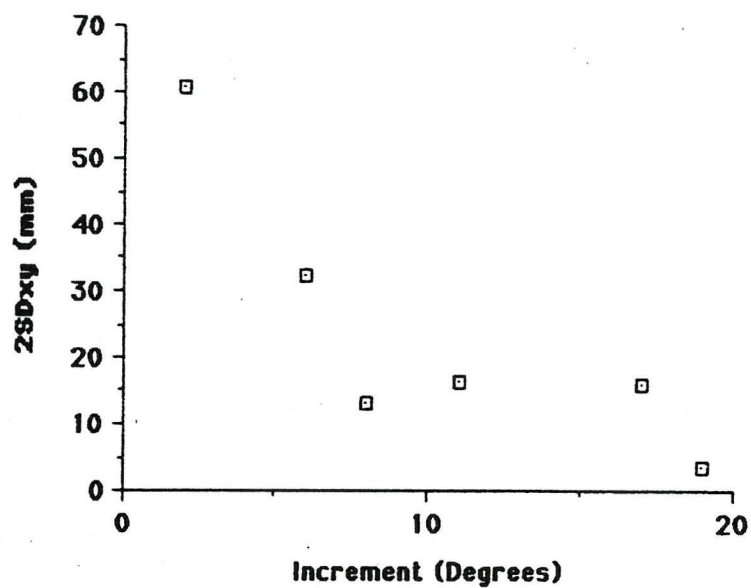


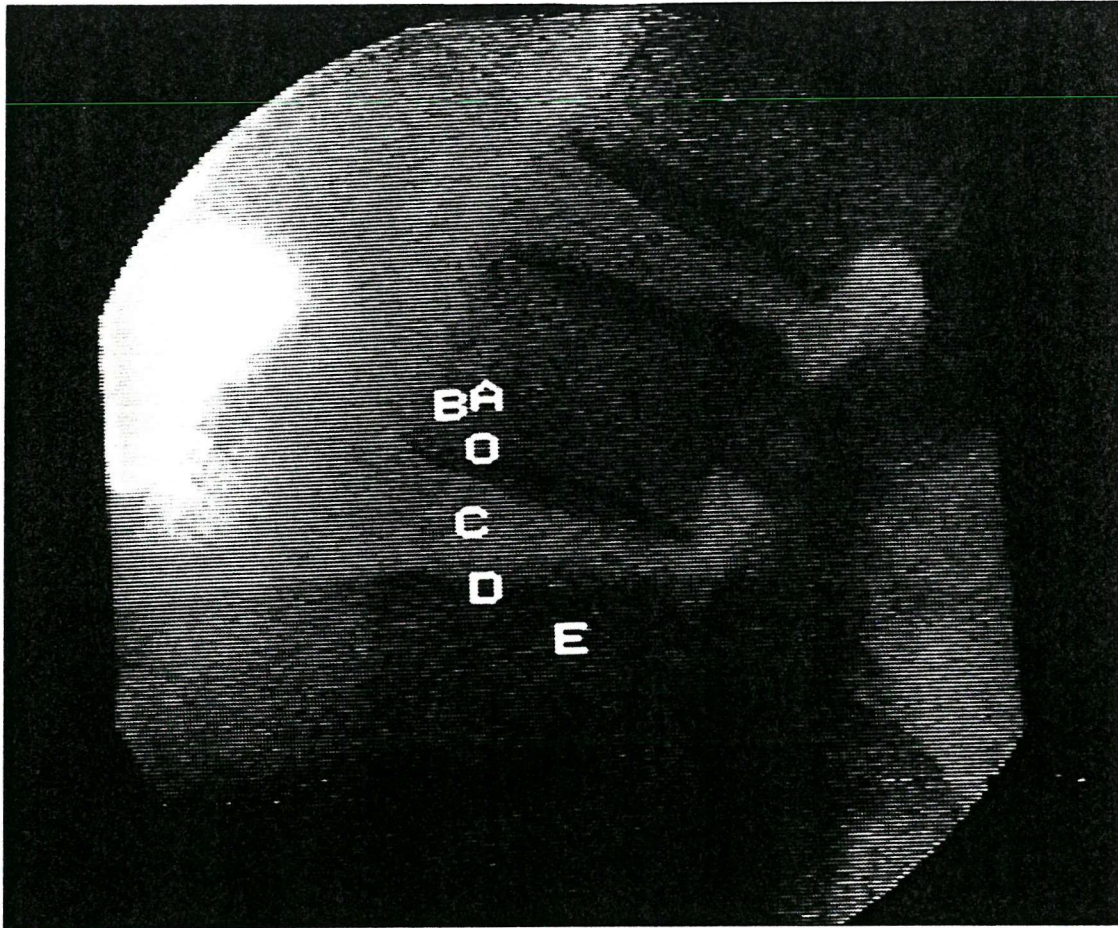
FIGURE 38

a) LATERAL IMAGE OF THE LUMBAR SPINE IN A HUMAN VOLUNTEER (SUBJECT 2)  
MARKED FOR THE CALCULATION OF ICR LOCATION AT L4-5

b) SCATTERPLOT OF OBSERVER VARIATIONS OF ICR LOCATION FOR A VARIETY  
OF INCREMENT SIZES FOR SUBJECT 2



FIGURE 39



LOCUS OF ICR LOCATIONS (A TO E) FROM FLEXION TO EXTENSION  
AT L4-5 IN SUBJECT 2

#### 11.4.2 The Cervical Spine

Penning (174) used ICRs to study sagittal plane translation in the cervical spine and Amevo, Worth and Bogduk (77,78) studied the effects of varying X-ray marking techniques on observer agreement. Although theoretically possible in the sagittal plane, the smaller image geometry may be expected to increase errors. To test the repeatability of this technique in the neck, therefore, a motion sequence in an asymptomatic volunteer was used. Analysis of this file was also carried out with the images enlarged by a factor of 2 to test the effects of image enlargement on repeatability of ICR location. Thirteen motion increments of various sizes at C4-5 were used, the largest being 17°. Ten ICR calculations were made for each increment and the variation in millimetres (2SDxy) was calculated.

Figure 40a and b show examples of the images before and after enlargement and their circles of observer variability for an 11° rotational increment at C3-4. The results are perhaps slightly better than for the lumbar spine and this may reflect better image quality in a less dense part of the body. However, this is unrepresentative and can, at this stage, only serve as an example of the variations in these particular individuals.

a)



b)

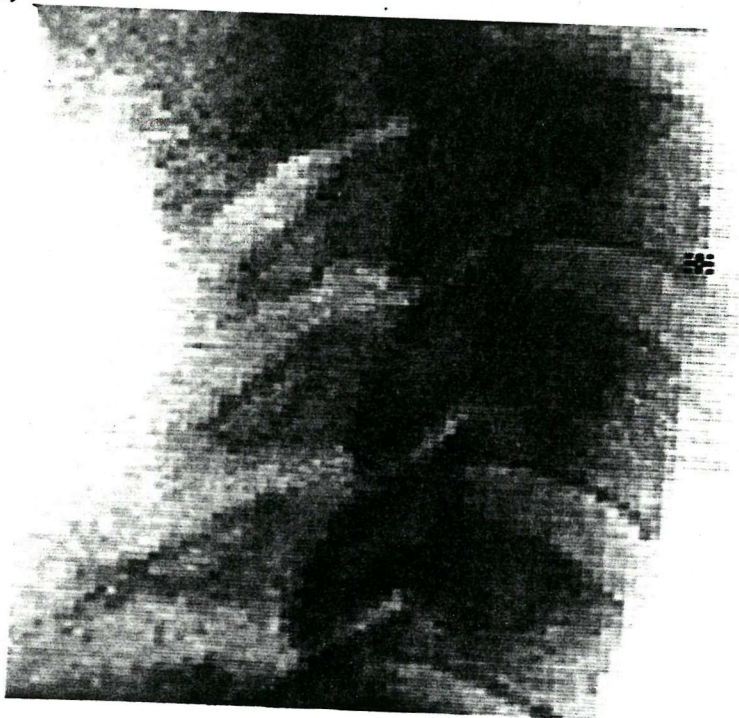


FIGURE 40

- a) UNENLARGED LATERAL CERVICAL SPINE IMAGE WITH MEAN ICR LOCATION  
AND 2SDx AND y ELLIPSE OF INTRA-OBSERVER VARIABILITY FOR  
10 ICR OBSERVATIONS AT C3-4
- b) AS 40a BUT USING A 2x ENLARGED IMAGE



## 12.0 THE QUANTIFICATION OF CORONAL PLANE MOTION

Coronal plane, or sidebending motion in the spine is coupled, by virtue of the alignment of the two posterior joints, with axial rotation. This effect is enhanced by weightbearing (175,176) and is most marked in the mid-cervical and mid-lumbar spines. In the lumbar spine, marking of the vertebral body corners is relatively unencumbered by unclear outlines given optimal radiography, but the influence of axial rotation means that the corner chosen is a rotating rim and not an anatomical point. Possibly it is for this reason that few previous researchers have chosen to mark vertebrae in this projection. As with sagittal plane motion, non-orthogonal alignment of the vertebrae is a problem, increasing geometric distortion and rounding the corners of the vertebral bodies to make reproducible marking difficult.

### 12.1 Calibration Studies of Rotations

Vertebral rotations in the coronal plane vary widely in range from  $1^{\circ}$  or  $2^{\circ}$  to  $20^{\circ}$  and more. The accuracy of their measurements is, therefore, fundamental to deciding the extent to which they can be used in clinical practice. As before with the sagittal plane studies (Section 11.0),  $30^{\circ}$  of sidebending motion in the calibration model was studied in  $5^{\circ}$  steps using the same radiographic set-up and video frame sampling procedure. The landmarks chosen were the corners of the adjacent vertebral end-plates (Figure 41).

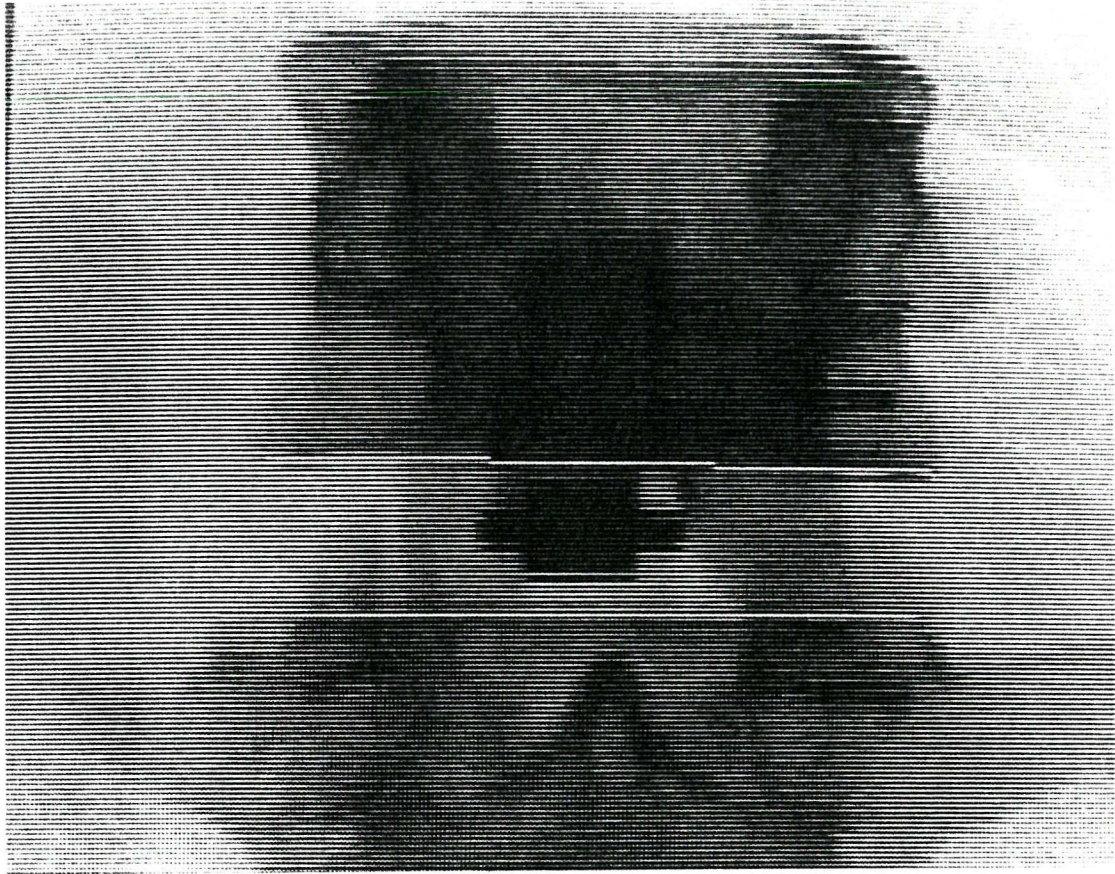
#### 12.1.1 Undegraded Images

The calibration model images were first obtained with purely coronal

plane rotation and the results, with the zero computed angle normalised to that of the protractor setting as before, can be seen in Figure 42. The standard deviation of the differences between computed and protractor readings were less than for the undegraded sagittal plane images, possibly because the length of the line generated is greater in this projection by virtue of the elliptical shape of the vertebral end-plates.

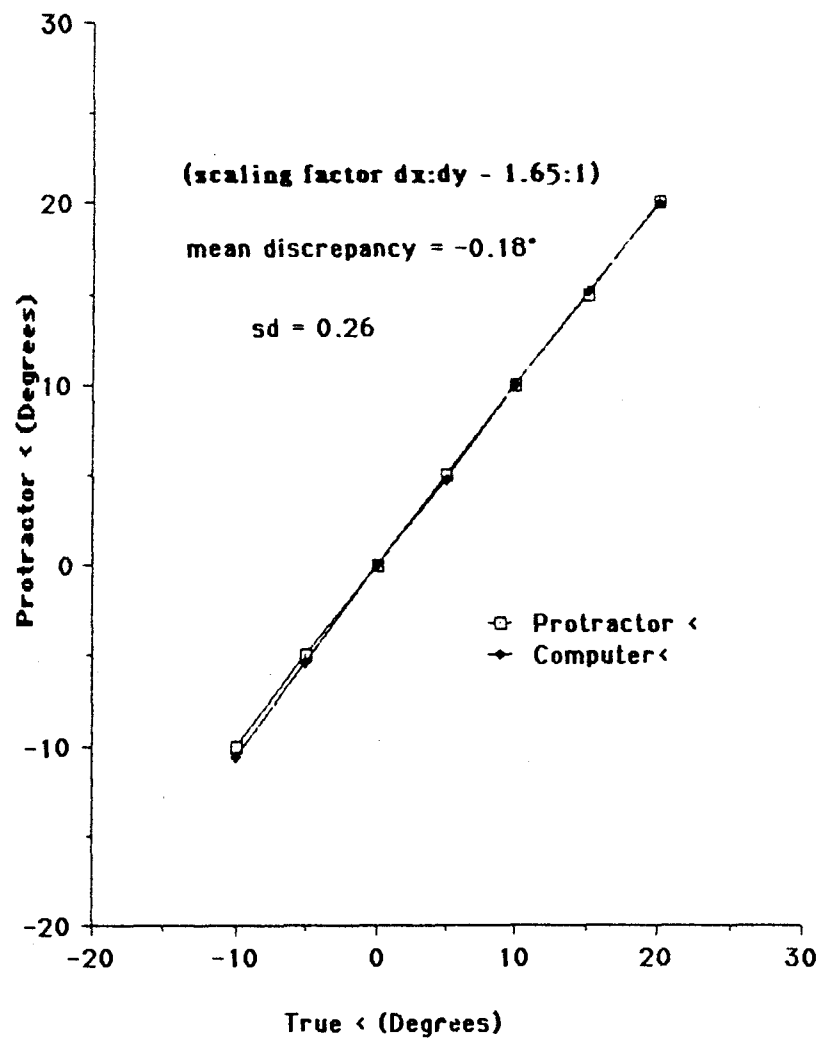


FIGURE 41



CALIBRATION MODEL (UNDEGRADED) MARKED FOR THE DETERMINATION  
OF CORONAL PLANE ROTATIONS

FIGURE 42



GRAPH COMPARING PROTRACTOR AND COMPUTER  
ESTIMATIONS OF LATERAL BENDING IN THE  
CALIBRATION MODEL

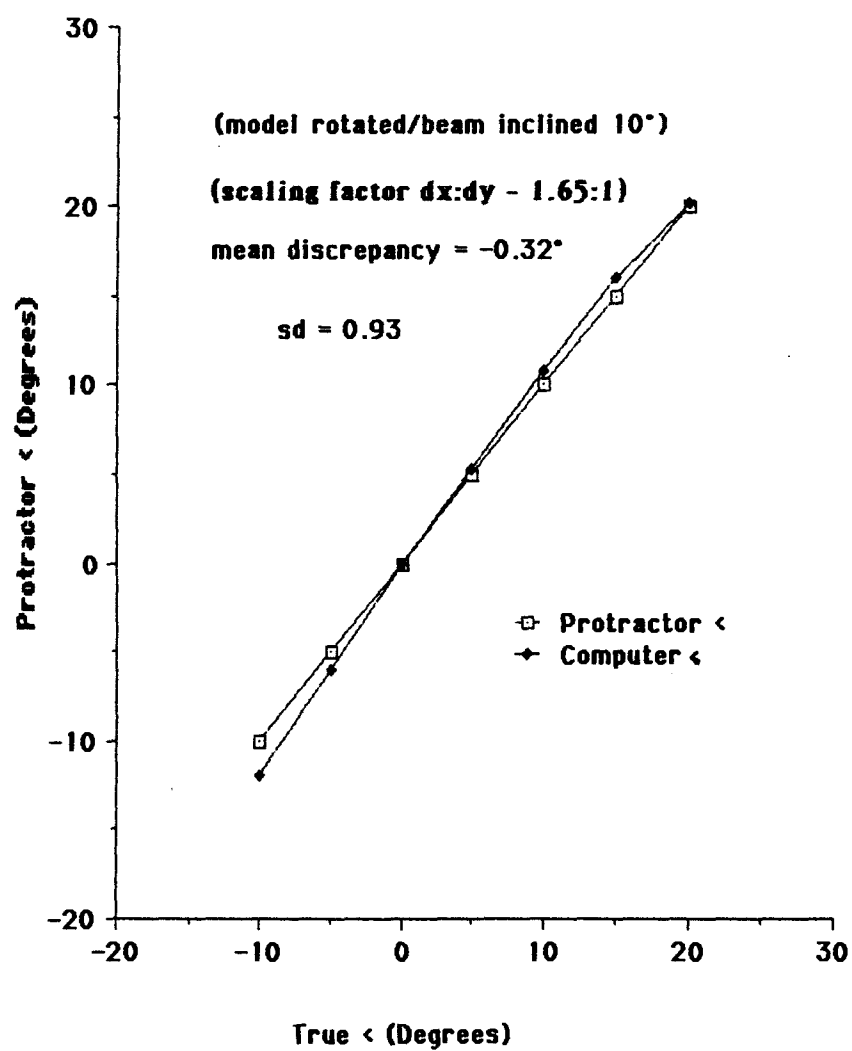
#### 12.1.2 Degraded Images

The effects of including  $10^\circ$  model rotation and X-ray tube inclination with interposed soft tissue as before are shown in Figure 43. At the 96% level, an error of  $\pm$  nearly  $2^\circ$  shows the necessity of keeping degrading effects low.

#### 12.1.3 In Vivo Simulation

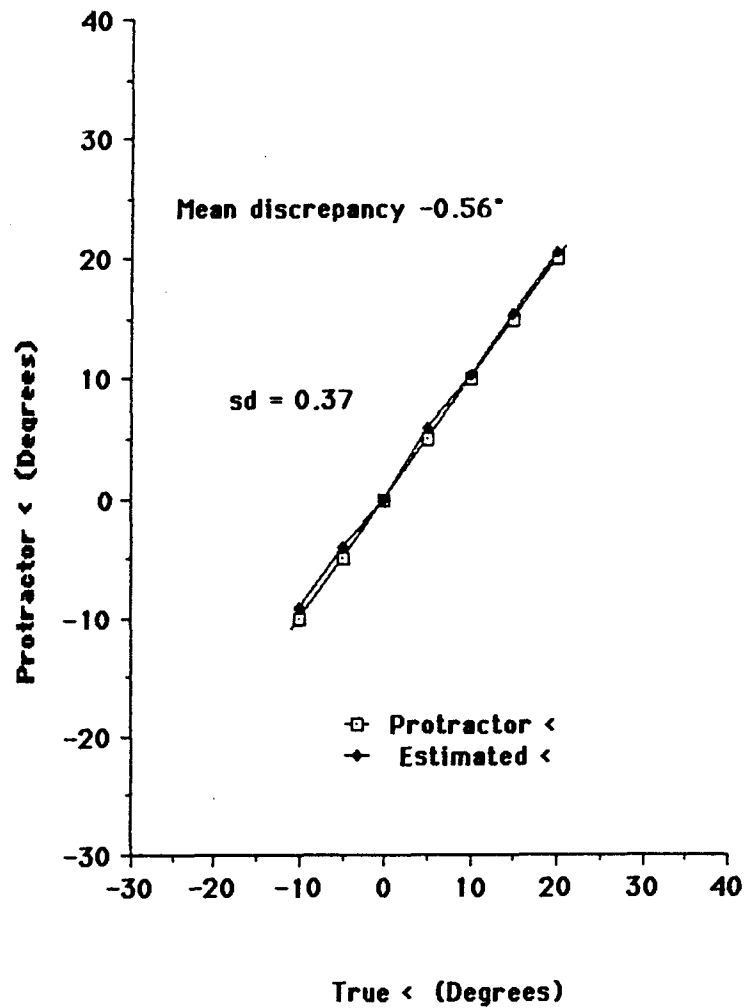
To simulate in vivo effects, the same soft tissue interposition was used and coupled motion was produced by rotating the model axially by  $0.5^\circ$  for every  $1^\circ$  of coronal plane rotation. As before, a range of  $30^\circ$  in  $5^\circ$  increments was used. The results, seen in Figure 44, suggest that inaccuracies of  $\pm 0.74^\circ$  might apply in clinical situations, given optimal radiography.

FIGURE 43



GRAPH COMPARING PROTRACTOR AND COMPUTER ESTIMATION OF  
LATERAL BENDING AS IN 41 BUT INCLUDING THE INFLUENCE  
OF SOFT TISSUE SCATTER AND POSITIONAL DISTORTION

FIGURE 44



GRAPH COMPARING PROTRACTOR SETTINGS AND COMPUTED  
ANGLES OF CORONAL PLANE ROTATION THROUGH 30°  
WITH COUPLED MOTION AND SOFT TISSUE  
SCATTER

## 12.2 Studies of Rotations in Human Volunteers

### 12.2.1 The Lumbar Spine

An X-ray sequence of coronal plane motion in the lumbar spine of a 25 year-old asymptomatic male volunteer was studied. Screening at this stage was carried out in the standing position with relatively little stabilisation over 36 seconds, including exposure during positioning. This time was divided between the right and left lateral bending sequences.

The recordings from videotape were digitised by sampling the motion sequences over a series of 16 equal time increments calculated to include the whole range of motion in each direction. These digitisations included the full range of motion with a few frames left over in each direction. The angles of the vertebrae from L2 to 5 with respect to the monitor's X-axis were determined by marking the same vertebral body corners in each frame (Figure 45). The marking procedure concentrated on the re-identification of the same anatomical landmarks from frame to frame.

#### 12.2.1.1 Absolute Lateral Flexion

The software allowed for the writing of batch commands for the automatic appearance of the screen cursor and the recording and calculation of these absolute angles. The angles were read from the microcomputer screen at the end of the procedure and were plotted against time for absolute lateral flexion. The results are shown in Figure 46.



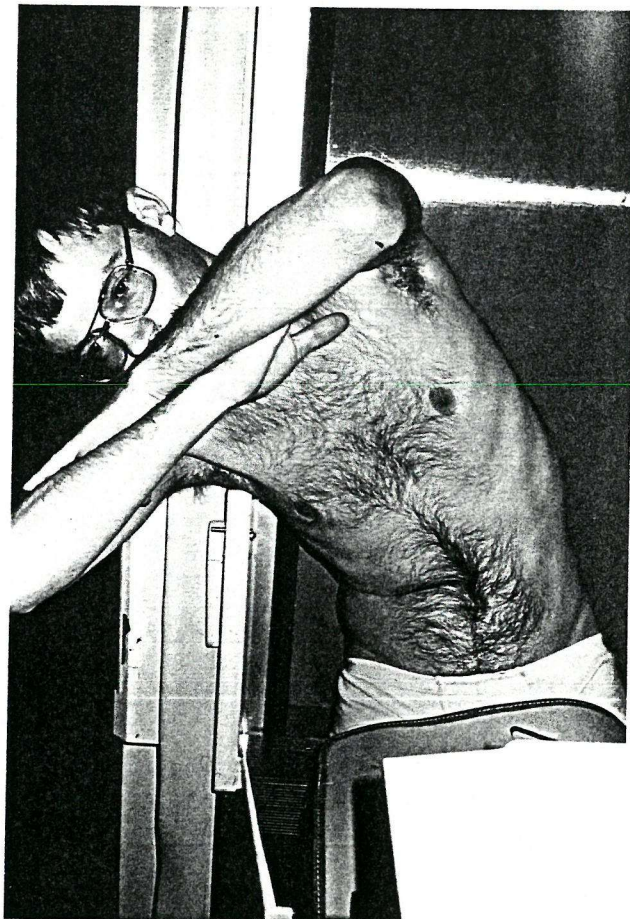


FIGURE 45a

SUBJECT IN LUMBAR LATERAL BENDING IN POSITION BESIDE INTENSIFIER

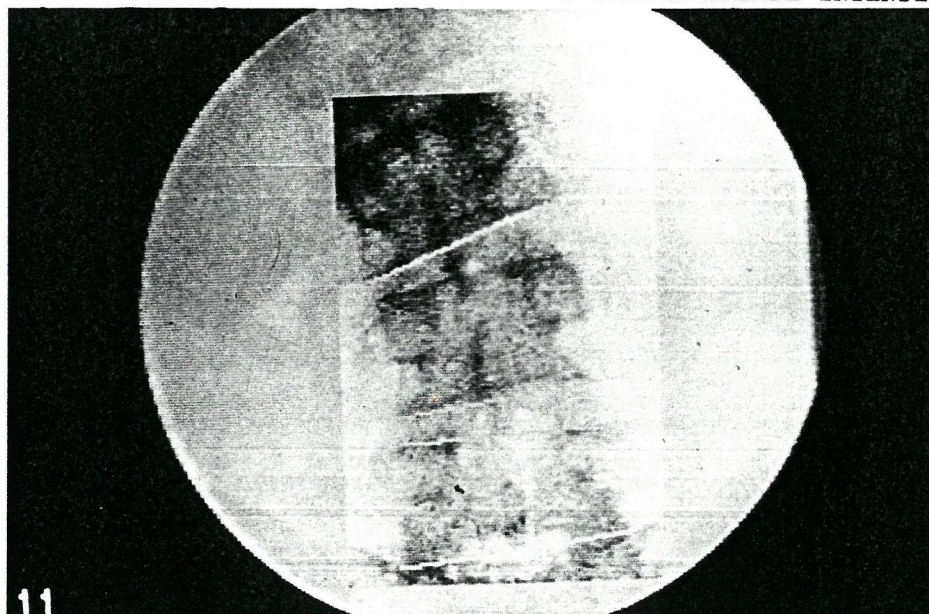
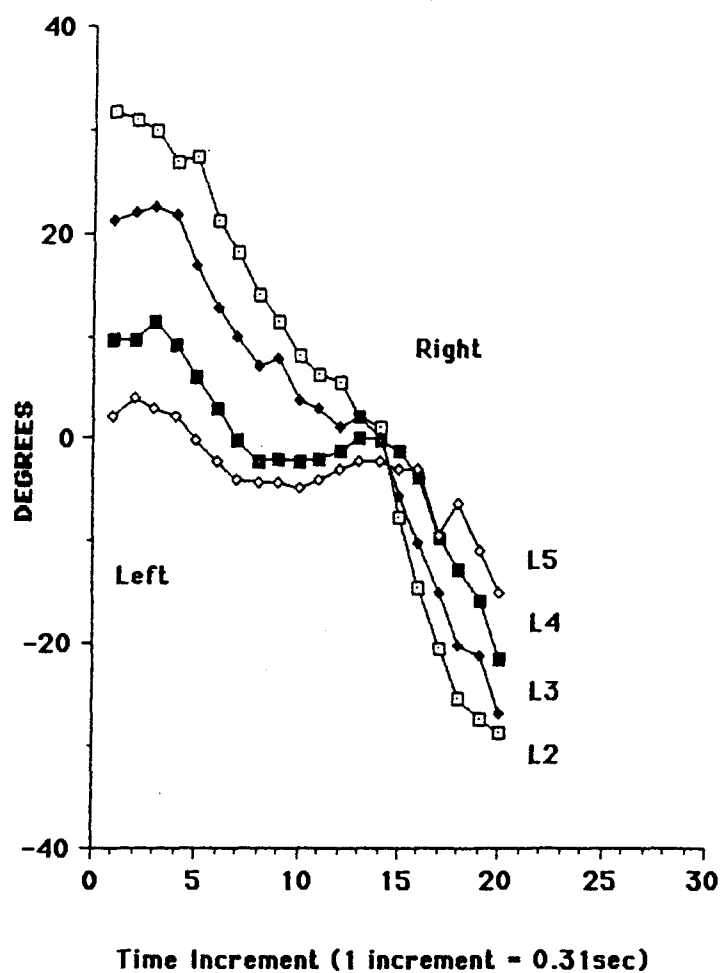


FIGURE 45b

COMPUTER IMAGE OF HUMAN LUMBAR SPINE IN THE ANTERIOR/POSTERIOR  
PROJECTION, CONTRAST ENHANCED AND MARKED FOR THE ESTIMATION  
OF INTERVERTEBRAL ANGLES

FIGURE 46



GRAPH SHOWING INCREMENTS OF CORONAL PLANE MOTION  
FOR L2-5 RELATIVE TO THE X-AXIS OF THE  
COMPUTER MONITOR



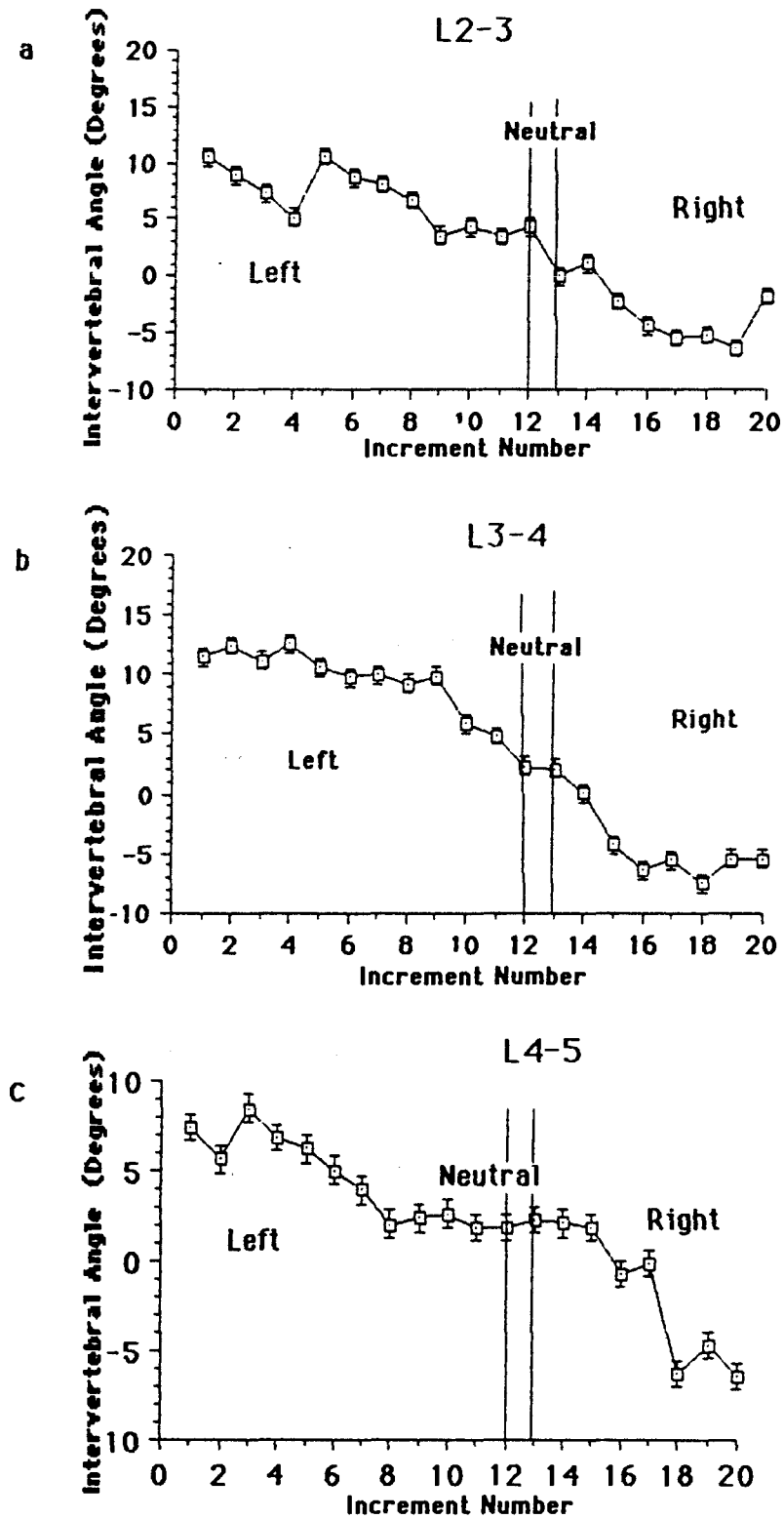
#### 12.2.1.2 Relative Lateral Flexion

Subtraction of the absolute angles of adjacent vertebrae throughout the motion sequence gave the angles between them and the coronal plane motion at L2-3, L3-4 and L4-5 is displayed in the graphs in Figures 47a-c. These show considerable irregularity in intervertebral motion despite the smooth overall movement of the trunk. It is unlikely that these irregularities can be attributed to noisy data as the variances of 10 repeated measurements of each intervertebral angle was less than that obtained in the calibration studies which attempted in vivo simulation. It is more likely that these irregularities reflect the contraction of deep spinal muscles and/or reflect the fluid dynamics within the intervertebral disc. The phenomenon has also been observed by Cholewicki et al (50), who recently carried out similar experiments based on the concepts which originated here.

#### 12.2.1.3 Interobserver Variations

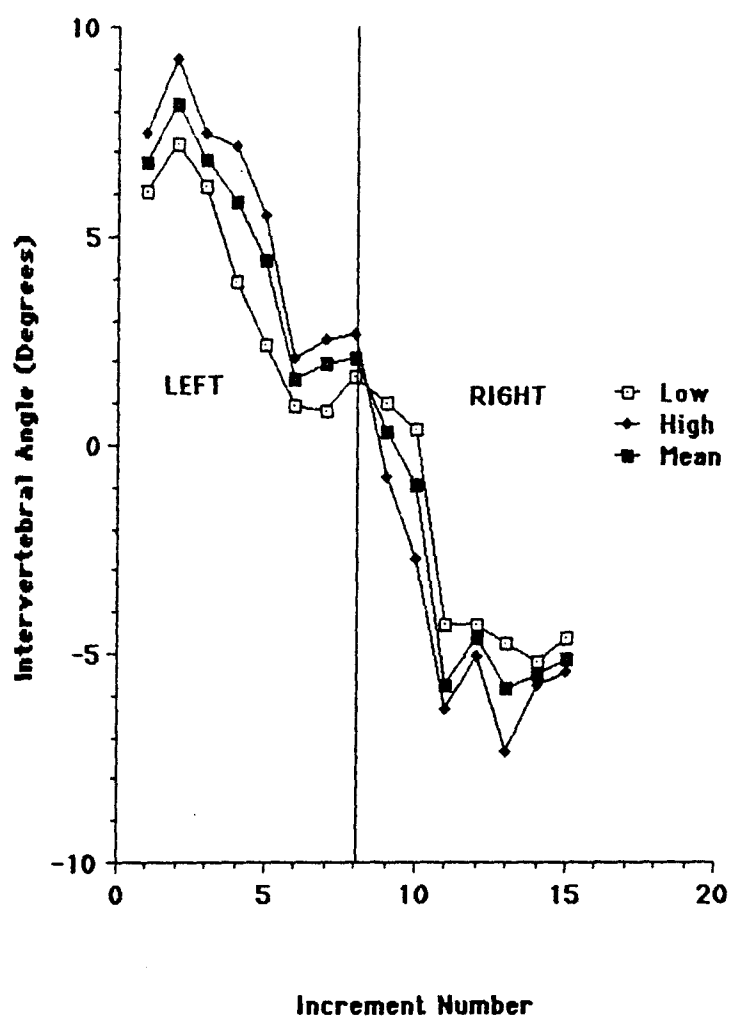
In order to examine the influence of multiple observers on the repeatability of measuring coronal plane motion, the same motion sequence was processed by 4 people. Two standard deviations of 10 repeated measurements of L3-4 intervertebral angle by two observers was  $0.65^{\circ}$ ; again less than the single observer figure obtained in the in vivo simulation. The four observers, who had varying experience with the system, then measured the L4-5 intervertebral angle throughout the motion. The result of this is shown in Figure 48.

FIGURE 47



(a-c) RELATIVE CORONAL PLANE MOTION IN ASYMPTOMATIC SUBJECT AT L2-3, L3-4 AND L4-5 (ERROR BARS = 2SD OF MEAN CALIBRATION ERROR)

FIGURE 48



RELATIVE CORONAL PLANE ROTATION AT THE L4-5 LEVEL BY  
FOUR OBSERVERS ILLUSTRATING RANGE AND  
MEAN MEASURES

It can be seen that a similar pattern is present for all observers. The variations in each measurement over all observers appeared not to bear any relationship to the size of the intervertebral angle measured (Figure 49), however, the combined SD between observers was 1.01, giving an inter-observer variation of approximately  $\pm 2^\circ$  at the 96% confidence level. This suggests that some observer training is necessary if this measurement is to have any value in clinical research. Rotations of  $2^\circ$  or less, such as are normal in the coronal plane at L5-S1 would not be quantifiable, but the regularity of rotations over greater ranges would, thus opening the possibility for study of the effects of pain syndromes and their treatment on kinematic behaviour.

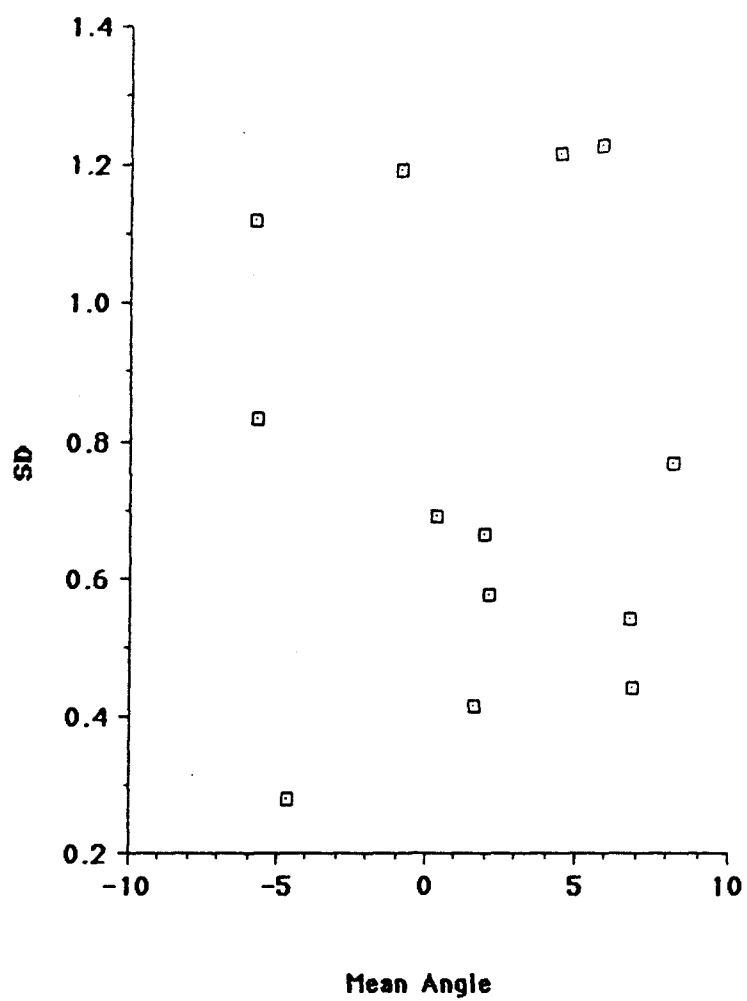
### 12.3 Translations in the Coronal Plane

This plane of translation is of limited clinical relevance for most spinal situations. In the absence of bony injury, the cervical and thoracic spines are designed to resist such motion by virtue of their rigid components. In the lumbar spine, however, this is restricted to the posterior joints, whose main function is to restrain a vertebra from forward translation on its inferior neighbour. However, were it not for an intact intervertebral disc, some considerable degree of lateral translation would be possible, albeit accompanied by axial rotation if taken to extremes. For this reason, lumbar spine joint laxity could result in lateral translation of individual vertebrae, and the assessment of this would be useful in diagnosis of back pain patients where mechanical instability is thought to be a causal

factor. It could also be a source of additional evidence to that obtained from studies of coronal plane motion in the same patient.

Unlike sagittal plane motion, very little information is available concerning ranges of translation. Pearcy, however (44), in a stereoradiographic study has suggested that only 1 or 2mm of translation can normally be expected. For the abnormal, very little is known. This would suggest that not only is direct measurement not an option, but the effects of coupling may well confound any attempt to assess the motion by locating serial ICRs.

FIGURE 49



VARIATION (SD) IN MEASUREMENT OF  
INTERVERTEBRAL ANGLES BY  
ANGLE SIZE

### 12.3.1 Calibration Studies of Translations

As for sagittal plane translation, the calibration model was used to assess both the accuracy and precision of assessments of translation using ICRs. In order to shed some light on where measurement limitations might lie, the model was used with and without the imposition of soft tissue scatter and the effects of coupling. These degrading effects were imposed using the same digitised images of the calibration model which were used in the coronal plane rotations studies.

#### 12.3.1.1 Accuracy

The calibration model was marked using the screen cursor as shown in Figure 50 and 10 observations were made of each of the settings. Degraded images were also marked and were the same as those used to calibrate for rotations in this plane using coupled motion features (see Section 12.1.3). The relationship between the ICR location error in millimetres on the screen and the size of the rotational increment can be seen in Figure 51. These findings are very similar to those resulting from the sagittal plane studies. The minimum rotational angle for a mean ICR location error of less than half the anterior-posterior dimension of the vertebral body is about 7°. Whether or not this scale of error would or would not allow distinction to be made between patients whose vertebrae did or did not translate in a clinically meaningful way must be left to future, large in-vivo studies; however, the work of others who digitised landmarks

on plain X-rays (75), suggests that there is a variation in range of translation in this plane which is reflected by centre length.

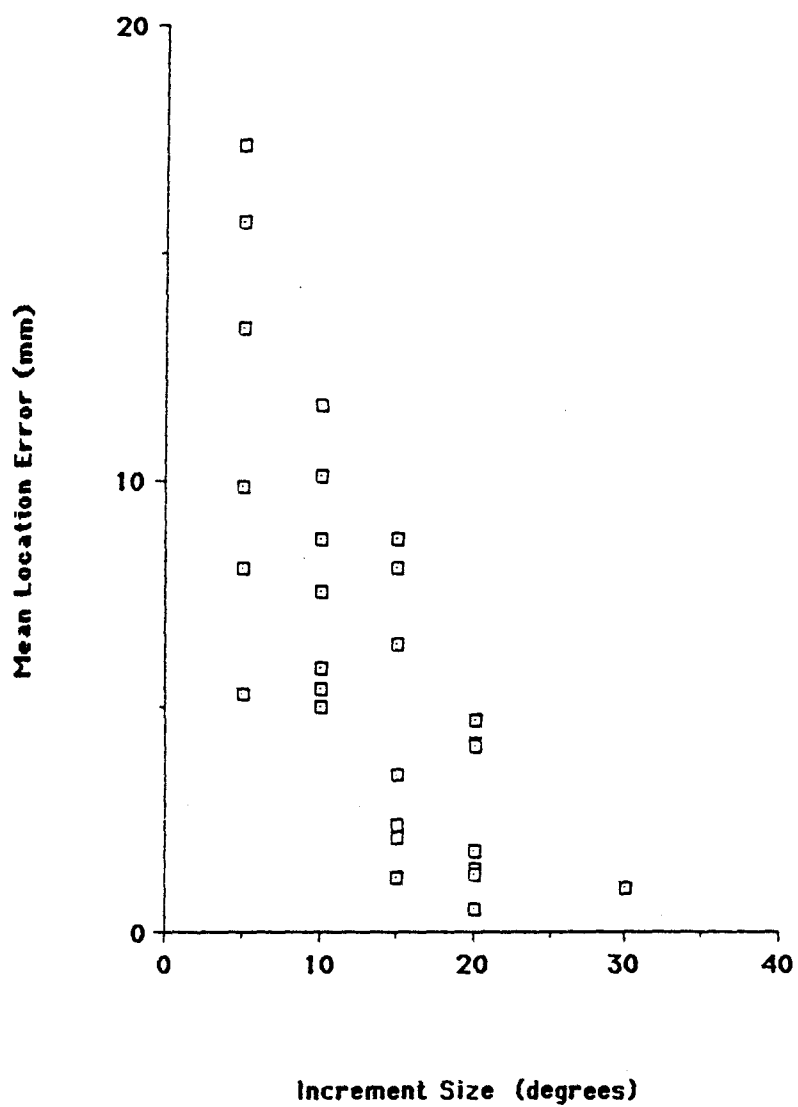
#### 12.3.1.2 Precision

Repeatability of measurement of ICRs in the calibration model in this plane was determined by two observers. Each observer carried out 10 measurements of each of 4 increments. The variation of locations for one observer by increment size is shown in Figure 52. This is very similar to the sagittal plane results (Figure 36) and may be even more promising for  $10^\circ$  rotations, despite the effects of coupled motion in this plane.

The results for two observers is expressed as circles whose radii are 2 standard deviations in x and y, and are placed with the mean locations as their centres (Figure 53a-d) in order to relate the error involved to the size of the vertebra. This is meant to represent a worst case situation and the results suggest that, given optimal radiography, a useful ICR locus should be obtainable for coronal plane lumbar spine motion in the model provided each increment exceeds  $5^\circ$ . This does not allow for the error-reducing effects of averaging (125), and the use of overlapping increments. While the former increases the laboriousness of the procedure, the latter is to be recommended in the interests of maximising the number of increments from which to obtain ICRs.

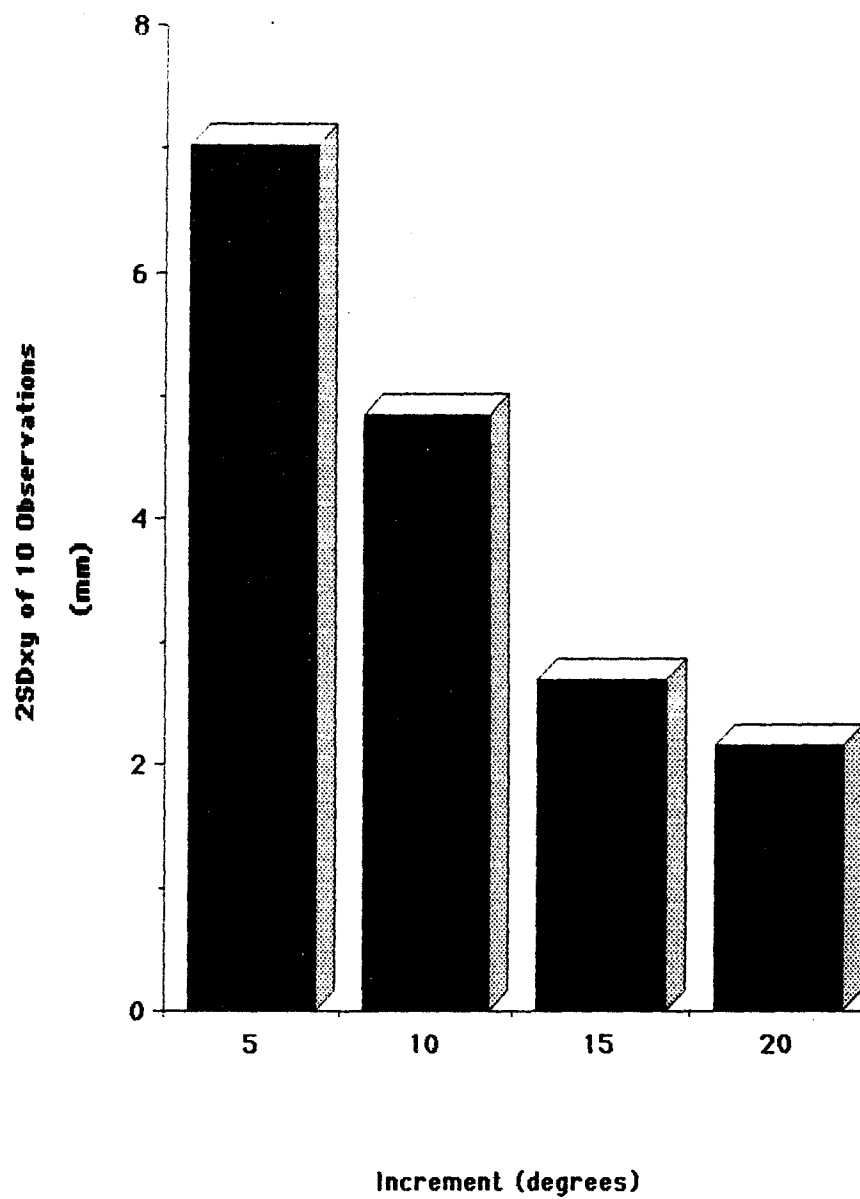


FIGURE 51



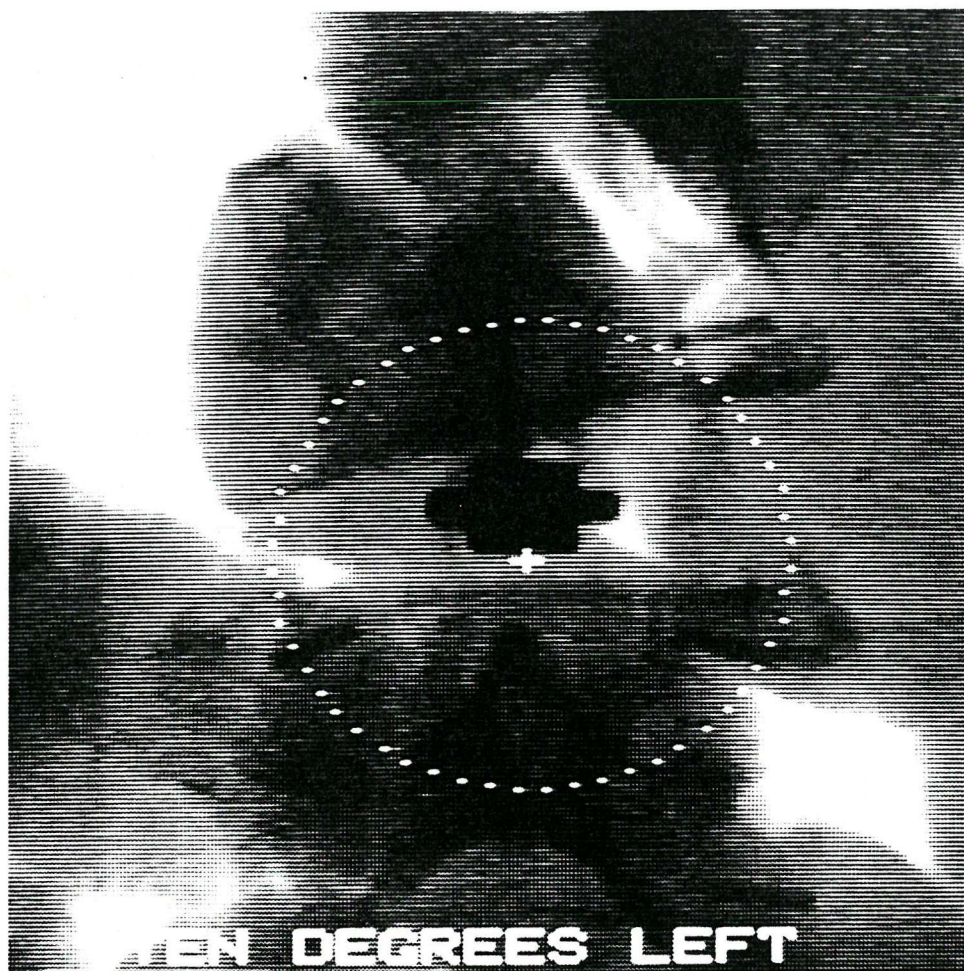
SCATTERPLOT SHOWING THE MEAN ICR  
LOCATION ERRORS OF CORONAL PLANE  
ICR LOCATIONS FOR A VARIETY  
OF INCREMENT SIZES

FIGURE 52



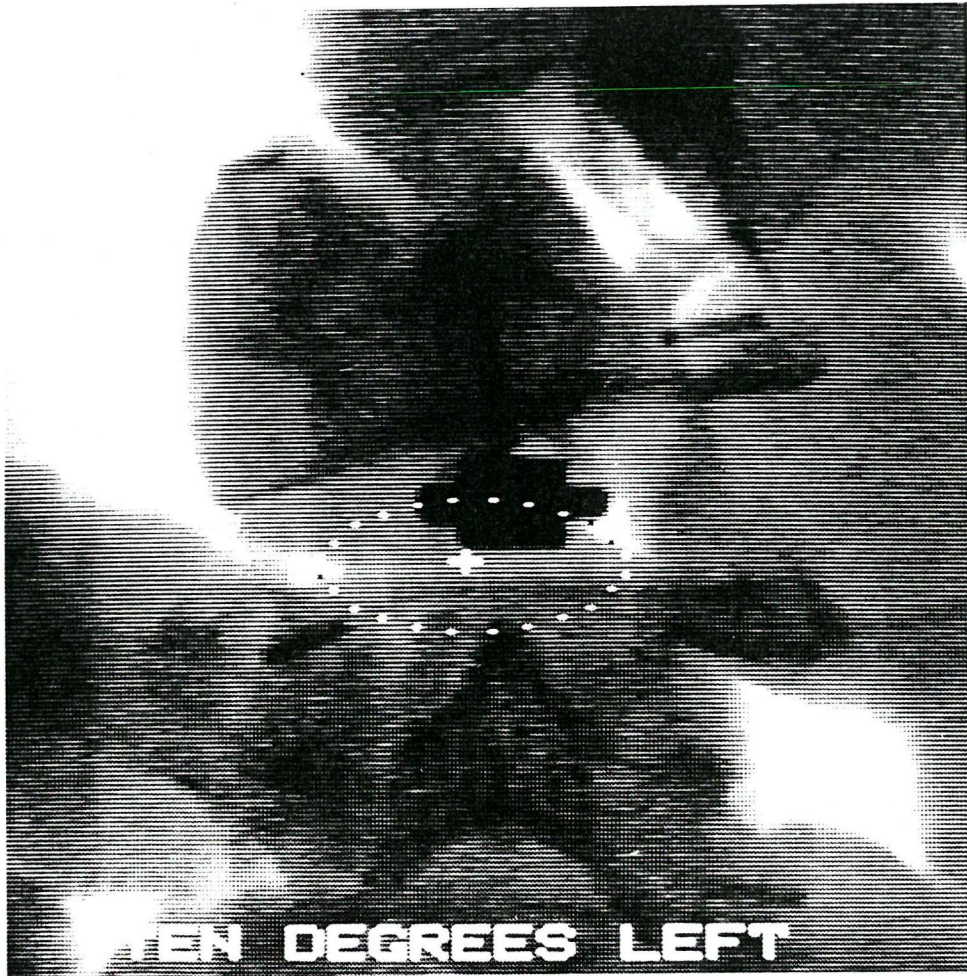
BAR GRAPH SHOWING THE INTRA-OBSERVER VARIATION OF ICR LOCATIONS  
IN THE CALIBRATION MODEL IN THE CORONAL PLANE FOR A  
VARIETY OF INCREMENT SIZES

FIGURE 53a



ELLIPSES OF INTER-OBSERVER REPEATABILITY ( $2SD_x$  AND  $y$ )  
AND MEAN LOCATIONS OF ICRs FOR INCREMENTS OF  $5^\circ$

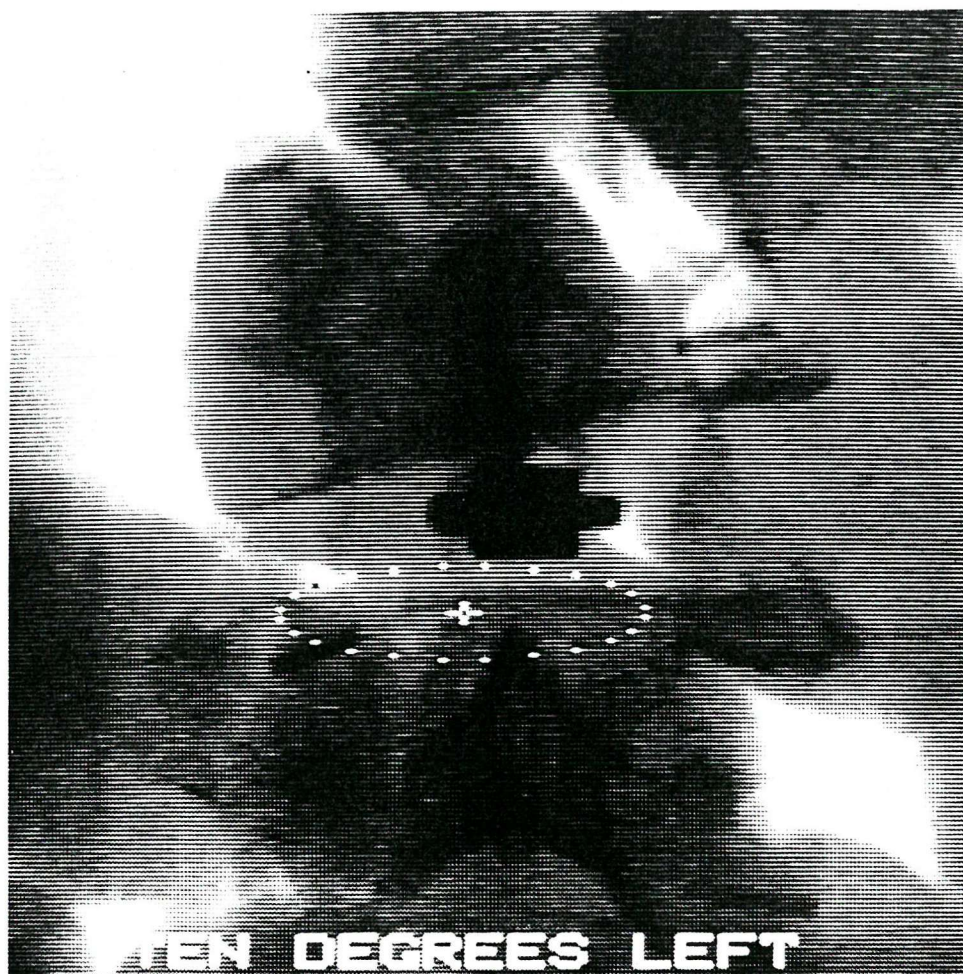
FIGURE 53b



ELLIPSES OF INTER-OBSERVER REPEATABILITY ( $2SD_x$  AND  $y$ )  
AND MEAN LOCATIONS OF ICRs FOR INCREMENTS OF  $10^\circ$

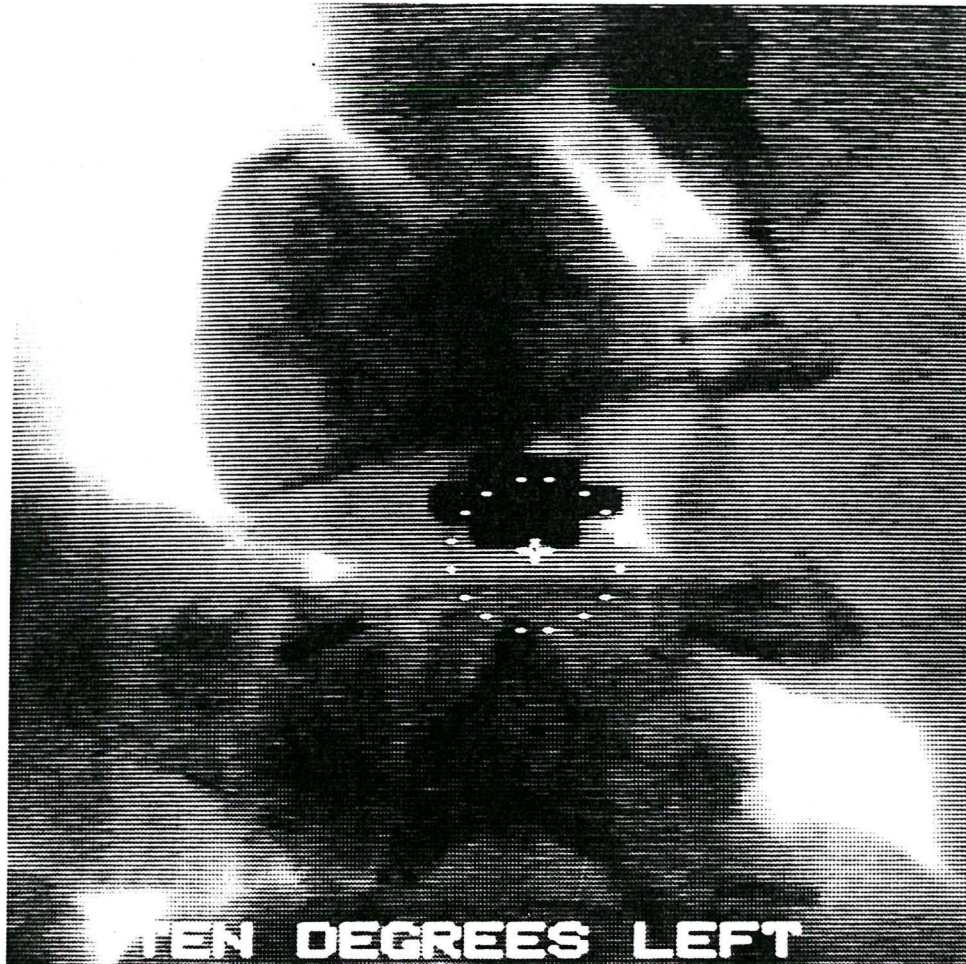


FIGURE 53c



ELLIPSES OF INTER-OBSERVER REPEATABILITY ( $2SD_x$  AND  $y$ )  
AND MEAN LOCATIONS OF ICRs FOR INCREMENTS OF  $20^\circ$

FIGURE 53d



ELLIPSES OF INTER-OBSERVER REPEATABILITY ( $2SD_x$  AND  $y$ )  
AND MEAN LOCATIONS OF ICRs FOR INCREMENTS OF  $30^\circ$

## 12.4 Studies of Translations in Human Volunteers

### 12.4.1 The Lumbar Spine

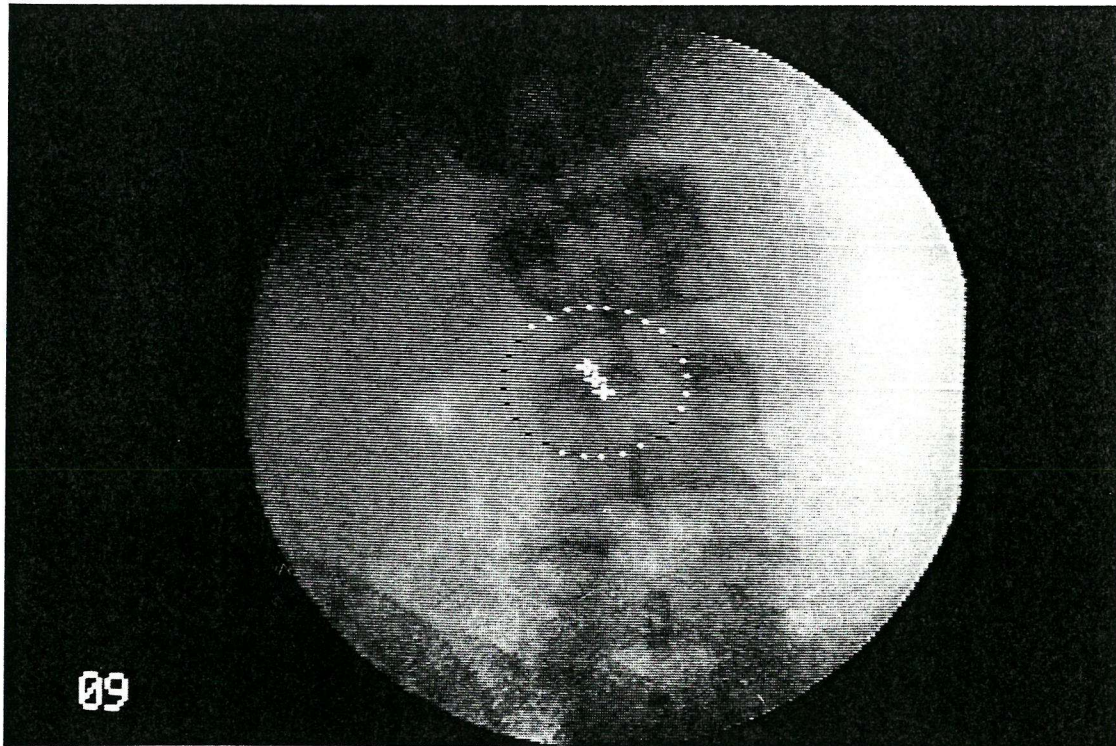
Six digitised frames from the sidebending sequence used in Section 12.2.1 were selected on the basis of representing approximately 4 equal increments of clockwise rotation at L3-4, each exceeding  $5^{\circ}$ . The total range of sidebending used was just under  $16^{\circ}$ . The increments overlapped and the ICR of each was computed 3 times and averaged, using the same technique as in the calibration studies. The results of this procedure are shown in Figure 54, which represents the track of ICRs from left to right sidebending. The area covered by these locations is consistent with translation in asymptomatic subjects noted in another in-vivo investigation (75).

### 12.4.2 The Cervical Spine

The tendency of soft tissues to compress during sidebending of the neck made radiographic tissue density difficult to control effectively without prohibitive lengths of exposure. When combined with the movement of soft tissues across possible anatomical landmarks, it became clear that some development of the radiographic procedure would be necessary to be able to record useful motion sequences. This was not attempted in the present study.



FIGURE 54



LOCUS OF ICRs FOR LEFT TO RIGHT SIDEBENDING AT THE  
L3-4 LEVEL IN A VOLUNTEER SUBJECT



### 13.0 EDGE-FINDING AS AN AID TO CO-ORDINATE MARKING

The problem of locating the same landmarks on successive images in sequence contributes greatly to the inaccuracies which are inherent in techniques such as this. Since these landmarks were, in fact, all bony edges, it was thought worthwhile to use the edge-enhancement algorithms supplied as part of the image processing software, to try to produce these edges automatically. Roberts and Sobel filters have been found to be useful for this purpose in other applications (177). The observer variation associated with the calculation of intervertebral angles on the digitised human images was therefore assessed before and after these forms of edge-enhancement.

#### 13.1 Application of the Median Filter

Image processing filters work by scanning each screen pixel and changing its grey level value according to a protocol which is usually influenced by the values of adjacent pixels. The Median filter sweeps each pixel as a 3x3 region, or mask.

a b c

d e f

g h i

The brightness value of the centre pixel (e) is changed in the process to the median value of all those immediately surrounding it. This has the effect of reducing high or low frequency noise which could be

magnified by the use of additional techniques; for example, edge-enhancement.

### 13.2 Application of the Roberts Gradient

In contrast to Median filtration, which is a form of averaging, or integration, and would tend to blur detail in an image (177), the Roberts filter uses differentiation to sharpen the image. The most commonly used method of differentiation in image processing is the gradient, in which grey level values of pixels are transformed according to the rate of change of grey levels encountered by sweeping in a given direction. This has the effect of delineating those areas of rapid brightness change by assigning large values for prominent edges in the image and small values in regions that are fairly smooth; thus constructing a white line around edges.

### 13.3 Application of the Sobel Operator

The Sobel operator applies two templates in turn to each pixel in the image to determine its grey-level value.

Template 1	Template 2
-1 -2 -1	-1 0 1
0 0 0	-2 0 2
1 2 1	-1 0 1

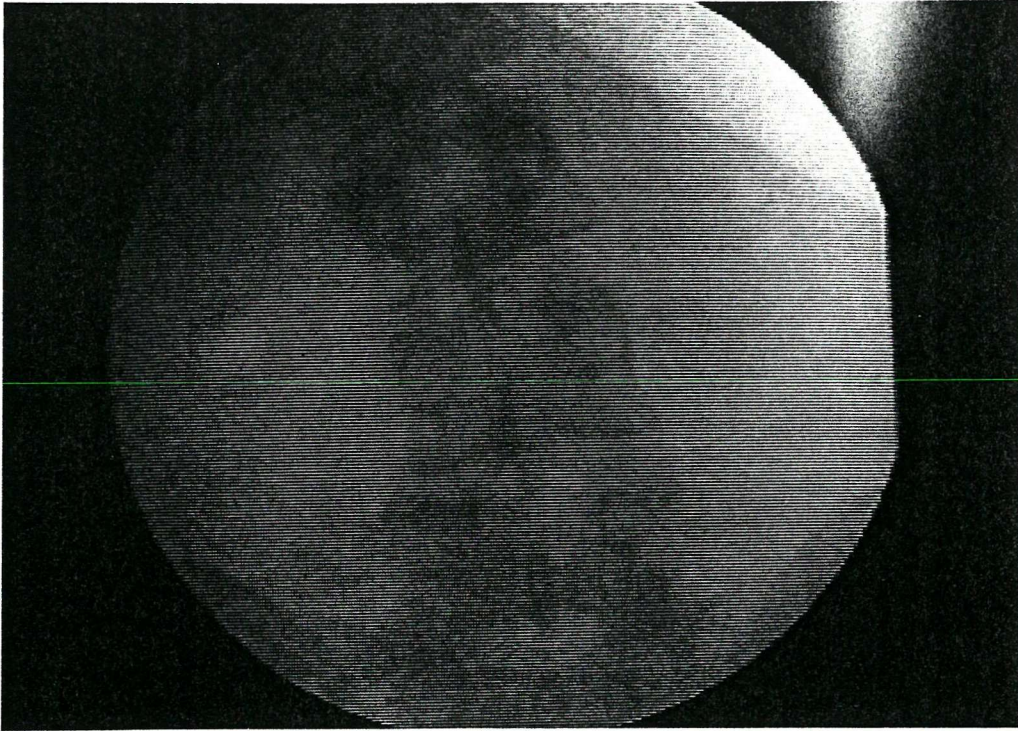
The value for the grey level of the central pixel in these 3x3 masks is determined from the sum of the responses of the two templates.

Template 1 gives the gradient in an x-direction and 2, the gradient in

y. Differences between regions are enhanced by this technique and by subsequent thresholding, when all grey levels above a given level are raised to peak white.

The images used, in their unprocessed form, are shown in Figures 55a and b. Both of these images were subsequently median-filtered to reduce the prevalence of high or low intensity noise prior to edge-finding. Sobel and Roberts filters were then applied to them.

a)



b)

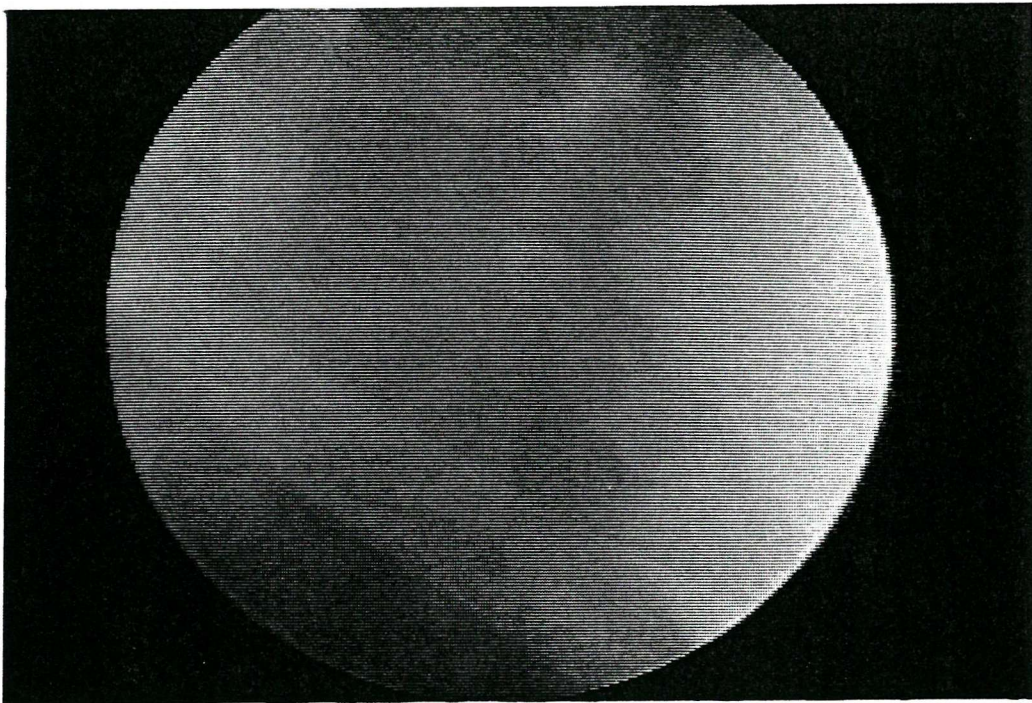


FIGURE 55

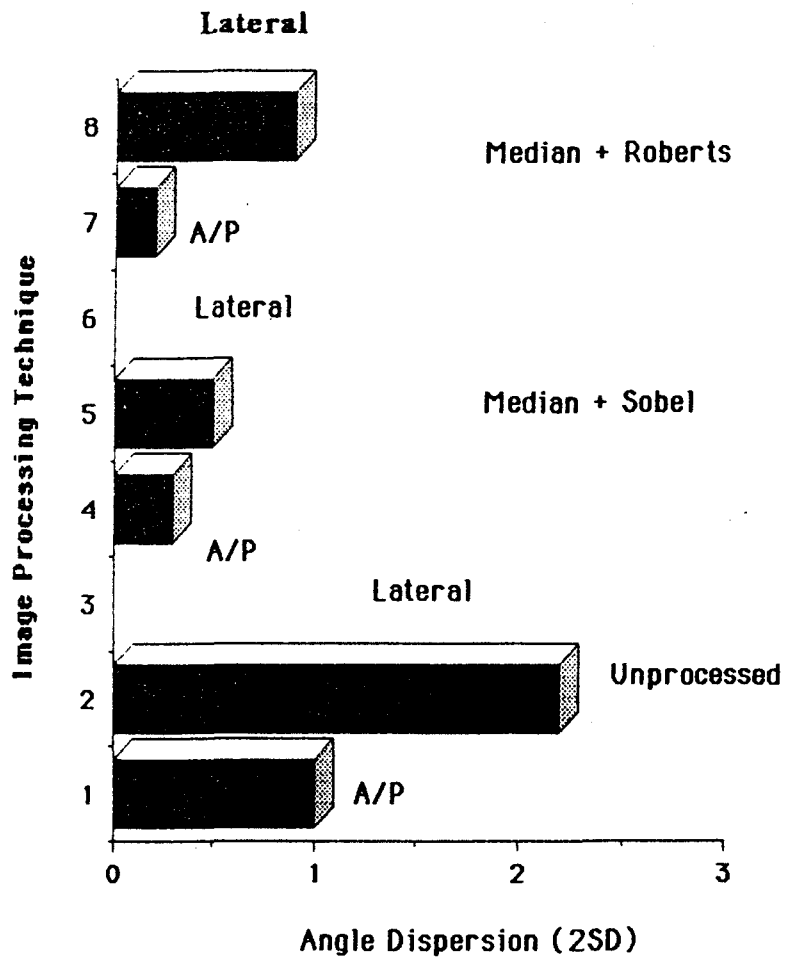
a) UNPROCESSED DIGITAL IMAGES OF ANTERIOR-POSTERIOR PROJECTIONS  
OF THE LUMBAR SPINE IN A VOLUNTEER SUBJECT

b) UNPROCESSED DIGITAL IMAGES OF LATERAL PROJECTIONS OF THE LUMBAR  
SPINE IN A VOLUNTEER SUBJECT

The dispersion of values for 10 observations of the L3-4 intervertebral angle by one observer using the three image processing techniques is shown in Figure 56. From these experiments, the image with the Roberts filter applied to the median-filtered anterior-posterior view produced the least variation in measurement of the intervertebral angle (Figure 57). In the lateral view, median plus Sobel filtration gave the best results (Figure 58). It is thought that the thicker line produced by this method is less likely to be lost and is more suitable where there is less radiographic contrast owing to greater soft tissue thickness.

Unfortunately, the movement of soft tissues across the plane of the penetrating X-rays could conceivably produce a different outline for successive positions. This could only be tested by repeated known rotations and X-ray exposures of human lumbar spines. Unethical in volunteers, the only satisfactory test situation would involve the use of cadavers with displacement transducers attached to the vertebrae. This was not possible in these studies. Nevertheless, there may, in the future, be scope for the development of a standardised mathematical treatment of co-ordinates derived by edge-finding which would render them more dependable.

FIGURE 56



DISPERSION OF VALUES FOR L3-4 INTERVERTEBRAL  
ANGLES USING 3 IMAGE PROCESSING TECHNIQUES



FIGURE 57

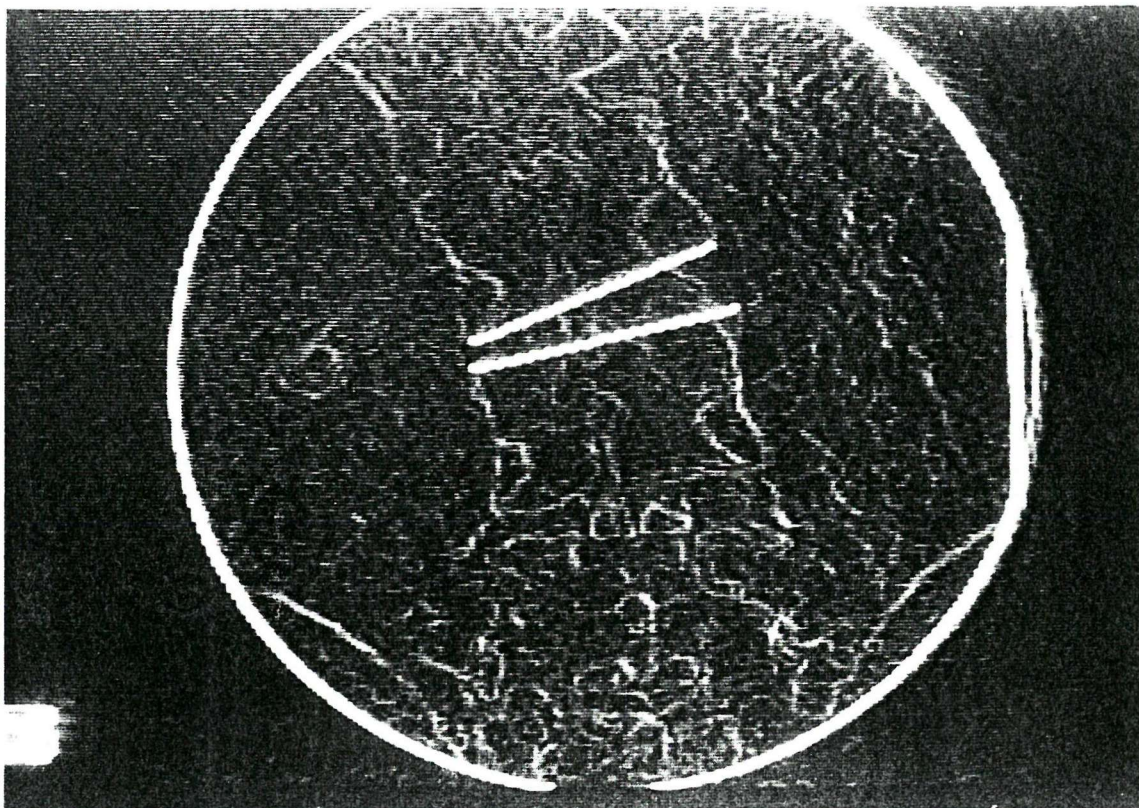


IMAGE AS 55a AFTER ADDING MEDIAN AND ROBERTS FILTRATION  
WITH MARKING OF L3 AND L4 VERTEBRAL BODIES

FIGURE 58

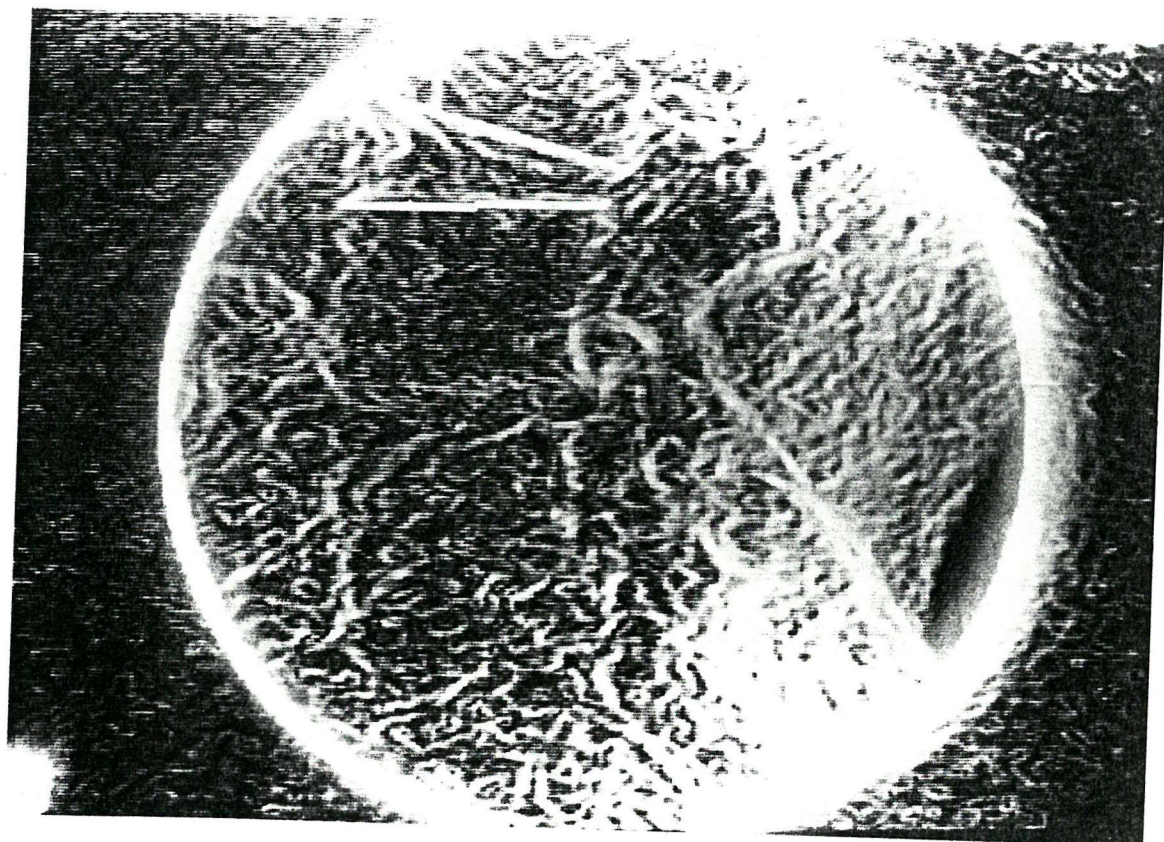


IMAGE AS 55b AFTER ADDING MEDIAN AND  
SOBEL FILTRATION



#### 14.0 RADIATION DOSAGE

At the outset of the studies, which used human subjects, local medical ethics committee approval was obtained for the screening of six volunteers at Odstock Hospital Spinal Unit in order to obtain recordings of spinal motion in the coronal and sagittal planes. Careful note was taken of the X-ray factors and screening times used (See Appendix V). In addition, thermoluminescent dosimeters were attached to a radiographic phantom (Figure 17) which was subjected to one minute's screening at 85KV and 2MA (see footnote \*). The siting for these was at the incident and exit points of the primary rays for anterior-posterior and lateral lumbar X-rays. These factors represented the average (mean) of those used to screen the volunteers.

The dosage attributable to one minutes' lumbar spine screening at average factors is shown in Table 2. In practice, about 10 seconds is the most that is required to record the motion sequence and, with careful explanation and rehearsal, the screening plus alignment can take less than 20 seconds. By way of comparison, the entry dosage normally associated with plain X-rays of the lumbar spine is about 20 mGy for anterior-posterior views and 50 mGy for lateral views (44). It is feasible, therefore, to be able to record motion sequences with less dosage than that associated with a single conventional X-ray of the same part.

\* Footnote: KV (kilovoltage) determines the penetrating ability of the X-rays; the greater the penetration generally, the less the absorbed dose. Ma (milliamperage) relates to the quantity of radiation given, and therefore absorbed. The exposure time has a decisive influence on the latter.

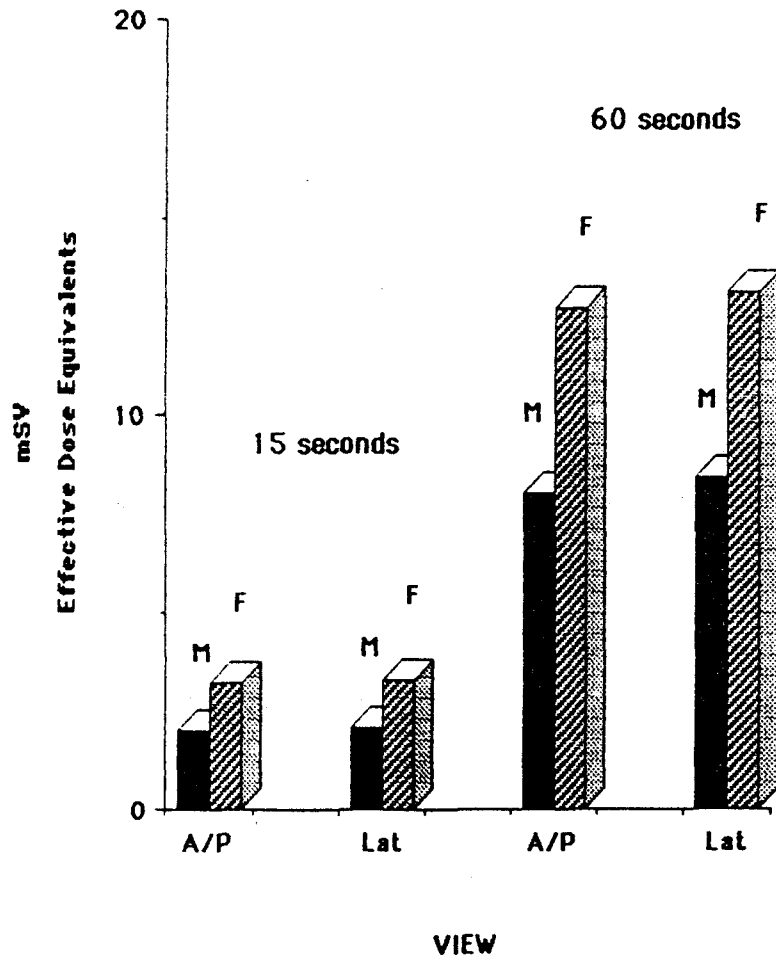
TABLE 2

ABSORBED RADIATION FROM ONE  
MINUTE OF LUMBAR SPINE SCREENING USING A PHANTOM

VIEW	MEAN ABSORBED DOSE (mGY)
Lumbar A/P	28.2
Lumbar Lateral	45.7

Given that the longest screening time is likely to be one minute, these values for absorbed radiation were converted into Effective Dose Equivalents for males and females. This measure incorporates cancer risk and is expressed in milliSieverts. The values shown in Figure 59 assume one-minute and (more typically) 15 second screening times, that the lumbar spine is screened with the x-rays entering the patient from the front, that the ovaries are not shielded in females and that the testes are shielded in males (as is customary when taking X-rays to view the lumbar spine). The one-minute screenings have an estimated cancer indication risk of 1 in 3,000, compared to a 1 in 5 natural incidence. By way of comparison, the International Commission on Radiological Protection draft recommendations (178) specify a limit of 20mSv per year for industrial exposure to ionising radiation. For

FIGURE 59



RADIATION DOSAGE (EFFECTIVE DOSE EQUIVALENTS)  
FOR MALES AND FEMALES FOR LUMBAR SPINE  
SCREENING TIMES OF 1 MINUTE AND  
15 SECONDS

medical diagnostic exposures the recommendations are less rigid, but are based on the premise that all procedures must be justified in terms of benefit to the patient. The Commission recommends that broadly, a limit of 5mSv over 5 years is to be aimed for.

At a later stage, when the technique was being used for the examination of patients, a further dosage study was carried out. This involved placing dosimeters on a male patient's abdomen and neck during the screening of the lumbar and cervical spines respectively. The results of this in terms of absorbed dose are shown in Table 3.

TABLE 3

ABSORBED RADIATION DOSAGE FOR A TYPICAL PATIENT  
SCREENING SEQUENCE INVOLVING THE CERVICAL AND LUMBAR SPINES

VIEW	ABSORBED DOSE (mGy)
Lumbar A/P	2.87
Lumbar Lateral	12.61
Cervical Lateral	2.60

(Note: Screening times are approximately 10 seconds for each view)

The values for Effective Dose Equivalents in mSv would represent 1/2 to 1/3 of these figures, depending on the circumstances of the radiography and continue to represent less radiation than a single plain film.

## 15.0 PATIENT STUDIES

### Patient 1.

This patient was a thirty-two year old ergonomist who, 12 years before, had been involved in an accident in which the car in which he was a passenger hit a tree. On impact, his seat became detached at one side, rotated, and tilted forward simultaneously. His head hit the dashboard, forcing it downward. X-rays of his neck taken in hospital showed no bony injury and further films taken at the extremes of flexion-extension range appeared to show no excessive translation at any level. Nevertheless, from the date of the accident, he suffered discomfort in his lower neck and upper back, continuously for the following 12 years. This became overtly painful if he undertook desk work or driving for longer than 10 minutes and it rendered him unemployable.

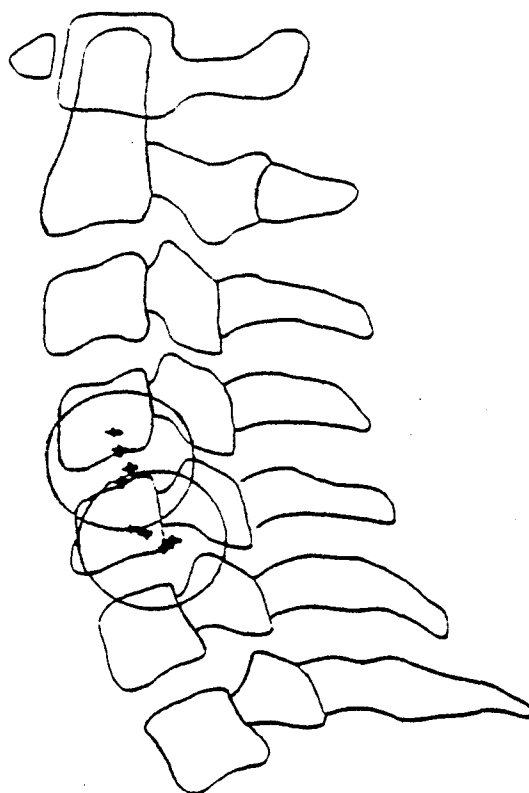
Clinical examination suggested that the level of mechanical insult, if there was one, was at either the C4-5 or C5-6 level. The patient underwent motion X-rays in the sagittal plane to investigate this and the positioning for this examination is as seen in Figure 30. The total screening time was 15 seconds and the ranges of rotation were  $13^{\circ}$  and  $20^{\circ}$  for the C3-4 and C4-5 levels respectively.

Figure 60 illustrates the locations of the ICRs for four increments at each of these levels. The increments were not of equal size, but varied from  $7^{\circ}$  to the overall range. The centres of the circles are the ICRs of the overall motion and their radii represent 2 standard deviations of 10 successive determinations by a single observer of the

smallest increment size. It can be seen that the grouping of ICRs is not large, suggesting that no excessive translation is occurring at these levels.



FIGURE 60



ICR LOCATIONS FOR FOUR MOTION INCREMENTS AT THE C4-5 AND C5-6  
LEVELS IN PATIENT 1 (CIRCLES HAVE CENTRES AT OVERALL ICR  
LOCATIONS - RADII REPRESENT INTRA-OBSERVER VARIATIONS  
(2SDxy) AT EACH LEVEL

Patient 2.

This 54-year old asymptomatic male volunteer had radiological evidence of disc degeneration at the L4-5 level (Figure 61). He had, however, experienced episodic debilitating back pain between the ages of 28 and 44, but had been trouble-free since then.

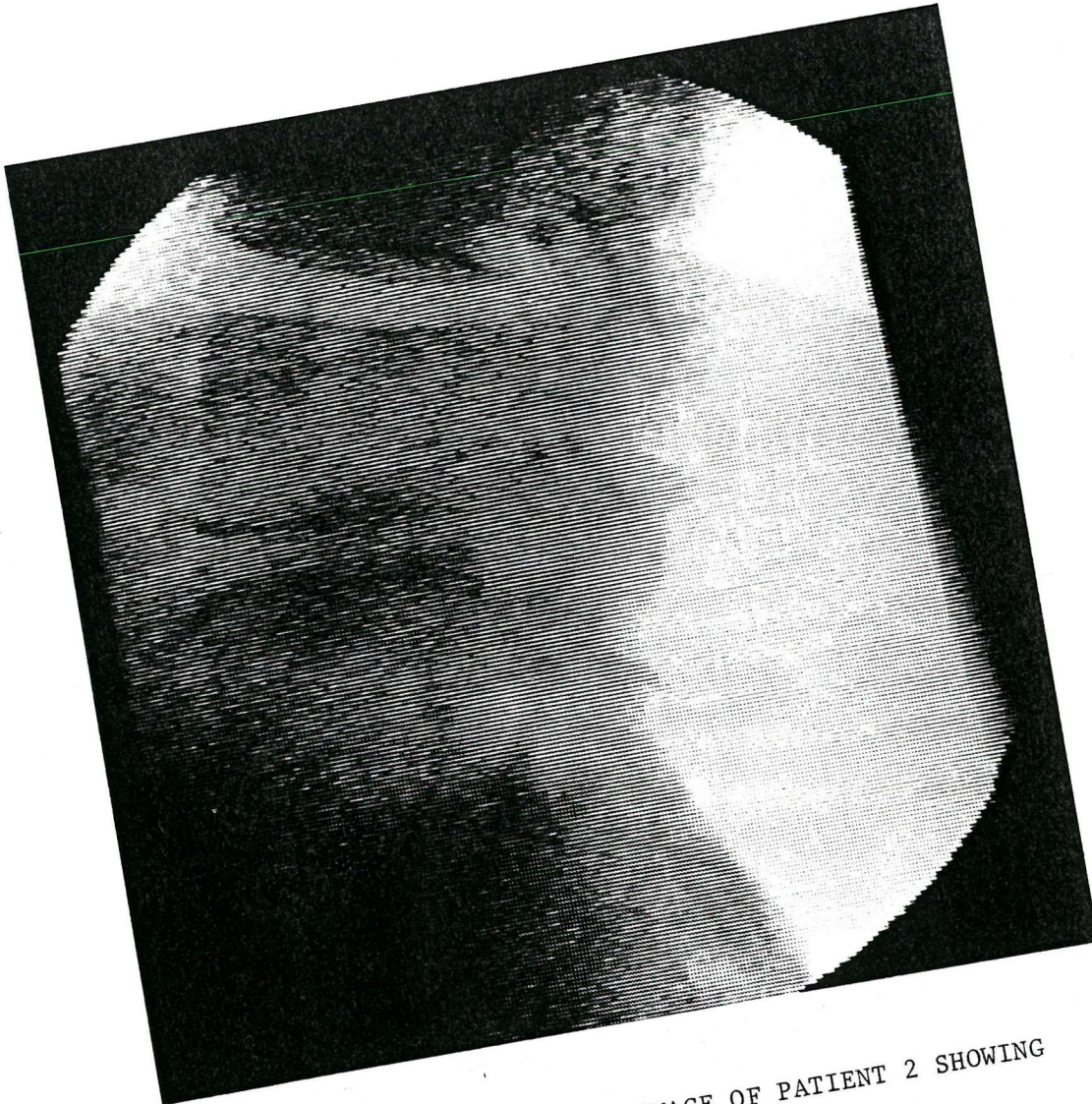
With regard to coronal plane motion, there was an absence of discernable motion at L4-5 in lateral bending. This can be seen in Figure 62c. The two levels above show a degree of irregularity in this motion (Figure 62a and b), some of which is also reflected in the overall motion (Figure 62d). (This irregularity was also a feature of the studies of other pain-free subjects). The error bars derive from the calibration studies as in section 12.2.1.2., and were of a higher order than those which resulted from a study of observer variability.

The locus of ICRs at L3-4 for sidebending is shown in Figure 63 and this suggests a mechanically stable segment. The absence of any rotation at L4-5 made ICR location untenable at that level.

For sagittal plane motion, the availability of anatomical landmarks and the image quality generally allowed for the measurement of rotations from L3-5 (Figure 64 a and b). Here the degenerate disc level (L4-5), (Figure 64b) showed about  $10^{\circ}$  of motion, whereas the L3-4 level above, (Figure 64a) which was mobile during sidebending, was essentially immobile in the sagittal plane. The range of rotation in this plane at L4-5 allowed for the determination of only one ICR, which was located just inferior to the L4-5 disc, indicating that

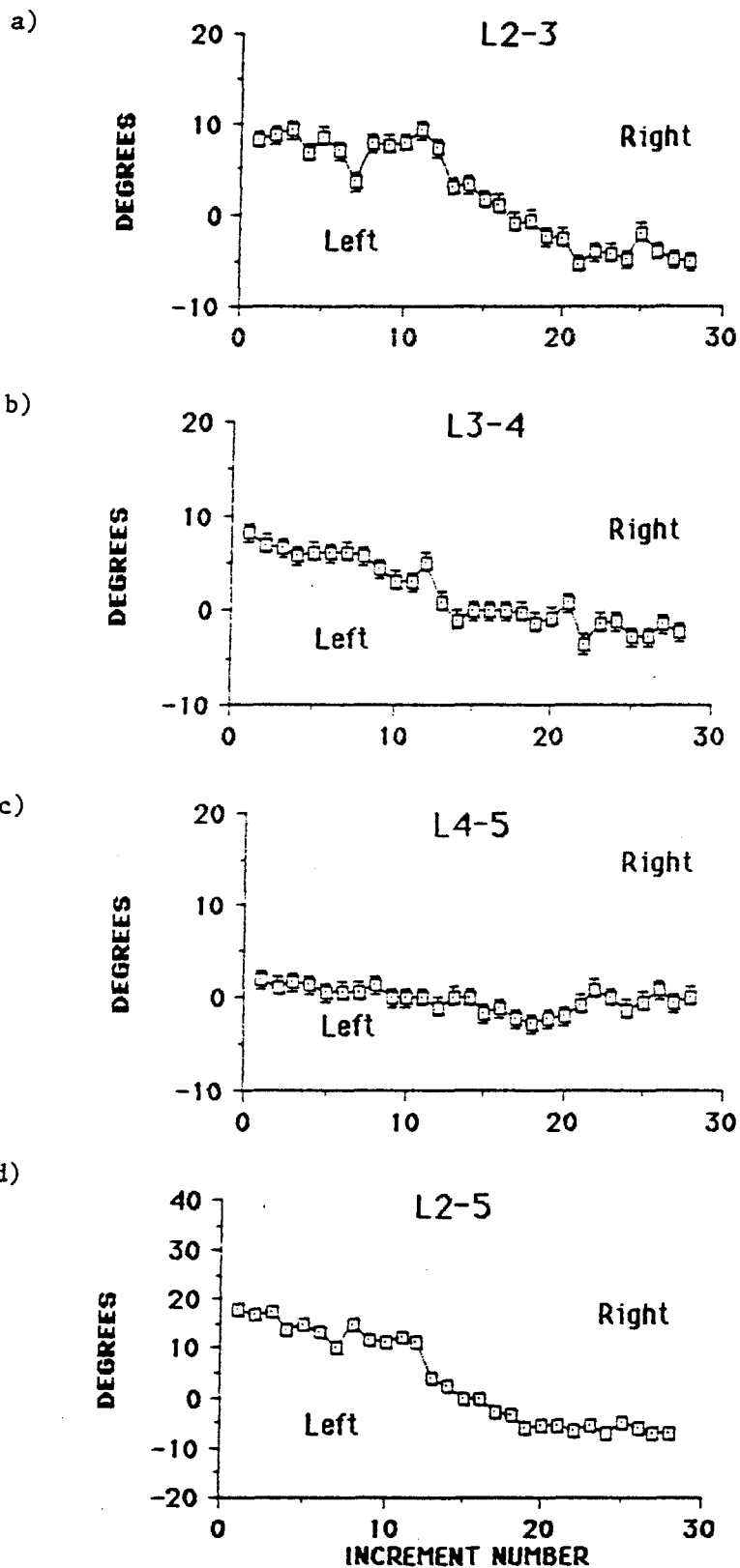
despite disc degeneration, the segment did not translate and was therefore inherently stable. This may be consistent with this patient's pain-free status.

FIGURE 61



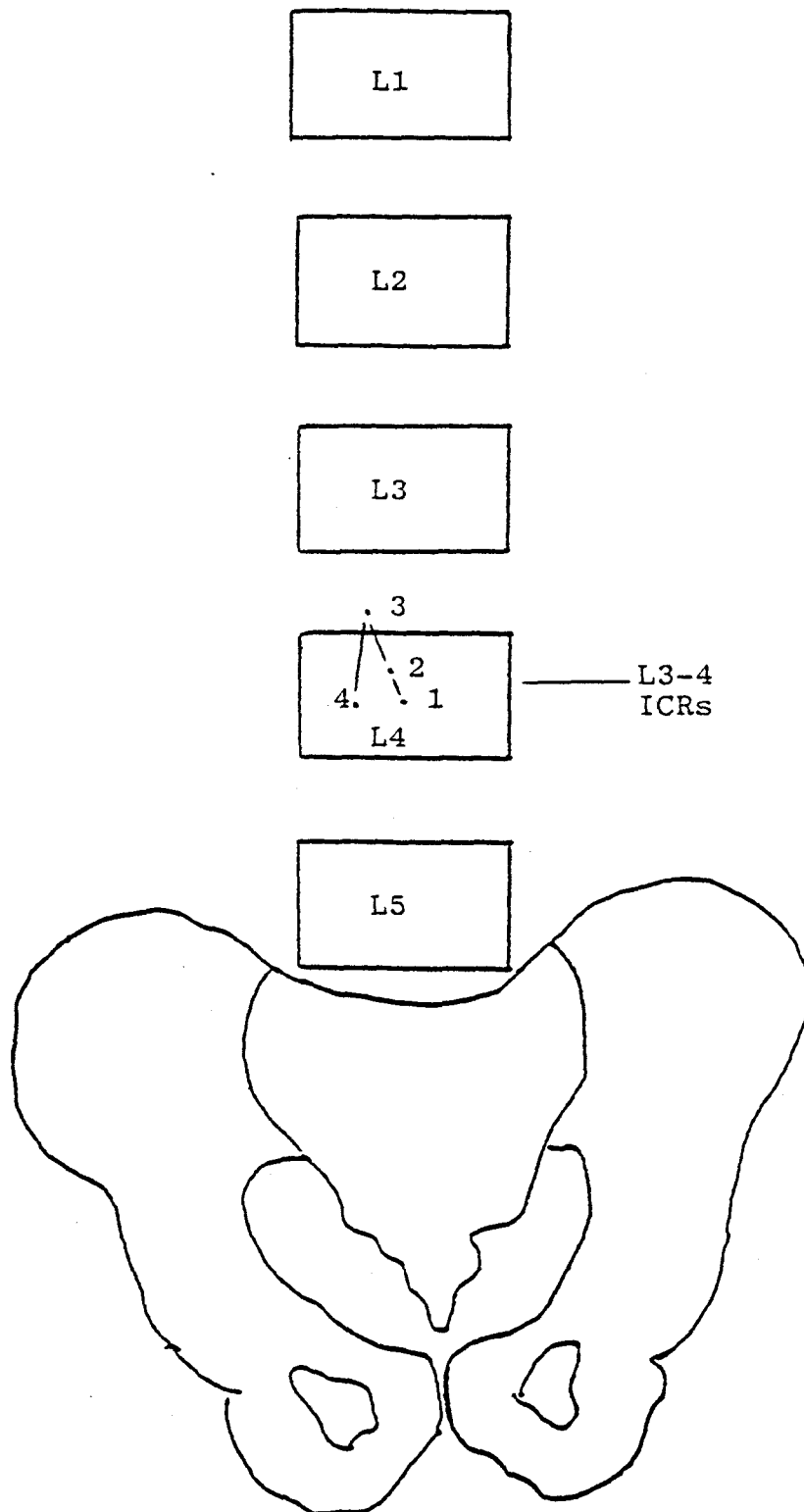
DIGITISED LATERAL LUMBAR IMAGE OF PATIENT 2 SHOWING  
DISC DEGENERATION AT THE L4-5 LEVEL

FIGURE 62



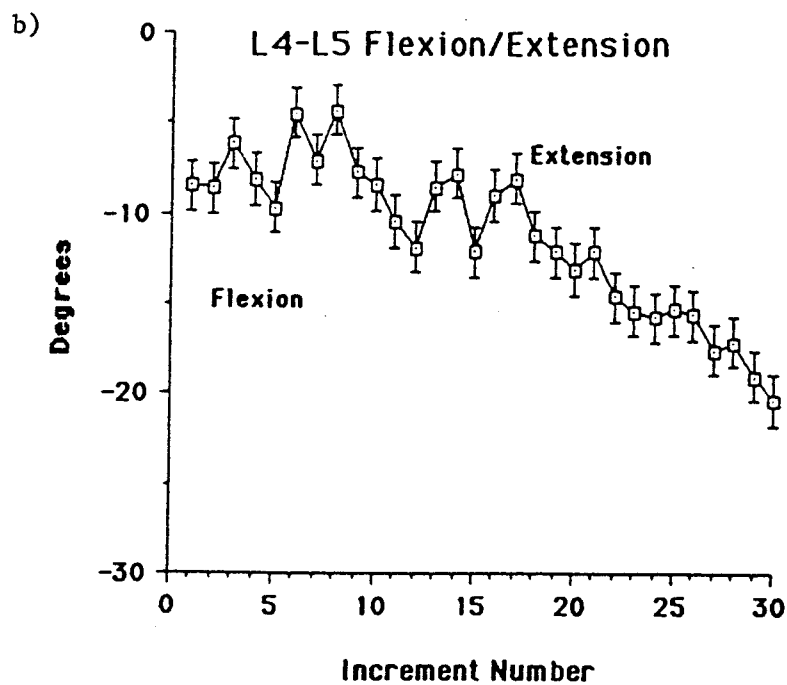
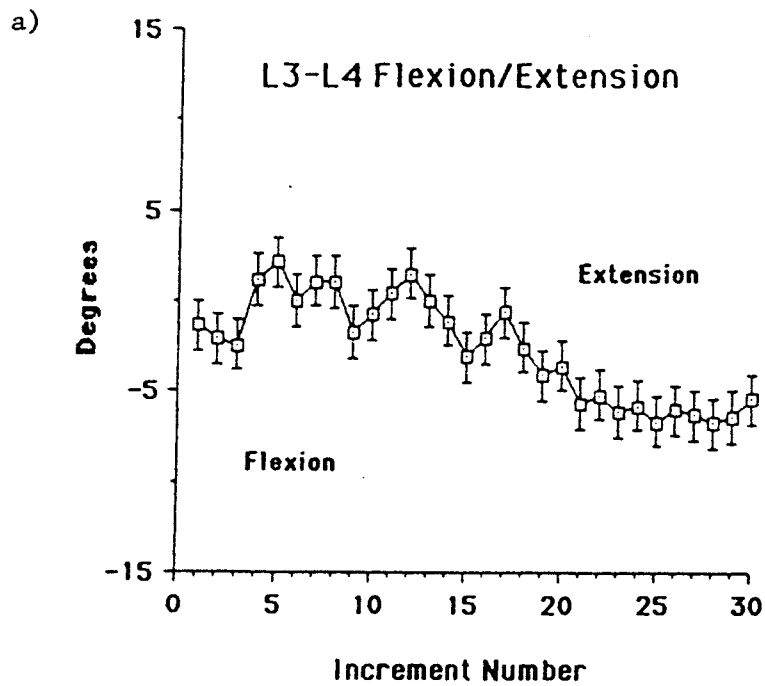
(a-d) GRAPHS OF 28 INCREMENTS OF SIDEBENDING  
FOR L2-5 IN PATIENT 2

FIGURE 63



LOCUS OF ICRs FOR CORONAL PLANE MOTION AT  
L2-3 IN PATIENT 2

FIGURE 64



INCREMENTAL MOTION IN FLEXION-EXTENSION OF PATIENT 2  
AT THE L3-4 AND L4-5 LEVELS

Patient 3.

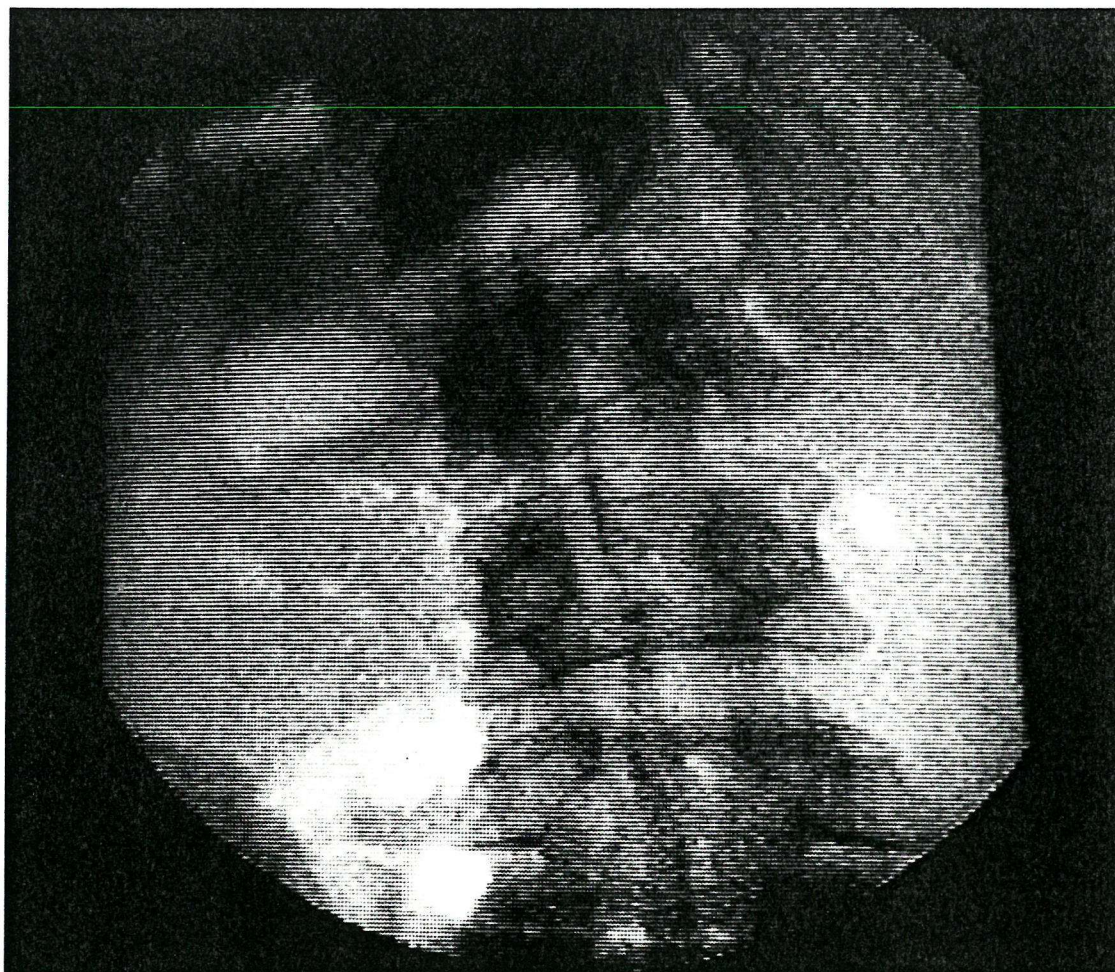
This was a 48 year-old company director who had suffered from frequent low back pain over 28 years. The main problem was initially one of stiffness and he suffered over many years from the effects of a common condition known as osteochondritis of the spine, in which the vertebrae, during adolescence, remain in a cartilagenous state until relatively late in one's development. This leaves them subjected to adult weight before they become firm, causing unevenness in the outlines of the bones. In this patient, this led to thinning of the intervertebral discs which may have contributed to the stiffness which he complained of.

His back had been manipulated on literally hundreds of occasions, including under anaesthetic and this relieved his symptoms. For the last 15 years, however, he became heavily involved in squash playing and periodically suffered acute, debilitating episodes of lower back pain on unguarded movements. He also experienced pain any time he undertook prolonged standing. The question of instability of the mid-lumbar spine became essential to deciding on his clinical management and this was investigated using the DVF technique.

Figure 65a-d shows views of the extremes of range of his lumbar spine in the coronal and sagittal planes. The standard deviation of the repeated determination of intervertebral angles in the coronal plane was  $0.51^{\circ}$  and  $0.70^{\circ}$  in the sagittal plane. Using  $\pm 2SD$  as error bars, the detailed graphical description of the ranges of coronal and sagittal plane motion can be seen in Figures 66 and 67.



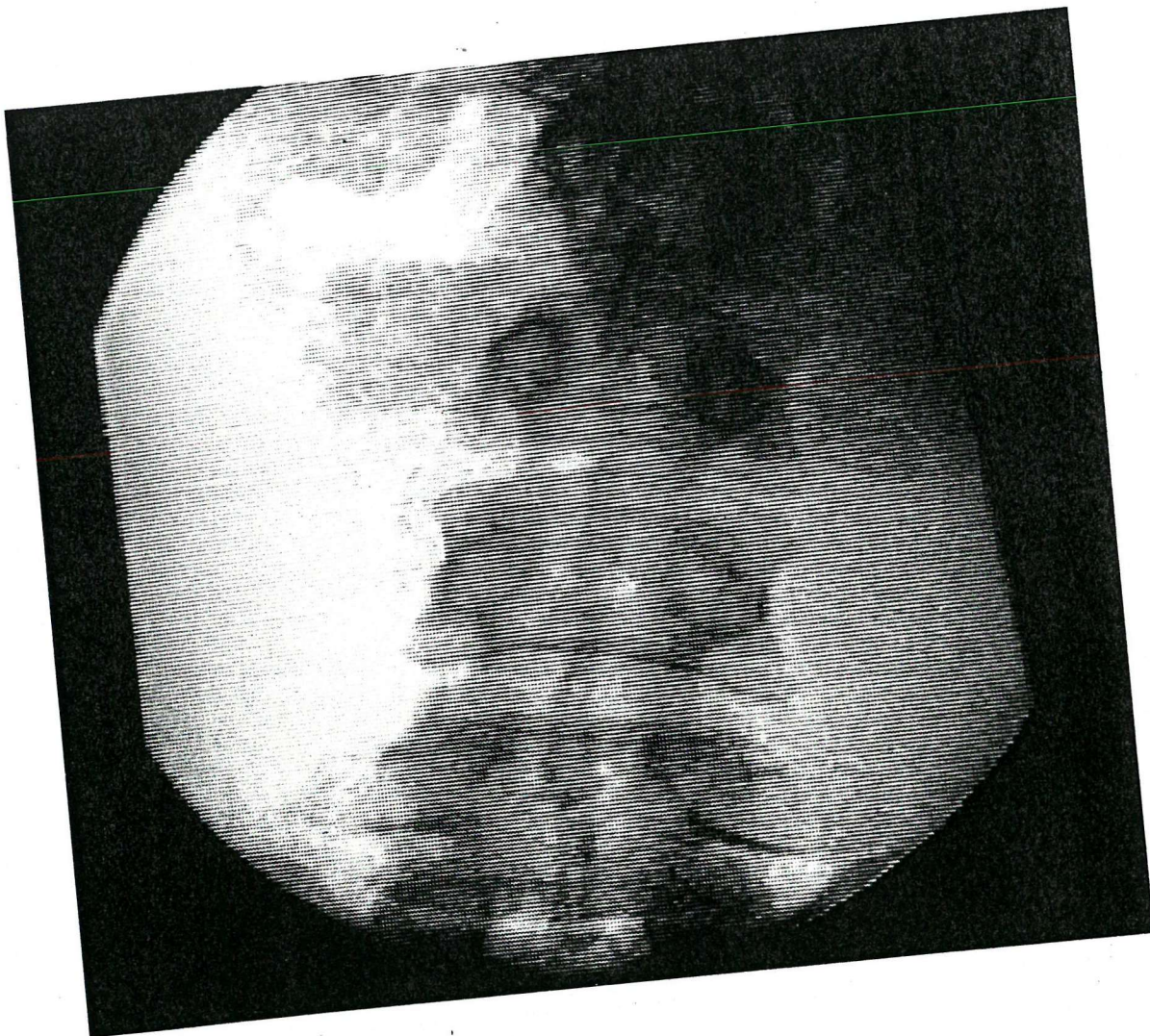
FIGURE 65a



IMAGES OF THE EXTREMES OF RIGHT SIDEBENDING  
MOTION IN PATIENT 3

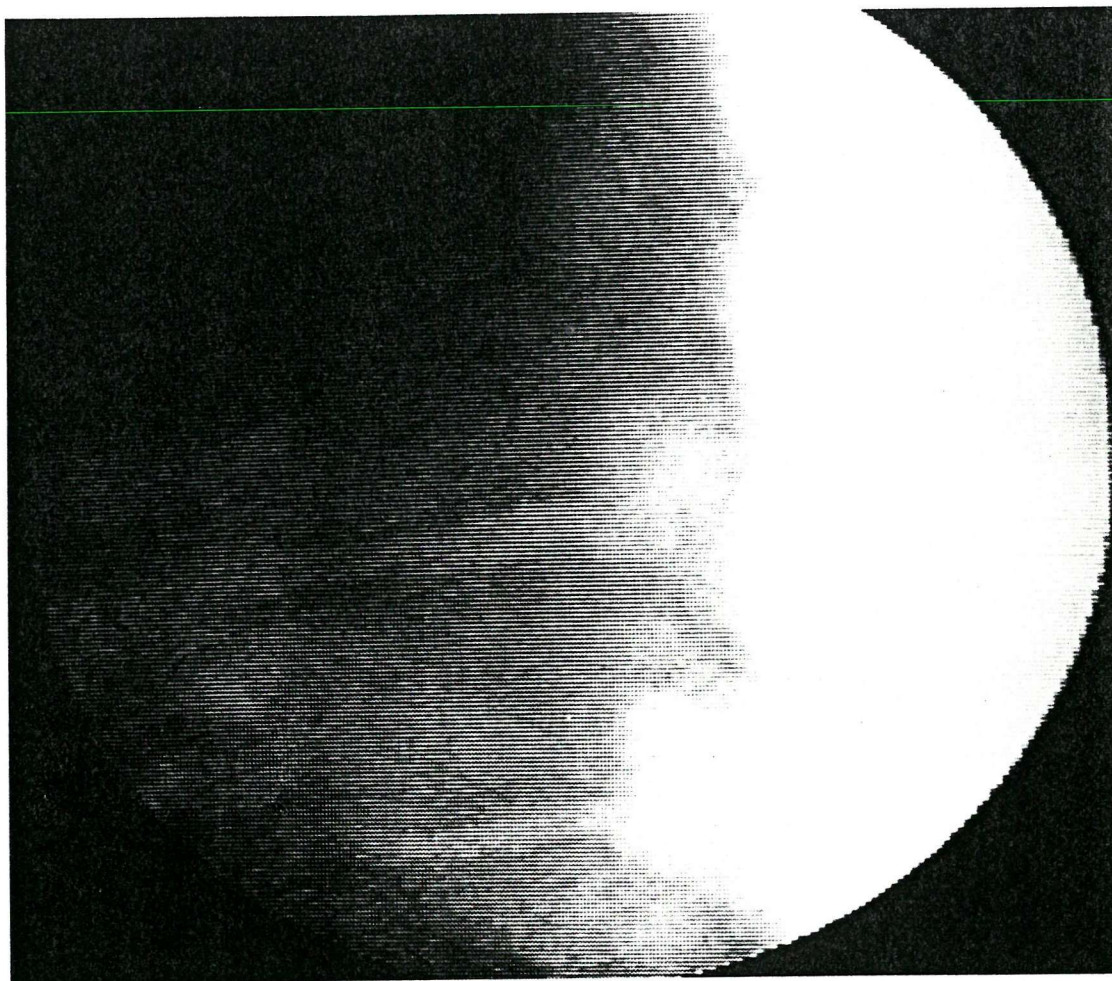


FIGURE 65b



IMAGES OF THE EXTREMES OF LEFT SIDEBENDING  
MOTION IN PATIENT 3

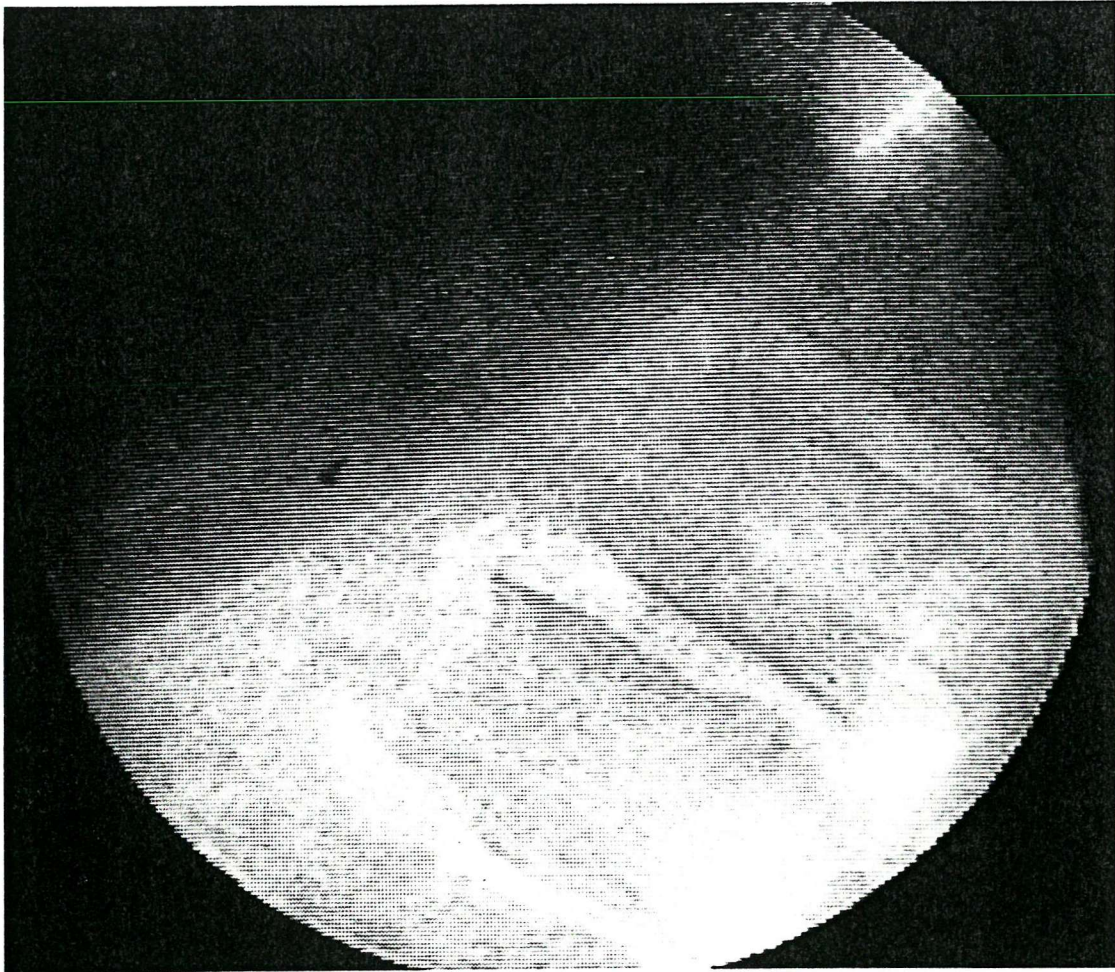
FIGURE 65c



IMAGES OF THE EXTREMES OF FLEXION  
MOTION IN PATIENT 3

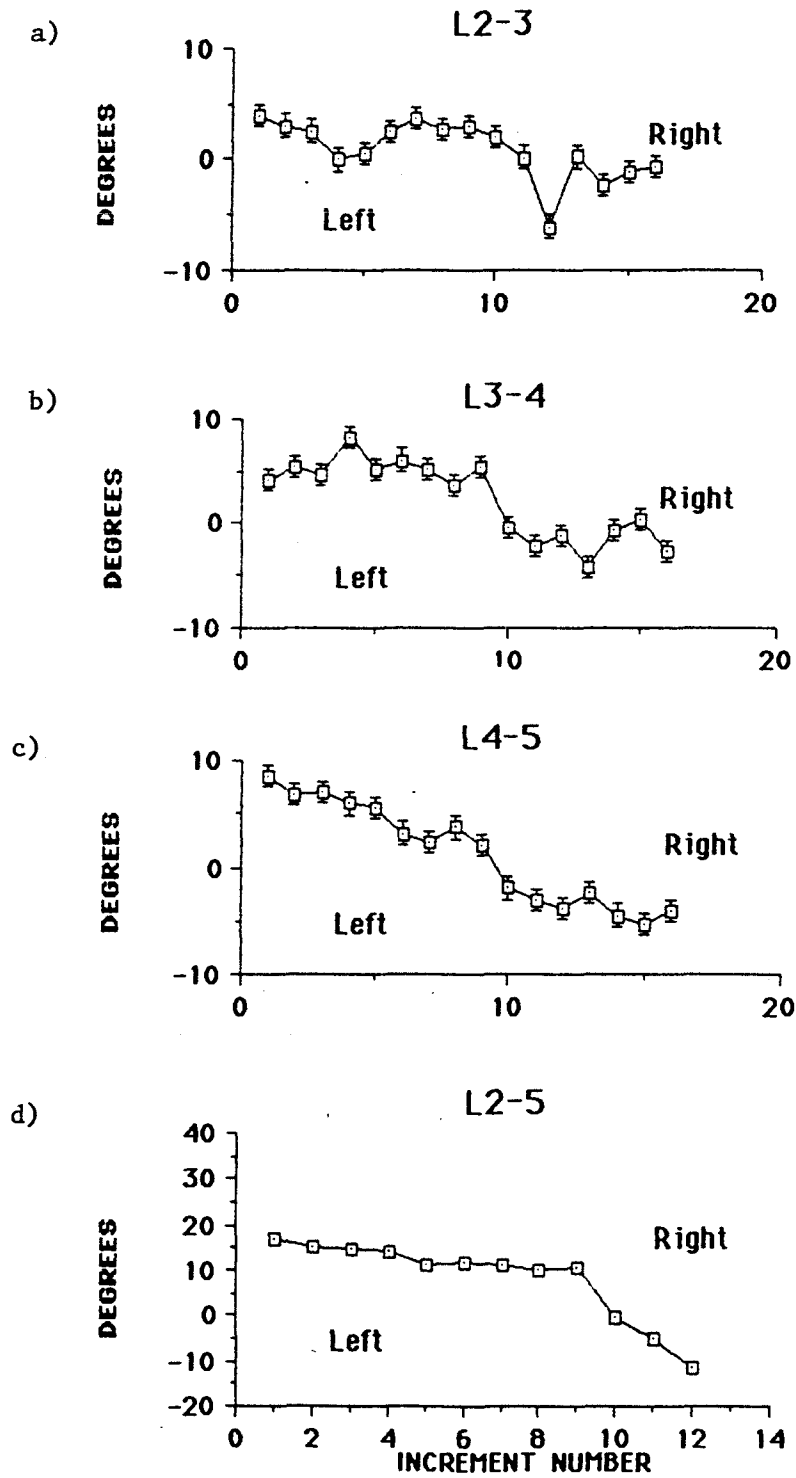


FIGURE 65d



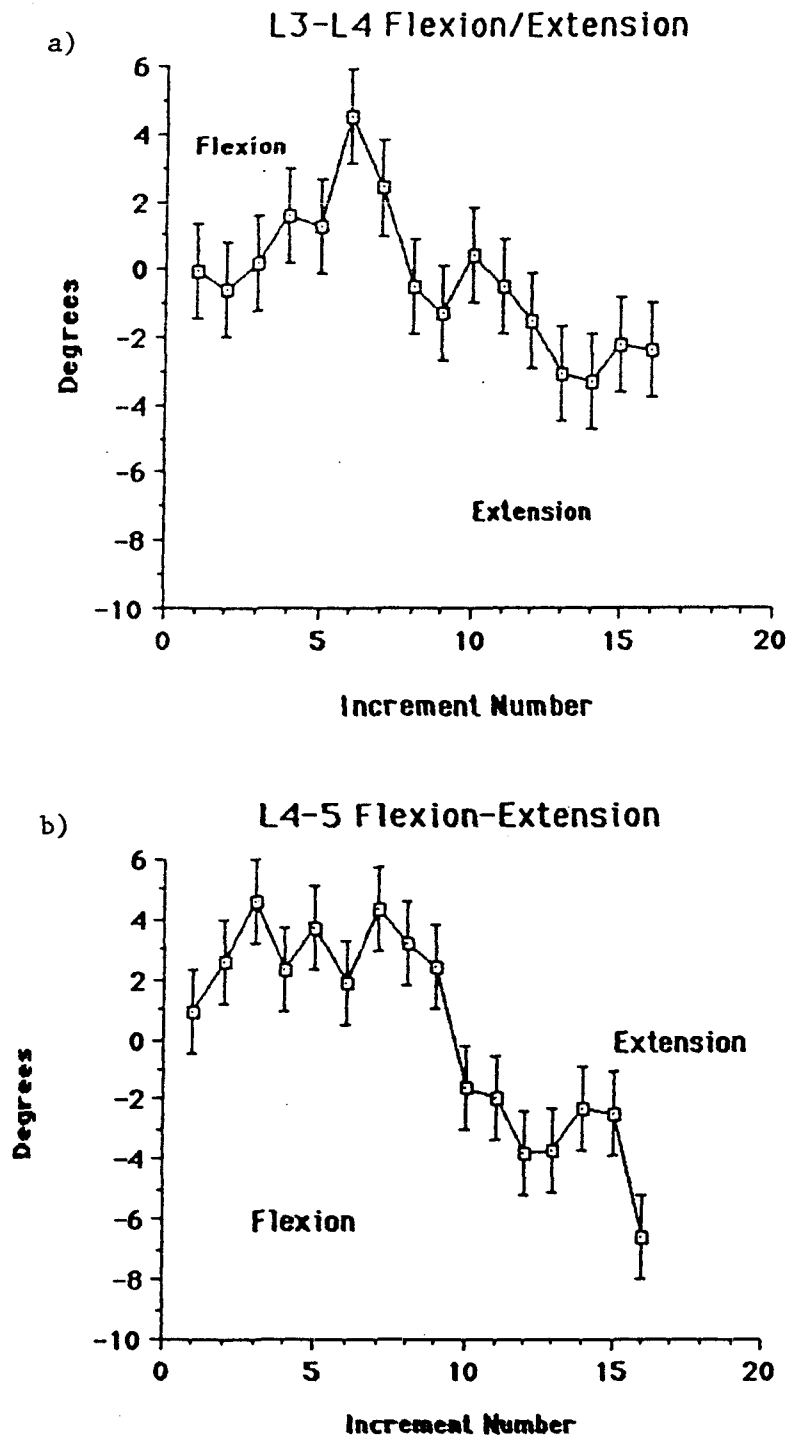
IMAGES OF THE EXTREMES OF EXTENSION  
MOTION IN PATIENT 3

FIGURE 66



GRAPHS SHOWING 12 INCREMENTS OF SIDEBENDING  
FOR L2-5 IN PATIENT 3

FIGURE 67



GRAPHS SHOWING 16 INCREMENTS OF FLEXION-EXTENSION  
AT L3-4 and L4-5 IN PATIENT 3

From Figures 65a and b and 66d it can be seen that left side bending is more restricted than right and coupled motion is lost in left side bending. The right side bend overall appears related to activity at the L2-3 and L3-4 levels.

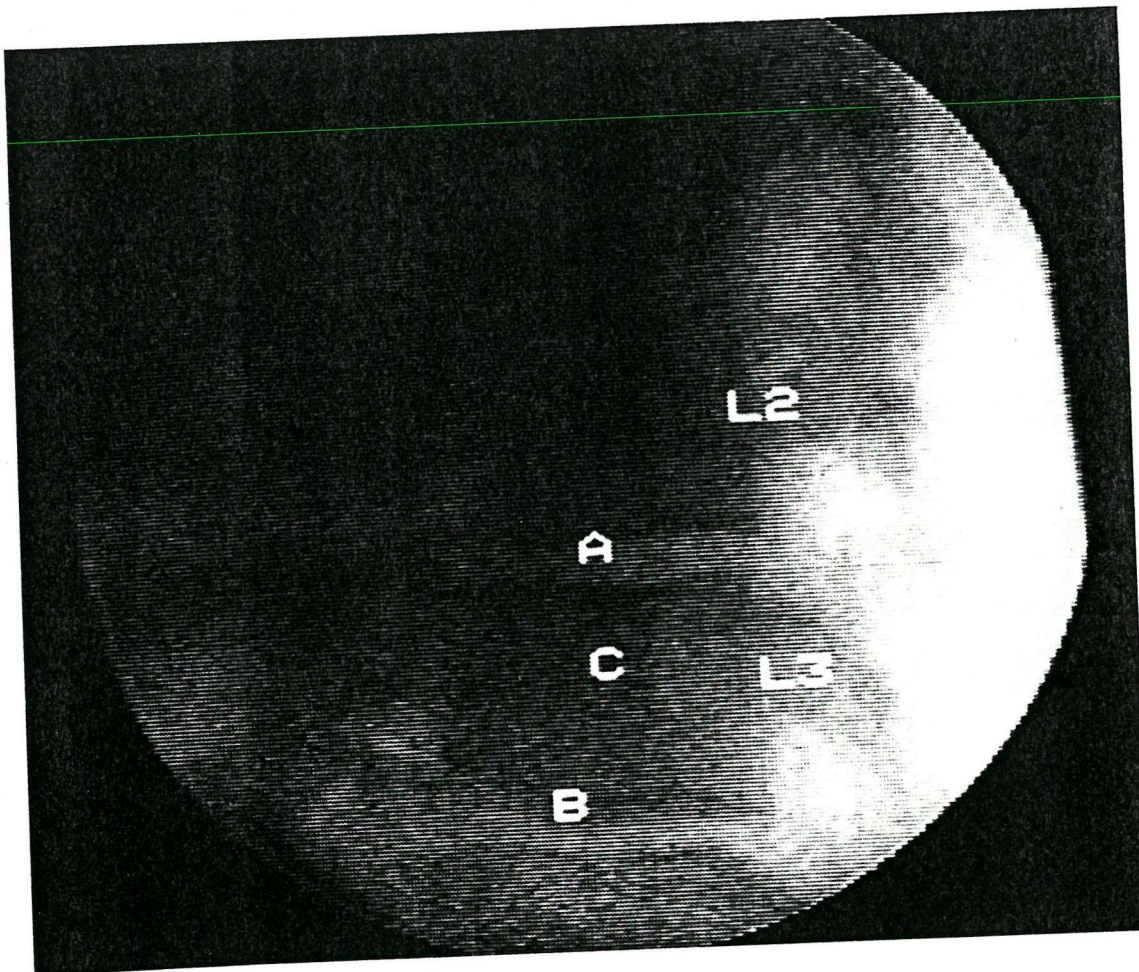
For sagittal plane motion at L3-4, there is clearly a phase of flexion, even though the trunk as a whole is extending. At L4-5, this extension motion is rather sudden, perhaps suggesting loss of tension in the holding ligaments at that level. The ranges of rotation are less than  $7^{\circ}$  in both directions at L3-4, therefore an ICR was not determined at this level. However, there did seem to be a transient reversal of the direction of the rotation at this level in the sagittal plane. Posterior slippage of L2 on L3 was suggested by the appearance of the extension view (Figure 65d), and two overlapping ICRs plus the overall ICR were calculated for this level. The results can be seen in Figure 68, in which the ICR (B), which represents the extension phase, drops well below the inferior border of L3, suggesting that this level, at least in extension, is unstable.

The ICR tracks for L3-4 and L4-5 are well contained and are of about 12mm diameter (Figure 69). These are based on up to 5 overlapping increments of at least  $7^{\circ}$ . It was not possible to determine the ICRs for L2-3 in this plane because of the length of the lumbar spine in this rather tall individual. This denies us, for the present, information about the stability of this segment in the coronal plane and points to one requirement in future work, namely the use of the largest-possible diameter intensifier.

In summary, the use of the technique in this patient allows the confirmation of excessive translation in sagittal plane motion at L2-3; however, the interpretation of the rotations must await further detailed studies of normals and other symptomatic subjects.

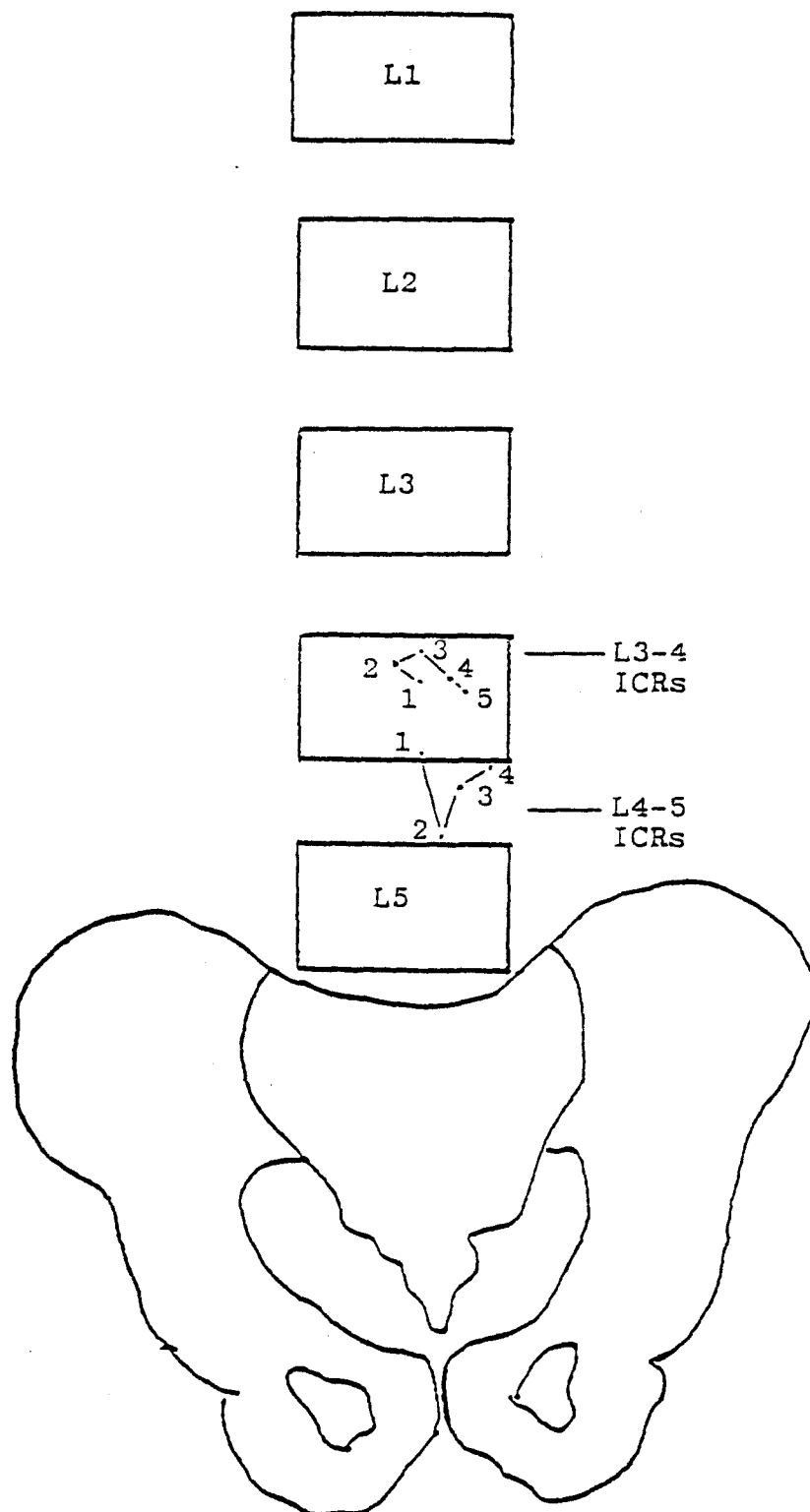


FIGURE 68



ICRs FOR SAGITTAL PLANE MOTION AT L2-3 IN PATIENT 3  
(A = FLEXION PHASE, B = EXTENSION PHASE,  
C = OVERALL MOTION)

FIGURE 69



TRACK OF ICRs FOR CORONAL PLANE ROTATIONS AT  
L3-4 and L4-5 IN PATIENT 3

### 15.1 A Procedure for Processing Patient Files

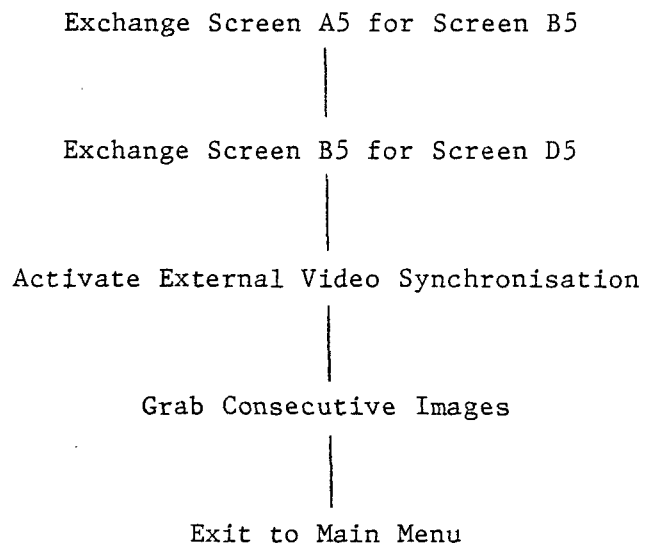
Experience with both volunteer and patient subjects suggested possibilities for streamlining the image processing and a procedure for doing this is summarised in the flow diagram below. It was noticed, for example, that traces of the monitor's startup test pattern were left imposed on the first images to be digitised from videotape in a given session. This required clearing screens and preparing to grab images. The following batch of commands, activated by a single initial command, was used to achieve this. (See Appendix IIc for command sequence.)

```
Clear A5 to grey level 100
|
Clear B5 " " " "
|
Clear C5 " " " "
|
Clear D5 " " " "
|
Select 256x256 pixel mode
|
Set to grab consecutive images
```

As stated above, patients were asked to bend from the neutral position to the extremes of the plane required, thus giving two separate motion sequences. Since 16 images would fit a single file, a procedure was

established which would grab 8 in either direction. To prepare for this, the above batch file also set up the computer to receive 256x256 pixel images and placed it in external synchronisation mode. The grab command (GRAB WSQ 8 n;), was then entered where n is the time interval between frames.

Once the series of 8 images had been digitised, it was then necessary to move them to a different part of the frame buffer (see Figure 19) in order to make space for the next 8 images. (See Appendix IIId for command sequence). This was also done by a batch command which achieved the following:



The next set of 8 images was then digitised using the same command (GRAB WSQ 8 n;).

To place the 16 digitised images in a numbered order so that they could be previewed in sequence throughout the motion, a further batch command was used. This began by re-ordering the images and ended by assigning numbers on the screen (See Appendix IIe) for command sequence).

Previewing the images in sequence was reminiscent of watching them on videotape. The smaller number of frames, played at a convenient speed and constantly repeated, was a useful feature for visual assessment of individual segmental levels for comparison with the later computed indices. It also allowed the operator to anticipate any landmark which may become obscure, or travel off the screen during the sequence. Previewing required the following commands:

```
MOD SYNCI;
```

```
GRAB RSQ 16 8 8;
```

The sequence could be stopped by pressing any key.

## 15.2 Pre-Processing Prior to Co-ordinate Marking

In order to anticipate observer errors, operators could measure the intervertebral angles in all relevant vertebrae 10 successive times using the frame which was thought to present the lowest quality image. Two standard deviations of the mean result might then be used as the error, provided this exceeded the variation determined from the calibration studies by the same observer.

Subjectively, improvement in poorly definable edges for marking was sometimes possible using linear contrast stretching. Comprehensive testing of the effects of this on observer error variability was not carried out; however, it often increased operator confidence in placing co-ordinates. This procedure involves determining the grey scale range within a cursor area, selected closely around the

vertebrae to be marked, then expanding this range to the full extent allowed by the system (256 grey levels).

Perusal of the intervertebral angles makes clear the prospects for ICR calculation. A rotation of, for example,  $7^\circ$  between two vertebrae would allow for only one ICR calculation, whereas an increment of  $20^\circ$  would allow several equal and overlapping increments to be used. The practicability of determining ICRs in a given subject rests initially on the range of rotation and on the quality of the image. Five calculations of a single ICR at each level was used to determine the circle of repeatability, provided this exceeded the calibration error.

#### 16.0 CONCLUSION, FURTHER WORK AND FUTURE TRENDS

This thesis has proposed a technique for obtaining kinematic information about the intervertebral linkages and has shown that this can be achieved with acceptable accuracy and low radiation dosage by digitising images from videofluoroscopy. The calibration studies have indicated the accuracy of the present system from ideal to extreme conditions. This accuracy could undoubtedly be improved by averaging and Cholewicki et al, (50) in a recent publication using a similar system, have suggested that for determining rotations 4 repetitions is the optimum for maximising this effect. This, however, begins to defeat the object of reducing the laboriousness of exhaustive repetitions of observations and is the main reason why the results given here have largely excluded the effects of averaging.



The calibration of rotational motion has produced a methodology which is capable of usefully measuring angles greater than about  $2^{\circ}$  with no systematic error related to size of angle. For human subjects, the application of this across a whole motion range raises the question of optimum sampling of images. It would probably be quite acceptable, for most clinical purposes, to sample 16 frames instead of 32. This must be considered in relation to frequency and to the velocity of the motion performed by the subject, which should, as far as possible, be standardised. The question of whether motion is best performed as one, or in two separate sequences of neutral to extreme in either direction was, for this work, determined by the diameter of the image intensifier. This was not large enough to image, from one positional setting, the whole range of motion. However, it is suggested that a "neutral to extreme in each direction" protocol would best avoid artefacts in relation to differences in kinematic profile in each direction. Overall, there is room for greater standardisation in relation to radiography than was possible here.

The determination of ICRs appears, so far, to be satisfactory. Using the present technique, which takes note of previously reported work into optimisation (49), ICRs for the lumbar spine in the asymptomatic volunteer subjects seem consistent with what appears in the literature. Similar work in the cervical spine seems to benefit from the use of image enlargement. The limitations of accuracy with respect to ICRs do, however, need to be scrupulously borne in mind. Foremost among these is the necessity that the vertebra in question rotates by at least  $7^{\circ}$ . This allows for at least one ICR location,

which is still valuable evidence of the presence or absence of abnormally large translations. (Multiple ICRs show how the translation is distributed throughout the rotational range).

No conclusions can be drawn about the significance of irregular motion from the human subject studies reported here. This is clearly beyond the scope of the present work. Future work, however, should establish the kinematic characteristics in symptomatic and asymptomatic populations. This should be studied in relation to other clinical findings in order to provide coherent diagnostic categories.

Improvement in the appearance of the images in these studies was limited to the use of linear contrast stretching and did, subjectively, increase operator confidence in co-ordinate placement with some images. However, doubt remains as to whether this actually confers both accuracy and precision. The whole question of the influence of image quality on reliability of marking is an open one which will require studies involving various aspects of images. For the present, an intra-observer study of at least one of the calculations for each patient, plus the use of averaging, should keep the limitations of the technique in perspective.

As new forms of imaging emerge, fluoroscopy may cease to be the most appropriate technique. However, this must be approached with discernment. Magnetic resonance, although attractive for the appearance of the images it provides, offers the engineer a slice which changes its outline for each position. Moreover, natural

movement of the spine within body coils is not an option in the foreseeable future. However, new and innovative techniques employing the principles developed in this study should be adaptable to suit many imaging systems.

#### 16.1 Extension into 3-D

Future advances in this technique would include its extension to 3-D, the standardisation and automation of the procedures (both computing and radiographic) and the addition of display graphics and statistics to the output. Central to this would be the development of a biplanar videofluoroscopic system for orthogonal, low-dose in vivo imaging of the human spine in motion. This would require an X-ray machine with two tubes and intensifiers, capable of synchronous, alternative pulsing which would reduce the already low radiation dosage considerably. No such system currently exists commercially and it would require some simple adaptation of standard equipment to assemble it. The radiographic protocols would be rigorous and closely allied to ongoing image processing research. This would necessitate the use of more advanced patient stabilisation devices and surface goniometry to monitor overall body movements. This equipment could also incorporate the means to measure muscle activity during the motion and should be sited in close proximity to the laboratory where the analyses for clinical use would take place.

Such studies would initially involve the establishment of the smooth operation of the X-ray system in tandem with the current 2-D image processor. Concurrently, however, it would be necessary to create a

new image processing system which would be based on parallel processing, to provide a responsive and user-oriented interface through which spine kinematics could be determined in 3-D. This would involve supplying images to a transputer system for the initial 3-D reconstruction. The use of transputer arrays would also allow pseudo-3D views to be generated and played in sequence as movies using a realistic time scale. The power made available by parallel processing would, in addition, allow the operator to dynamically alter the viewpoint whilst observing the 3-D images.

Much more work needs to be done to improve the appearance of the images. Future work of the above nature would require a user interface which would allow experimentation with a range of noise reduction filters, edge detection algorithms and image enhancement operations. Experience with the images used so far has highlighted the wide variety of image types which must be accommodated if the system is to be used comprehensively. If the operator is not satisfied with the quality of an automatically produced image, there should be available a multiple choice presentation panel with these different filters algorithms and operations.

The calculation of segmental kinematics would, as before, proceed from user-determined screen co-ordinates. However, assuming rigid body conditions for the vertebrae, the track of each one could be calculated from one view to the next. This would greatly reduce the laboriousness of the data input operations.

Under 3-D conditions, mathematical description of clinical problem types would be possible. We have already provided a degree of numerical robustness in the calculation of ICRs, by providing a more appropriate algorithm for computation than that taken previously from the literature (Appendix III). The 3-D equivalent to this is the Helical Axis of Motion (HAM) or Screw Displacement Axis. Using this approach, the relative displacement of a vertebra from one position to another would be defined in terms of its rotation about, and translation along, the HAM. This potentially enables coupled motion to be included within the measurement. The use of the HAM in in vivo spinal kinematics has, until now, not been achievable, largely due to the complexity and laboriousness of its calculation. The more powerful computing procedures suggested here would make the use and development of the HAM a real possibility.

The HAM can be expected to be at least as sensitive to measurement errors as the 2-D ICR. However, by maximising the rotational increments involved as shown in this thesis for ICRs and by increasing the number of reference points on the moving image (40), these errors should be reducible. The problem of errors will continue to need special attention as will the degree of detail appropriate to the measurement of spinal kinematics. For screening purposes, there may be simpler approaches which this system would facilitate and these should be explored.

The socio-economic importance of mechanical disorders of the spine and the interest in objective kinematic information among engineers and

clinicians are such that these advances would be well worth attempting. Given, from this present work, the opportunity to gather such data in an essentially non-invasive way, the possibilities are tantalising.

## APPENDIX I

### SCALE OF THE PROBLEM OF BACK PAIN

The socio-economic effects of back pain and other mechanical musculoskeletal disorders are vast. When in the United Kingdom, in the mid-1970's, it was realised that the problem caused more working days lost to industry than strikes, a government working group (I1) was set up to consider the current provision for the care of sufferers and to make recommendations for change. At the time, the lost working time from back pain was 13 million days per annum. By 1987-88, this figure had grown to 46.5 million (I2).

The 1987-88 figures for spinal problems represented 12% of all incapacities, an increase by 3% of the 1982-83 statistics; however, for back pain, the % change was much higher at 26%. This is said to represent an estimated £1 billion cost to industry and 300,000 referrals to National Health Service Hospitals each year (I3).

The attention focused on spinal pain by such figures has led to renewed efforts to understand the conditions which cause it. These conditions are largely mechanical in nature (I2) and are difficult to classify in conventional terms. The reason for this is that their most consistent features are of a mechanical, rather than a pathological nature. The quantification of these mechanical features, a discipline in its infancy, is the issue which this thesis addresses.



## REFERENCES

I1 Department of Health and Social Security: Working Group on Back Pain. Report to the Secretary of State for Social Services. London:HMSO, 1979

I2 Statistical Tables Series - Back Disorders. Department of Health and Social Security. Newcastle Upon Tyne, 1989

I3 Glass JB. Acute lumbar strain: clinical signs and prognosis. Practitioner 1979;222:821-5

APPENDIX II  
COMMAND SEQUENCES FOR IMAGE PROCESSING

APPENDIX IIa  
FRAME-GRABBING FROM VIDEOTAPE - COMMAND SEQUENCE

Select 256x256 pixel mode	MOD XY256;
and synchronise with videotape	MOD SYNCE;
player. Grab 16 consecutive	GRAB CON;
images at 'n' separation.	GRAB WSQ 16 n;
(return to activate grab sequence)	
EX	
Write the result to	FILES WRITE (device) (filename) (global);
the hard disc.	

APPENDIX IIb

MARKING AND CALCULATION OF ONE VERTEBRAL ANGLE

COMMAND SEQUENCE

Set to input	AR ANDC A1 254;
a linear construction	EX
	CO GRA 7;
Overlay cursor	CO OV 1 0 255 0;
(green) on grey background	CURS OV=1;
image.	VEC A1 255 -1;
	THRE LO A1 A1 255 0;
Digitise 2 co-ordinates	EX
and return cursor colour	AR INV A1;
to grey.	EX
	AR INV A1;
	EX
Search for and label	BIN LAB A1 A1;
the resulting line and	STA A1 6 3;
display the angle which	EX
the line subtends with	CO GR;
the monitor's x-axis.	SGEO IMAG H1 A1 3;
	EX

## APPENDIX IIc

### CLEAR ALL SCREENS AND SYNCHRONISE WITH VIDEO

Clear A5, B5,

C5, D5 to grey

level 100.

ARI CLEAR A5 100;

CLEAR B5 100;

CLEAR C5 100;

CLEAR D5 100;

EX

Select 256x256 pixel

mode and synchronise with

with video player to grab

consecutive images.

MOD XY256;

MOD SYNCE;

GRAB CON;

APPENDIX II d

PREPARE FOR SECOND SET OF 8 IMAGES

Exchange screens containing	EXCH A5 C5;
images for blank screens	EXCH B5 D5;
which will receive next set	MOD SYNCE;
of 8 images.	GRAB CON;
	EX

## APPENDIX IIe

### ORDER AND NUMBER DIGITISED IMAGES

1. Rearrange screens so  
that when played in  
sequence, images will  
be in order.  
  
EXCH A5 C5;  
  
EXCH A1 A4;  
  
EXCH A2 A3;  
  
EXCH A5 C5;  
  
EXCH A5 D5;  
  
EXCH A1 A4;  
  
EXCH A2 A3;  
  
EXCH A5 D5;  
  
EXCH C5 A5;
2. Place lettering in peak  
white at defined position  
in screens A<sub>1</sub>, A<sub>2</sub>, A<sub>3</sub>, A<sub>4</sub>.  
  
ASCII A1 255 10 10 BA=0 HI=2;  
  
01;  
  
ASCII A2 255 10 10 BA=0 HI=2;  
  
02;  
  
ASCII A3 255 10 10 BA=0 HI=2;  
  
03;  
  
ASCII A4 255 10 10 BA=0 HI=2;  
  
04;
3. Exchange the previous  
large screen (A<sub>5</sub>) just  
labelled for the next  
screen (B<sub>5</sub>) containing 4  
images and repeat the  
labelling procedure.  
  
EXCH A5 C5;  
  
EXCH A5 D5;  
  
ASCII A1 255 10 10 BA=0 HI=2;  
  
05;  
  
ASCII A2 255 10 10 BA=0 HI=2;  
  
06;

4. Repeat Stage 3

for next large screen.

ASCII A3 255 10 10 BA=0 HI=2;

07;

ASCII A4 255 10 10 BA=0 HI=2;

08;

EXCH A5 D5;

EXCH A5 B5;

ASCII A1 255 10 10 BA=0 HI=2;

13;

ASCII A2 255 10 10 BA=0 HI=2;

14;

ASCII A3 255 10 10 BA=0 HI=2;

15;

ASCII A4 255 10 10 BA=0 HI=2;

16;

5. Repeat Stage 3

for last large screen.

EXCH A5 B5

ASCII A1 255 10 10 BA=0 HI=2;

09;

ASCII A2 255 10 10 BA=0 HI=2;

10;

ASCII A3 255 10 10 BA=0 HI=2;

11;

ASCII A4 255 10 10 BA=0 HI=2;

12;

## APPENDIX III

### I.C.R. PROGRAMME

```
::MODUL-HEADER::/##/

# MODUL-NAME: UICR.PAS

#ENVIRONMENT: PASCAL

# TYPE: kimagenametype

# GLOBAL: incos0simage

# SUB-MODULS:

# DECLARATION:
# DESCRIPTION: PROCEDURE TO CALCULATE AND DISPLAY I.C.R.

      (ALSO IMPOSES A RIGID BODY CONSTRAINT ON THE IMAGES
      OF EACH MOTION SEGMENT, THEREBY, HOPEFULLY REDUCING
      OPERATOR READING ERRORS).

::MODUL-HEADER-END::

>

procedure UICR;

type
  intarray = ARRAY[1..11,1..2,1..9] of integer;
  realarray1 = ARRAY[1..11,1..2] of real;
  realarray2 = ARRAY[1..11,1..2,1..3] of real;
  realarray3 = ARRAY[1..11,1..2,1..9] of real;
  smallstring = PACKED ARRAY[1..6] of char;
  smallarray = ARRAY[1..2] of smallstring;
  namearray = ARRAY[1..16] of kimagenametype;

var
  icrexit: boolean;
  imagecode,chan,chan1,xpos,ypos,xrad,yrad,shapecode: integer;
  ercode,nopics,nopnts,lastchannel,v: integer;
  x,y,xstore,ystore: intarray;
  theta: realarray1;
  avx,avy: realarray2;
  pic,picref: kimagenametype;
  name: namearray;
  lowup: smallarray;

procedure VALUES(var x,y: intarray);

var
  im,ver,n: integer;
```



```

begin
  for im := chan to lastchannel do
    for ver := 1 to 2 do
      for n := 1 to nopnts do
        writeln('VALUES of x and y[im,v,n]: ',x[im,ver,n],y[im,ver,n],
              im,ver,n);
      end;
    end;
  end;

procedure ERROR(rcode: integer);

begin
  writeln('error text',rcode);
  {calls error text from incose.txt using rcode}
  {may be easier to do it direct}
end;

procedure SETUP(var rcode: integer);

const
  icrinfo = 11;

begin
  rcode := 0;
  chan := 9;
  lowup[1] := 'Lower ';
  lowup[2] := 'Upper ';

  MPRINT(icrinfo);

  name[1] := 'C1';
  name[2] := 'C2';
  name[3] := 'C3';
  name[4] := 'C4';
  name[5] := 'D1';
  name[6] := 'D2';
  name[7] := 'D3';
  name[8] := 'D4';
  name[9] := 'A1';
  name[10] := 'A2';
  name[11] := 'A3';
  name[12] := 'A4';
  name[13] := 'B1';
  name[14] := 'B2';
  name[15] := 'B3';
  name[16] := 'B4';

end;

procedure INPUTS(var nopics,nopnts,chan,lastchannel: integer;
                var pic: kimagenametype);
var
  count: integer;

```

```

begin
  writeln('How many images do you wish to use?');
  readln(nopics);
  {error check}
  writeln('How many points on each vertebra do you wish to digitise?');
  readln(nopnts);
  {error check}
  writeln('Please enter the name of the first image {eg. A3} ....');
  MIMAGT(pic);
  {error and capital check}

  for count := 1 to 16 do
    if name[count] = pic then chan := count;

  lastchannel := chan + nopics - 1;
  if lastchannel > 16 then ERROR(1);

end;      inputs

procedure PLOT(xpos,ypos,image,hheight,hwidth : integer);
var
  colour,counter : integer;
  pic : kimagenametype;

  procedure POINT(xpos,ypos: integer;
                  pic: kimagenametype);

  begin

    KWDWCH(pic,false,1,rcode);
    KPNTGW(1,ypos,xpos,colour);
    if colour > 127 then colour := colour - 128
      else colour := colour + 128;
    KWDWCH(pic,true,1,rcode);
    KPNTPW(1,ypos,xpos,colour);

  end;

begin

  pic := name[image];

  for counter := (ypos-hheight) to (ypos+hheight) do POINT(xpos,
    counter,pic);
  for counter := (xpos-hwidth) to (xpos+hwidth) do POINT(counter,
    ypos,pic);
end;

Procedure DIGITISE(var x,y : intarray;
                   nopics,nopnts,chan,lastchannel: integer;
                   pic: kimagenametype);

```

```

const
  lineref = 1;
  line = 2;

var
  linref,channel,point,v,p: integer;
  indum: char;

begin
  picref := incos0simage;
  linref := lineref;

  for channel := chan to lastchannel do begin

    pic := name[channel];

    if channel = chan then
      KWDWCH(pic,true,line,rcode)
    else
      KWDWCH(name[channel-1],true,line,rcode);

    KWDWCH(picref,true,lineref,rcode);
    UEXCHA(lineref,line,rcode);

    xpos := 128;
    ypos := 128;
    if channel = chan then begin
      xrad := 8;
      yrad := 8;
      shapecode := 1;
    end;

    rcode := 0;

    for v := 1 to 2 do begin

      point := 0;

      repeat
        point := point + 1;
        for p := 1 to 3 do writeln(' ');

        if (v<>1) or (point<>1) then begin
          writeln('Would you like to change the position of the
                    last point ?');
          writeln(' ');
          writeln('          Y (yes) or RETURN (no)');
        end
      else begin
        for p := 1 to 2 do writeln(' ');
        writeln('          Press return for next position.....');
      end;
    end;
  end;

```

```

        writeln(' ');
        writeln('New position: ',lowup[v],' Vertebra. Point no. ',
            point);
        for p := 1 to 2 do writeln(' ');
        read(indum);

        if (indum = 'y') or (indum = 'Y') then begin
            point := point - 1;
            writeln('      Please enter new position for point no. ',
                point);
            PLOT(x[channel,v,point],y[channel,v,point],channel,2,2);
        end;
        KWDWCH(picref,true,lineref,ercode);
        CURSOR(linref,xpos,ypos,xrad,yrad,shapecode,ercode);
        x[channel,v,point] := xpos;
        y[channel,v,point] := ypos;

        PLOT(x[channel,v,point],y[channel,v,point],channel,2,2);

        until point = nopnts;
    end;

    if channel = lastchannel then
        KWDWCH(picref,true,lineref,ercode)
    else
        KWDWCH(name[channel+1],true,lineref,ercode);

        KWDWCH(pic,true,line,ercode);
        UEXCHA(lineref,line,ercode);
    end;

end;                                {digitise procedure}

procedure STORE(var x,y,xstore,ystore: intarray);

var
    im,m,n: integer;

begin
    for im := chan to lastchannel do
        for m := 1 to 2 do
            for n := 1 to nopnts do begin
                xstore[im,m,n] := x[im,m,n];
                ystore[im,m,n] := y[im,m,n];
            end;
        end;
    end;                                {store procedure}

Procedure RIGIDBODY(chan,lastchannel,nopnts,v : integer;
    var x,y: intarray;
    var theta: realarray1;
    var avx,avy: realarray2);

```

```

var
  th,meanx,meany,dy,dx,ty,tx : realarray3;
  first : boolean;
  q,im,iml,s,sy,sx,toty,totx,sumy,sumx,n : integer;
  sum,f,a,chi : real;

procedure ANGLEROT(first : boolean;
                   chan,im,nopnts : integer;
                   var x,y: intarray;
                   var theta: realarray1;
                   var avx,avy: realarray2);
var
  n,m : integer;
  pause:integer;
begin
  rewrite (OUTPUT,'LS:');

  f := 0;
  toty := 0; totx := 0;
  for n := 1 to nopnts do begin
    m := n;
    if m = nopnts then m := 0;
    dx[im,v,n] := x[im,v,m+1] - x[im,v,n];
    dy[im,v,n] := y[im,v,m+1] - y[im,v,n];
    if sqr(dx[im,v,n] < 0.001 then dx[im,v,n] := 0.001;
    th[im,v,n] := arctan(dy[im,v,n]/dx[im,v,n]);

    toty := toty + y[im,v,n];
    totx := totx + x[im,v,n];
  end;

  theta[im,v] := 0;
  f := 2 * 3.14;
  avy[im,v,1] := toty/nopnts;
  avx[im,v,1] := totx/nopnts;
  if not first then begin
    while sqr(f) > 1.0E-8 do begin
      sum := 0;
      for n := 1 to nopnts do
        sum := sum + th[im,v,n] - th[chan,v,n];
      s := 1;
      if sum > 0 then s := -1;
      for n := 1 to nopnts do
        th[im,v,n] := th[im,v,n] + (s*f);
        theta[im,v] := theta[im,v] - (s*f);

      f := f * 0.75;
    end;
  end;

```

```

    for n := 1 to nopnts do begin
        dy[im,v,n] := avy[im,v,1]-y[im,v,n];
        dx[im,v,n] := avx[im,v,1]-x[im,v,n];
        sx := 1; sy := 1;
        if dx[im,v,n] > 0 then sx := -1;
        if dy[im,v,n] > 0 then sy := -1;
        if sqr(dx[im,v,n]) < 0.001 then dx[im,v,n] := 0.001;
        a := sqrt(sqr(dy[im,v,n]) + sqr(dx[im,v,n]));
        chi := arctan(dy[im,v,n]/dx[im,v,n]) - theta[im,v];
        y[im,v,n] := trunc(avy[im,v,1] + sy * (a*sin(abs(chi))));
        x[im,v,n] := trunc(avx[im,v,1] + sx * (a*cos(chi)));
    end;
end;

theta[chan,v] := 0;
end;                                { ANGLEROT procedure }

procedure CENTRALISE(chan,im,nopnts : integer;
                    var x,y: intarray;
                    var meanx,meany: realarray3);

var
    n : integer;

begin

    for n := 1 to nopnts do begin
        ty[im,v,n] := y[im,v,n];
        tx[im,v,n] := x[im,v,n];
    end;

    f := 200;
    sy := 1;
    sx := 1;
    while sqr(f) > 1E-6 do begin
        sumy := 0;
        sumx := 0;
        for n := 1 to nopnts do begin
            ty[im,v,n] := ty[im,v,n] + (f*sy);
            tx[im,v,n] := tx[im,v,n] + (f*sx);
            sumy := sumy + y[chan,v,n] - trunc(ty[im,v,n]);
            sumx := sumx + x[chan,v,n] - trunc(tx[im,v,n]);
        end;
        sx := 1;
        sy := 1;
        if sumy < 0 then sy := -1;
        if sumx < 0 then sx := -1;
        f := f * 0.75;
    end;

    for n := 1 to nopnts do begin
        y[im,v,n] := trunc(ty[im,v,n]);
        x[im,v,n] := trunc(tx[im,v,n]);
    end;

```

```

        meany[im,v,n] := (meany[(im-1),v,n]*(im-chan) + y[im,v,n])/2;
        meanx[im,v,n] := (meanx[(im-1),v,n]*(im-chan) + x[im,v,n])/2;
    end;
end;                                { CENTRALISE procedure }

procedure RESITE(im,nopnts : integer;
                 var theta: realarray1;
                 var avx,avy: realarray2;
                 var meanx,meany: realarray3;
                 var x,y: intarray);
var
    difavy,difavx,realy,realx : real;
    n : integer;

begin

    totx := 0; toty := 0;
    difavy := avy[im,v,1] - avy[lastchannel,v,2];
    difavx := avx[im,v,1] - avx[lastchannel,v,2];

    for n := 1 to nopnts do begin

        realy := meany[im,v,n] + difavy;
        realx := meanx[im,v,n] + difavx;
        y[im,v,n] := trunc(realy);
        x[im,v,n] := trunc(realx);
        dy[im,v,n] := avy[im,v,1] - y[im,v,n];
        dx[im,v,n] := avx[im,v,1] - x[im,v,n];
        sx := 1; sy := 1;
        if dx[im,v,n] > 0 then sx := -1;
        if dy[im,v,n] > 0 then sy := -1;
        if sqr(dx[im,v,n]) < 0.001 then dx[im,v,n] := 0.001;
        a := sqrt(sqr(dy[im,v,n]) + sqr(dx[im,v,n]));
        chi := arctan(dy[im,v,n]/dx[im,v,n] + theta[im,v]);
        realy := avy[im,v,1] + sy * a*sin(abs(chi));
        realx := avx[im,v,1] + sx * a*cos(chi);
        y[im,v,n] := trunc(realy);
        x[im,v,n] := trunc(realx);
        totx := totx + x[im,v,n];
        toty := toty + y[im,v,n];

    end;

    avx[im,v,3] := totx/nopnts;
    avy[im,v,3] := toty/nopnts;

end;                                { RESITE procedure }

begin                                { main body }

    first := true;
    im := chan;

```

```

    ANGLEROT(first,chan,im,nopnts,x,y,theta,avx,avy);

    first := false;

    for n := 1 to nopnts do begin
        meany[chan,v,n] := y[chan,v,n];
        meanx[chan,v,n] := x[chan,v,n];
    end;

    for im := (chan+1) to lastchannel do begin
        VALUES(x,y);

        ANGLEROT(first,chan,im,nopnts,x,y,theta,avx,avy);
        VALUES(x,y);
        CENTRALISE(chan,im,nopnts,x,y,meanx,meany);
        VALUES(x,y);

    end;
    toty := 0; totx := 0;
    for n := 1 to nopnts do begin
        toty := toty + trunc(meany[lastchannel,v,n]);
        totx := totx + trunc(meanx[lastchannel,v,n]);
    end;

    for im := chan to lastchannel do begin
        avy[im,v,2] := 0;
        avx[im,v,2] := 0;
    end;

    avy[lastchannel,v,2] := toty/nopnts;
    avx[lastchannel,v,2] := totx/nopnts;

    for im := chan to lastchannel do begin
        RESITE(im,nopnts,theta,avx,avy,meanx,meany,x,y);
    end;

end;                                { rigid procedure }

procedure CONSTRAINT(var x,y,xstore,ystore: intarray);

var
    im,m,n: integer;
    indum: char;

begin

close (OUTPUT);

    for n := 1 to 3 do writeln(' ');
    writeln('Do you want to apply a rigid body constraint ? ');
    writeln(' ');
    writeln('                                Y [yes] or N [no]..... ');

```



```

    for n := 1 to 2 do writeln(' ');
    read(indum);
    if (indum <> 'Y') and (indum <> 'y') then
        for im := chan to lastchannel do
            for m := 1 to 2 do
                for n := 1 to nopnts do begin
                    x[im,m,n] := xstore[im,m,n];
                    y[im,m,n] := ystore[im,m,n];
                end;
            end;
        end;

    { constraint procedure }

    procedure FINDICR(chan,lastchannel,nopnts: integer;
        var x,y: intarray;
        var avx,avy: realarray2;
        var theta: realarray1);
    type
        realarray4 = ARRAY[1..11,1..9] of real;
        intarray4 = ARRAY[1..11,1..9] of integer;
    var
        sx,sy,im,n,v: integer;
        a,e,f,g,x1,x2,x3,x4,y1,y2,y3,y4,totalx,totally,totang,chi: real;
        b,c,d,h,cosang,sinang,angrot,phil,phi2: real;
        xcr,ycr,xcr1,ycr1: integer;
        m1,m2,p,q,r: real;
        icrx,icry: intarray4;
        realicrx,realicry,angle: realarray4;
        dx,dy,xt,yt: realarray3;

    begin

    rewrite (OUTPUT,'LS:');

    for v := 1 to 2 do
        for n := 1 to nopnts do begin
            xt[chan,v,n] := x[chan,v,n];
            yt[chan,v,n] := y[chan,v,n];
        end;

    for im := (chan+1) to lastchannel do begin

        for n := 1 to nopnts do begin

            dx[im,2,n] := avx[im,1,3] - x[im,2,n];
            dy[im,2,n] := avy[im,1,3] - y[im,2,n];

            sx := 1; sy := 1;
            if dx[im,2,n] > 0 then sx := -1;
            if dy[im,2,n] > 0 then sy := -1;

```

```

    if sqr(dx[im,2,n]) < 0.001 then dx[im,2,n] := 0.001;
    a := sqrt(sqr(dx[im,2,n]) + sqr(dy[im,2,n]));
    chi := arctan(dy[im,2,n]/dx[im,2,n]) - (theta[im,1] - theta[(im-1),1]);
    xt[im,2,n] := avx[im,1,3] + sx * a * cos(chi);
    yt[im,2,n] := avy[im,1,3] + sy * a * sin(abs(chi));
    xt[im,2,n] := xt[im,2,n] - (avx[im,1,3] - avx[(im-1),1,3]);
    yt[im,2,n] := yt[im,2,n] - (avy[im,1,3] - avy[(im-1),1,3]);

end;

totalx := 0; totaly := 0; totang := 0;

for n := 2 to nopnts do begin

    x1 := xt[(im-1),2,(n-1)];    y1 := yt[(im-1),2,(n-1)];
    x2 := xt[im,2,(n-1)];        y2 := yt[im,2,(n-1)];
    x3 := xt[(im-1),2,n];        y3 := yt[(im-1),2,n];
    x4 := xt[im,2,n];            y4 := yt[im,2,n];

    phil := arctan((y3-y1)/(x3-x1));
    phi2 := arctan((y4-y2)/(x4-x2));
    angrot := phil-phi2;

{      The following block calculates the ICR}

    a := x1;      b := y1;
    e := x2;      f := y2;
    c := x3;      d := y3;
    g := x4;      h := y4;

    x1 := a + c;   x2 := e + g;
    y1 := b + d;   y2 := f + h;

    m1 := (a - c)/(d - b);
    m2 := (e - g)/(h - f);

    p := y1 - m1*x1;
    q := y2 - m2*x2;
    r := m2 - m1;

    xcr := round((p - q)/(2*r));
    ycr := round((m2*p - m1*q)/(2*r));

    writeln('Centre of rotation is at : ',xcr,ycr);
    writeln(' ');
    writeln('Angle of rotation is : ',(angrot*57.3),' degrees');

close(OUTPUT);

```

```

if      (xcr < 0) or (xcr > 255)
  or (ycr < 0) or (ycr > 255) then

  writeln('The I.C.R. is outside the screen')

else

  icrx[im,1] := xcr;
  icry[im,1] := ycr;

  PLOT(icrx[im,1],icry[im,1],(im-1),20,20);
end;
end;
end;

begin                                {main UICR procedure}

  SETUP(rcode);
  INPUTS(nopics,nopnts,chan,lastchannel,pic);
  DIGITISE(x,y,nopics,nopnts,chan,lastchannel,pic);
  STORE(x,y,xstore,ystore);
  for v := 1 to 2 do
begin
  RIGIDBODY(chan,lastchannel,nopnts,v,x,y,theta,avx,avy);
end;
VALUES(x,y);
CONSTRAINT(x,y,xstore,ystore);

  FINDICR(chan,lastchannel,nopnts,x,y,avx,avy,theta);

end;                                UICR procedure

```

## APPENDIX IV

### GLOSSARY OF TERMS

Aberrent Motion - Motion beyond physiological range or sequence

Ankylosing Spondylitis - An inflammatory rheumatic disease in which the spinal ligaments progressively calcify causing rigidity

Asymptomatic - Without symptoms

Cineradiography - A radiographic technique for obtaining motion X-rays using an image intensifier and a cine camera

Computed Tomography - A radiographic technique for obtaining transverse views of a body part

Contralateral - On the opposite side

Collagen - An organic substance which forms part of the tendons and ligaments of the body

Digital Subtraction Radiography - A radiographic technique normally used for the real-time imaging of vascular catheters

Discography - The X-ray imaging of the flow of contrast substance within the intervertebral disc

Dysesthesias - Tingling sensation in the distribution of a sensory nerve usually caused by its compression

Electrogoniometer - A device for measuring the angular movement of a joint in one plane using an electronic device such as a potentiometer or displacement transducer

Goniometer - A common type of commercially-available inclinometer using the bubble principle

Grey Level - A term used to describe the value given to the intensity of a picture element on a VDU

Image Intensifier - A device for amplifying the intensity of a fluorescent X-ray image for recording

Inclinometer - A device for measuring the angular movement of an object in one plane using a pendulum or bubble-suspended needle

Methylmethacryolate - An organic chemical used as a cement in orthopaedic surgery

Myelography - The x-ray imaging of the flow of contrast substance in the spinal canal

Neurogenic Claudication - Cramping of the legs on walking as a result of reduced blood flow around the lower spinal nerve roots

Osteolysis - Attenuation of bone

Palpation - Examination by feeling with the hands

Posterolateral - Towards the back and side

Proteoglycans - Organic molecules which are present as colloid in the intervertebral disc

Radiculography - The X-ray imaging of the flow of contrast substance around the nerve roots of the spine

Retroposition - Backward displacement

Roentgenography - A radiographic technique

Roentgenogram - An X-ray plate

Spine - Cervical	- A series of seven vertebrae contained in the neck
- Thoracic	- A series of twelve vertebrae contained in the thorax
- Lumbar	- A series of five vertebrae in the region of the loin
- Lumbosacral	- The junction between the lumbar spine and the sacrum below

Spinal Fusion - A surgical procedure for immobilising sections of the vertebral column

Spondylolisthesis - A spinal abnormality in which the body of a vertebra slips forward, away from its spinous process (see Figure 13), normally as a result of a defect in the neural arch between them

Stereoroentgenography - A radiographic technique for locating an object in 3-dimensional space utilising two X-ray sources

Stress Radiographs - X-rays taken at the extremes of joint range for investigating increased range of motion

Symptomatic - Having symptoms

Videofluoroscopy - A radiographic technique for recording moving X-ray images from an image intensifier using a TV camera

APPENDIX V  
RADIOGRAPHIC DATA PERTAINING TO THE SCREENING OF  
SIX VOLUNTEER SUBJECTS

X-ray factors

Name	Position	KV	Ma	Time (min)	Total
N. Hudson-Cook	A/P L	85	2	0.6	
	Lat L	125	2	1.1	
	A/P C	43	2	0.4	
	Lat C	64	2	0.2	2.3
C. Foley	A/P L	97	2	1.1	
	Lat L	125	3	1.0	
	A/P C	55	2	0.1	
	Lat C	43	2	0.9	3.1
R. Allen	A/P L	110	1	2.1	
	Lat L	94	2	1.1	
	A/P C	61	2	0.8	
	Lat C	58	2	2.1	6.1
R. Peach	A/P L	94	2	0.9	
	Lat L	124	2	1.4	
	A/P C	70	2	1.1	
	Lat C	70	2	2.0	5.8
A. Menzies	A/P L	73	2	0.6	
	Lat L	113	2	0.8	
	A/P C	58	1	0.5	
	Lat C	61	1	0.9	2.8
A. Parker	A/P L	82	2	0.7	
	Lat L	113	2	1.1	
	A/P C	58	1	0.6	
	Lat C	58	1	1.0	3.4
Average Screening Times By View					
	A/P L			1.0	
	Lat L			1.1	
	A/P C			0.7	
	Lat C			1.2	4.0

## APPENDIX VI

### LIST OF PUBLICATIONS FROM THIS RESEARCH

1. A Computer/X-ray Method for Measuring Spinal Segmental Movement - A Feasibility Study. Transactions of the Second Annual Conference of the Pacific Consortium for Chiropractic Research, Belmont, California, June 1987
2. Spine Kinematics: A Digital Videofluoroscopic Technique. Proceedings of the IEEE Engineering in Medicine and Biology Society 10th Annual International Conference, New Orleans, Nov. 1988
3. An Image Processing Method For Spine Kinematics - Preliminary Studies. Clinical Biomechanics - 1988;3:5-10
4. A Digital Videofluoroscopic Technique for Spine Kinematics. Journal of Medical Engineering and Technology - 1989;13:1/2:109-113
5. Spine Kinematics: A Digital Videofluoroscopic Technique. Journal of Biomedical Engineering - 1989;11:224-228
6. An Image Processing Technique for the Radiographic Assessment of Vertebral Derangements. Journal of Photographic Science - 1989;37:131-133

7. Image Presentations for Spinal Kinematic Analysis Using Digital Videofluoroscopy. Proceedings of the Third International Conference on Image Processing and its Applications - Electronics division of the Institution of Electrical Engineers, University of Warwick, July, 1989
8. The Digital Videofluoroscopic Assessment of Spine Kinematics. Proceedings of the International Conference on Spinal Manipulation - Foundation for Chiropractic Education and Research, Washington, DC, May, 1990
9. The Analysis of Spine Kinematics Using Digital Videofluoroscopy. Proceedings of the 7th Meeting of the European Society of Biomechanics Society, Aarhus, Denmark, July, 1990
10. The Analysis of the Stability of the Cervical and Lumbar Spines Using Digital Videofluoroscopy. (Abstract) Proceedings of the 6th IMEKO Conference on Measurement in Clinical Medicine and 8th Hungarian Conference on Biomedical Engineering, Sopron, Hungary, August 1990
11. Incremental Lumbar Spine Motion in the Coronal Plane: An Observer Variation Study Using Digital Videofluoroscopy. European Journal of Chiropractic - 1990;38:56-61
12. Integrated Spinal Motion: A Study of Two Cases. Journal of the Canadian Chiropractic Association - 1991;35(1):25-30.



PUBLICATIONS IN PRESS

1. Spinal Imaging and the Practice of Chiropractic" Mick T,  
Phillips RB, Breen AC. In: Modern Developments in the  
Principles and Practice of Chiropractic (2nd edn), Haldeman S. (ed),  
Appleton and Lange, Norwalk CT (in press)

## PRESENTATIONS AT MEETINGS

February 1987 - An Image Processing Method for Spinal Motion X-rays.  
Research Seminar, Anglo-European College of  
Chiropractic

September 1987 - An Image Processing Method for Spine Kinematics -  
Preliminary Studies. International Chiropractic  
Conference, London

November 1987 - Digital Videofluoroscopy in the Assessment of Spine  
Kinematics. Research Seminar, Thames Polytechnic

November 1987 - Incremental Motion in the Lower Lumbar Spine -  
An Image Processing Study. Research Seminar, Anglo-  
European College of Chiropractic

April 1988 - A Digital Videofluoroscopic Technique for Spine  
Kinematics. North Sea Conference on Biomedical  
Engineering (Meeting of the International  
Federation for Medical and Biological Engineering)  
Maastricht, Netherlands

June 1988 - Digital Image Processing of Videofluoroscopic  
Vertebral Images - A Calibration Study. Research  
Seminar, Department of Mechanical Engineering, Southampton  
University

September 1988 - Spine Kinematics: A Digital Videofluoroscopic  
Technique. 28th Annual Scientific Meeting of the  
Biological Engineering Society, Salford

September 1988 - An Image Processing Technique of the Radiographic  
Assessment of Vertebral Derangements. Annual Scientific  
Meeting of the Royal Photographic Society: Recent Developments  
in Medical Imaging, Bath

October 1988 - Spinal Segmental Motion: Relevance and Methods of  
Assessment. Multi-disciplinary conference of the  
Physical Medicine Research Foundation, Toronto

November 1988 - Spine Kinematics: A Digital Videofluoroscopic  
Technique. Poster presentation at the Tenth Annual  
International Conference of The Engineering in  
Medicine and Biology Society of the Institution of  
Electrical and Electronic Engineers (IEEE), New  
Orleans.

January 1989 - Digital Image Processing of Spinal Motion X-rays.  
Seminar at IBM (UK) Scientific Centre, Winchester

February 1989 - Tomorrows World feature - BBC Television, London

April 1989 - Computer Analysis of Spinal Motion X-rays.

British Chiropractic Association Conference,  
Bournemouth

July 1989 - Image Presentations for Spinal Kinematic Analysis

Using Digital Videofluoroscopy. Third International  
Conference on Image Processing and its Applications.

Institution of Electical Engineers, University of  
Warwick

September 1989 - Image Enhancement Techniques for Spinal Kinematic

Studies Using Digital Videofluoroscopy. 29th Annual  
Scientific Meeting of the Biological Engineering  
Society, University of Bristol

November 1989 - Lumbar Spine Instantaneous Centres of Rotation

Determined by digital Videofluoroscopy. Annual  
Scientific Meeting of the Society for Back Pain  
Research, St. Mary's Hospital, London

May 1990 - The Digital Videofluoroscopic Assessment of Spine

Kinematics. International Conference on Spinal  
Manipulation - Foundation for Chiropractic Education  
and Research, Washington, DC

July 1990        -   The Analysis of Spine Kinematics Using Digital  
Videofluoroscopy. 7th Meeting of the European Society  
of Biomechanics, Aarhus, Denmark

August 1990    -   The Analysis of the Stability of the Cervical and  
Lumbar Spines Using Digital Videofluoroscopy. 6th  
IMEKO Conference on Measurement in Clinical Medicine  
and 8th Hungarian Conference on Biomedical  
Engineering, Sopron, Hungary

May 1991        -   The Definition and Detection of Spinal Instability.  
Conference of the European Chiropractors' Union,  
Dublin

## REFERENCES

- 1) Dowson D. Basic mechanics. In: Introduction to the Biomechanics of Joints and Joint Replacement. 1981; Mechanical Engineering Publications Ltd
- 2) Nachemson A. Lumbar Intradiscal Pressure. In: The Lumbar Spine and Back Pain (2nd edition), ed. Jayson MIV p 341; Pitman Medical. 1980
- 3) Schultz AB, Warwick DN, Berkson MH, Nachemson AL. Mechanical properties of human lumbar spine motion segments. Part I. Responses in flexion, extension, lateral bending and torsion. J Biomech Eng 1979; 101:46-52
- 4) Hukins DWL. Properties of spinal materials. In: The Lumbar Spine and Back Pain. (3rd edition), ed. Jayson MIV p 138-160; Longman Group 1987
- 5) White AA, Panjabi MM. The basic kinematics of the human spine. Spine 1978;3:12-20
- 6) Dimnet J, Fischer LP, Gonan G, Carret JP. Radiographic studies of lateral flexion in the lumbar spine. Journal of Biomechanics 1978;11:143-150
- 7) Dimnet, J, Pasquet, A, Krag, MH, Panjabi, M.M. Cervical spine motion in the sagittal plane: kinematic and geometric parameters. Biomechanics 1982;15(12):959-969
- 8) Todd TW, Pyle IS. A quantitative study of the vertebral column by direct roentgenologic methods. Amer J Phys Anthr 1928;12:321
- 9) Gianturco C. A roentgen analysis of the motion of the lower lumbar vertebrae in normal individuals and in patients with low back pain. Amer J Roentgenol 1944;52:261
- 10) Hasner E, Schalimtzek M, Snorrason E. Roentgenological examination of the function of the lumbar spine. Acta Radiol 1952;37:141-149
- 11) Tanz SS. Motion of the lumbar spine. A roentgenologic study. Am J Roentgenol 1953;69(3):399-412
- 12) Voesner ME, Mitts MG. The evaluation of cervical spine motion below C2: a comparison of cineroentgenographic and conventional roentgenographic methods. Am J Roentgenol 1972;115;1:148-154
- 13) Jirout J. The normal mobility of the lumbosacral spine. Acta Radiol (Diagn) (Stockh) 1957; 47:345-348
- 14) Jirout J. Changes in the mobility of cervical vertebrae in the frontal and horizontal plane after manipulation of segmental blockade. Neurochir 1977;40(3):135-138

- 15) Jirout J. Correlations of the functional disturbances in the cervical spine as roentgenographically in frontal and sagittal projections. Acta Univ Carol. (Med) (Praha) 1965 Suppl 21:128-9
- 16) Jirout J. Patterns of change in the cervical spine on lateroflexion. Neuroradiology 1971;2:164-6
- 17) Jirout J. Persistence of the synkinetic patterns of the cervical spine. Neuroradiology 1979;18:167-71
- 18) Jirout J. Studies in the dynamics of the spine. Acta Radiol 1956: 46:55-60
- 19) Jirout J. The influence of postural factors on the dynamics of the cervical spine. Neuroradiology 1972;4:239-44
- 20) Jirout J. The mobility of the cervical spinal cord under normal conditions. Brit Jnl Radiology 1959;32(38):744-751
- 21) Wood PHN, Badley EM. Epidemiology of back pain. In: Jayson MIV (ed). The lumbar spine and back pain 3rd edn. 1987;1-15: Churchill Livingstone
- 22) Moll JMH, Wright V. Normal range of spinal mobility: An objective clinical study. Ann Rheum Dis 1971;30:381-386
- 23) Reynolds TMG. Measurement of spinal mobility: A comparison of three methods. Rheumatol Rehabil 1975;14:180-185
- 24) Pearcy MJ. Measurement of back and spinal mobility. Clinical Biomechanics 1986;1:44-51
- 25) Troup JDG, Hood CA, Chapman AE. Measurements of the sagittal mobility of the lumbar spine and hips. Ann Phys Med 1968;9:308-321
- 26) Kottke FJ, Mundale MO. Range of mobility of the cervical spine. Archives of Physical Medicine and Rehabilitation 1959;379-382
- 27) Gonnella C, Paris SV, Kutner M. Reliability in evaluating passive intervertebral motion. Phys Ther 1982;62:436-444
- 28) Hart FD, Rose SJ. Reliability of a non-invasive method for measuring the lumbar curve. Proceedings of International Society for the Study of the Lumbar Spine. 1982 Orthop Trans 1983;7:105-106
- 29) Pennal GF, Conn GS, McDonald G, Dale G, Garside H. Motion studies of the lumbar spine - a preliminary report. J Bone Joint Surg 1972;54B(3): 442-452
- 30) Coyle B. Accuracy of measurement from points marked on X-rays. Communication at the Second Annual Conference on Research and Education of the Pacific Consortium for Chiropractic Research, 1987, Belmont, California

- 31) Triano JJ. Accurate determination of motion from plane films. Communication at the 8th annual meeting of the American Society of Biomechanics, October 3-5, 1984; University of Arizona, Tucson
- 32) Dunham WF. Ankylosing spondylitis: Measurement of hip and spinal movements. British Journal of Physical Medicine 1949;12:126-129
- 33) Sturrock RD, Wojtulewski JA, Dudley Hart F. Spondylometry in a normal population and in ankylosing spondylitis. Rheumatology and Rehabilitation 1973;12:135-142
- 34) Pearcy MJ. Measurement of back and spinal mobility. Clinical Biomechanics 1986;1:44-51
- 35) Aho A, Vartianinen O, Salo O. Segmentary mobility of the lumbar spine in antero-posterior flexion. Ann Med Intern Fennae 1955; 44:275
- 36) Allbrook D. Movements of the lumbar spinal column. J Bone & Joint Surg 1957;39B,2:339-45
- 37) Bronfort G, Jochumsen OH. The functional radiographic examination of patients with low-back pain: a study of different forms of variations. Journal of Manipulative and Physiological Therapeutics 1984;7:89-97
- 38) Bakke SM. Rontgenologische Beobachtungen uber die Bewegungen der Wirbelsaule. Radiol 1931 (suppl 13) pp15,17,25,35,38,107,116
- 39) Colachis SC, Strohm BR. Radiographic studies of cervical spine motion in normal subjects: flexion and hyperextension. Arch Phys Med and Rehab 1965 Nov:753-60
- 40) An KN, Chao EY. Kinematic analysis of human movement. Annals of Biomedical Engineering 1984;12:585-597
- 41) Drerup B, Frobin W, Haussler G. Evaluation of bi-plane radiographs by epipolar ray correlation. Soc. Photo-Optical Inst Eng 1978;166:192-198
- 42) Tibrewal SB, Pearcy MJ, Portek I, Spivey J. A prospective study of lumbar spinal movements before and after discectomy using biplanar radiography - correlation of clinical and radiographic findings. Spine 1985;10:455-460
- 43) Rab GT, Chao EY. Verification of roentgenographic landmarks in the lumbar spine. Spine 1977;2:287-293
- 44) Pearcy MJ. Stereo radiography of lumbar spine motion. Acta Orthopaedica Scandinavia 1985;56(suppl. 212)
- 45) Pearcy M, Burrough S. Assessment of bony union after interbody fusion of the lumbar spine using a biplanar radiographic technique. J Bone and Joint Surg 1982;64B:228-232



- 46) Selvik G. Roentgen stereophotogrammetry in Lund, Sweden. Proceedings of the Society for Photo-Optical Instrument Engineering (SPIE), 1978;166:184-191
- 47) Stokes IAF, Medlicott PA, Wilder DG. Measurement of movement in painful intervertebral joints. Medical and Biological Engineering and Computing 1980;18:694-700
- 48) Suh CH. The fundamentals of computer aided X-ray analysis of the spine. Journal of Biomechanics 1974;7:161-169
- 49) Panjabi MM. Centres and angles of rotation of body joints: a study of errors and optimisation. Journal of Biomechanics 1979;12:911-920
- 50) Cholewicki J, McGill SM, Wells RP, Vernon H. Method for measuring vertebral kinematics from fluoroscopy. Clinical Biomechanics 1991;6:73-78
- 51) Plamondon A, Gagnon M, Maurais G. Application of a stereoradiographic method for the study of intervertebral motion. Spine 1988;13(9):1027-1032
- 52) Pearcy MJ, Whittle MW. Movements of the lumbar spine measured by three-dimensional X-ray analysis. Journal of Biomedical Engineering 1982;4:107-112
- 53) Teves MC. The application of the X-ray image intensifiers I-IV. Philips Tech. 1955/6 Rev.17;69-97
- 54) Garrett JA, Smithson PH. Conventional X-ray imaging. Proceedings of the Institution of Electrical Engineers 1987;134A(2):107-114
- 55) Fielding JW. Normal and selected abnormal motion of the cervical spine from the second cervical vertebra to the seventh cervical vertebra based on cineroentgenography. J Bone Joint Surg 1964;46A(8):1779-1781
- 56) Fielding JW. Cineroentgenography of the normal cervical spine. J Bone Joint Surg 1957;39A(6):1280-1288
- 57) Jones MD. Cineradiographic studies of the normal cervical spine. California Medicine 1960;93(5):293-296
- 58) Buonocore E, Hartman JT, Nelson CL. Cineradiograms of cervical spine in diagnosis of soft-tissue injuries. J.A.M.A. 1966;198(1):25-29.
- 59) Howe JCW. Cineradiographic evaluation of normal and abnormal cervical spine function. The Journal of Clinical Chiropractic 1974;4:42-54
- 60) Jones MD. Cineroentgenographic studies of patients with cervical spine fusion. American Journal of Roentgenology 1962;87(6):1054-1057

- 61) Jones MD. Cineradiographic studies of abnormalities of the high cervical spine. Archives of Surgery 1967;94:206-213
- 62) Van der Ven HW. The preparation and performance of thin vacuum-deposited CsI (Na) scintillation layers. Nucl Instrum & Meth 1969;75:347-348
- 63) Breen A, Allen R, Morris A. A Computer/X-ray method for measuring spinal segmental movement: a feasibility study. Communication at the Second Annual Conference on Research and Education of the Pacific Consortium for Chiropractic Research, June 13-14 1987, Belmont Calif
- 64) Leung STK. The value of cineradiographic motion studies in diagnosis of dysfunctions of the cervical spine. AECC Student Project 1977
- 65) Skippings RS, Taylor MJ. Paradoxical motion of atlas in flexion: a fluoroscopic study of chiropractic patients. AECC Student Project 1985
- 66) Castleman KR. Digital image processing. Prentice Hall 1979; Englewood Cliffs
- 67) Panagiotacopoulos ND. Digital image processing: a potential non-invasive technique in the diagnosis of diseased intervertebral discs. Spine 1982;7(5):506-11
- 68) Moores BM. Digital X-ray imaging. Proceedings of the Institution of Electrical Engineers 1987;134A(2):115-125
- 69) Wallace WA, Johnson F. Detection and correction of geometrical distortion in X-ray fluoroscopic images. Journal of Biomechanics 1981;14:123-125
- 70) Frymoyer JW, Frymoyer WW, Wilder DG, Pope MH. The mechanical and kinematic analysis of the lumbar spine in normal living human subjects in vivo. Journal of Biomechanics 1979;12:165-172
- 71) Hoag JM, Kosek M, Moser JR. Kinematic analysis and classification of vertebral motion. J Amer Osteopath Ass 1960;59:part 1:899-908, part 2:982-986
- 72) Panjabi MM, Krag MH, Goel VK. A technique for measurement and description of three-dimensional six degree-of freedom motion of a body joint with application to the human spine. Journal of Biomechanics 1981;14:447-4601
- 73) Schaffer WO, Spratt KF, Weinstein J, Lehman TR, Goel V. The consistency and accuracy of roentgenograms for measuring sagittal translation in the lumbar vertebral motion segment. Spine 1990;15(8):741-750

- 74) Rosenberg P. The R-Center method: a new method for analysing vertebral motion by X-rays. The Journal of the American Osteopathic Association 1955;55(2):103-111
- 75) Gonan GP, Dimnet J, Carret JP, de Mauroy JC, Fischer LP, de Mourgues G. Utilite de l'analyse cinematique de radiographies dynamiques dans le diagnostic de certaines affections de la colonne lumbaire. Acta Orthopaedica Belgica 1982;48(4):589-629
- 76) Panjabi MM, Krag MH, Dimnet JC, Walter SD, Brand RA. Thoracic spine centers of rotation in the sagittal plane. Orthop-Res 1984;1(4):387-94
- 77) Amevo B, Macintosh, JE, Worth, D, Bogduk N. Instantaneous axes of rotation of the typical cervical motion segments: I. an empirical study of technical errors. Clinical Biomechanics 1991;6:31-37
- 78) Amevo B, Worth D, Bogduk N. Instantaneous axes of rotation of the typical cervical motion segments: II. optimisation of technical errors. Clinical Biomechanics 1991;6:38-46
- 79) Gertzbein SD, Seligman J, Holtby K, et al. Centrode patterns and segmental instability in degenerative disc disease. Spine 1985;4:257-261
- 80) Panjabi MM, Krag MH, Chung DQ. Effects of disc injury on mechanical behaviour of the human spine. Spine 1984;9(7):707-713
- 81) Seligman JV, Gertzbein SD, Tile M, Kapasouri A. Computer analysis of spinal segment motion in degenerative disc disease with and without axial loading. Spine 1984;9:566-573
- 82) Kammerer R, Bauer W, Honegger HW. On-line analysis of rapid motion with a microcomputer. Journal of Neuroscience Methods 1987;19:89-94
- 83) Hoschek J, Weber U, Ladstatter P, Schelske HJ. Mathematical kinematics in engineering of endoprostheses evaluation of the results of gait analysis. Arch Orthop Trauma Surg 1984;103:342-347
- 84) Thurston AJ. Repeatability studies of a television/computer system for measuring spinal and pelvic movements. Journal of Biomedical Engineering 1982;4:129-132
- 85) Whittle MW. Calibration and performance of a 3-dimensional television system for kinematic analysis. Journal of Biomechanics 1982;15:185-196
- 86) Gore TA, Higginson GR, Stevens J. The kinematics of hip joints - normal functioning. Clin Phys Physiol Meas 1984;5:233-252
- 87) de Lange A, Kauer JMG, Huiskes R. Kinematic behaviour of the human wrist joint: a roentgen-stereophotogrammetric analysis. Journal of Orthopaedic Research 1985;3:56-64

- 88) Ohwovoriole EN, Mekow C. A technique for studying the kinematics of human joints; Part II: The humeroscapular joint. *Orthopaedics* 1987;10:3:457-462
- 89) Langrana NA. Spatial kinematic analysis of the upper extremity using a biplanar videotaping method. *J Biomech Eng* 1981;103:11-17
- 90) De Seze S, Djian A, Abdelmoula M. Etude radiologique de la dynamique cervicale dans le plan sagittal. (Une contribution radio-physiologique a l'etude pathogenique des arthroses cervicales). *Revue Due Rhumatisme* 1951;No.3:(2):112-116
- 91) Aho A, Vartiainen O, Salo O. Segmentary antero-posterior mobility of the cervical spine. *Annales Medicinae Internae Fenniae* 1955;44:287-299
- 92) Bhalla SK, Simmons EH. Normal ranges of intervertebral joint motion of the cervical spine. *The Canadian Journal of Surgery* 1969;12:181-187
- 93) Penning L. Functional pathology of the cervical spine, 1968: Excerpta Medica Foundation, Amsterdam
- 94) White AA, Johnson RM, Panjabi MM, Southwick WO, Biomechanical analysis of clinical stability in the cervical spine. *Clinical Orthopaedics and Related Research* 1975;109:85-95
- 95) White AA, Panjabi MM. The role of stabilization in the treatment of cervical spine injuries. *Spine* 1984;9(5):512-522
- 96) Panjabi MM, Goel VK, Clark CR, Keggi KJ, Southwick WO. Biomechanical study of cervical spine stabilization with methylmethacrylate. *Spine* 1985;10(3):198-203
- 97) Gregersen GG, Lucas DB. An in vivo study of the axial rotation of the human thoracolumbar spine. *J Bone Joint Surg* 1967;49A:247
- 98) Coetsier M, Vercauteren M, Moerman P. A new radiographic method for measuring vertebral rotation in scoliosis. *Acta Orthopaedica Belgica* 1977;43(5):598-605
- 99) White AA. Analysis of the mechanics of the thoracic spine in man. *Acta Orthopaedica Scandinavica* 1969;(suppl.127):8-105
- 100) Panjabi MM, Brand RA, White AA. Mechanical properties of the human thoracic spine as shown by three-dimensional load-displacement curves. *J Bone Joint Surg* 1976;58A:642
- 101) Hart FD, Strickland D, Cliffe P. Measurement of spinal mobility. *Ann Rheum Dis* 1974;33:136-139
- 102) Willner S. Spinal pantograph: a non-invasive technique for describing kyphosis and lordosis in the thoraco-lumbar spine. *Acta Orthop Scand* 1981;52:525-529

- 103) Lindahl O. Determination of the sagittal mobility of the lumbar spine: a clinical method. *Acta Orthop Scand* 1966;37:241-254
- 104) Hilton RC, Ball J, Benn RT. In-vitro mobility of the lumbar spine. *Ann Rheum Dis* 1979;38:378-383
- 105) Porter RW, Wicks M, Ottewell D. Measurement of the spinal canal by diagnostic ultrasound. *J Bone Joint Surg* 1978;60B:2:481-485
- 106) Hibbert CS, Delaygue C, McGlen B, Porter RW. Measurement of the lumbar spinal canal by diagnostic ultrasound. *Brit J Radiol* 1981;54:870-874
- 107) Benson DR, Schultz AB, Dewald RL. Roentgenographic evaluation of vertebral rotation. *J Bone Joint Surg* 1976;58A:1125-1129
- 108) Drerup B. Principles of measurement of vertebral rotation from frontal projections of the pedicles. *Journal of Biomechanics* 1984;17(12):923-935
- 109) Drerup B. Improvements in measuring vertebral rotation from the projections of the pedicles. *Journal of Biomechanics* 1985;18:369-378
- 110) Mehta MH. Radiographic estimation of vertebral rotation in scoliosis. *J Bone Joint Surg* 1973;55B(3):513-520
- 111) Matteri RE, Pope MH, Frymoyer JW. A biplane radiographic method of determining vertebral rotation in postmortem specimens. *Clinical Orthopaedics* 1976;116:95
- 112) Scholten PJM, Veldhuizen AG. The influence of spine geometry on the coupling between lateral bending and axial rotation. *Engineering in Medicine* 1985;14(4):167-171
- 113) Lovett RW. A contribution to the study of the mechanics of the spine. *Am J Anat* 1903;2:457-462
- 114) Reichmann S, Berglund E, Lundgren K. Das Bewegungszentrum in der Lendenwirbelsäule bei Flexion und Extension. *Z Anat Entwickl-Gesch* 1972;138:283-287
- 115) Miles M, Sullivan WE. Lateral bending at the lumbar and lumbosacral joints. *The Anatomical Record* 1961;139(3):387-398
- 116) Stokes IAF, Frymoyer JW. Segmental motion and instability. *Spine* 1987;12(7):688-691
- 117) Posner IRA, White AA, Edwards WT & Hayes WC. A biomechanical analysis of the clinical stability of the lumbar and lumbosacral spine. *Spine* 1982;7(4):374-389
- 118) Banks SD. The use of spinographic parameters in the differential diagnosis of lumbar facet and disc syndromes. *Journal of Manipulative and Physiological Therapeutics* 1983;6(3):113-116

- 119) Shirazi-Adl A, Ahmed AM, Shrivastava SC. A finite element study of a lumbar motion segment subjected to pure sagittal plane moments. *Journal of Biomechanics* 1986;19(4):331-350
- 120) Ogston NG, King GJ, Gertzbein SD, Tile M, Kapasouri A, Rubenstein JD. Centrode patterns in the lumbar spine. Baseline studies in normal subjects. *Spine* 1986;11(6):591-595
- 121) Gertzbein SD, Holtby R, Tile M, Kapasouri A, Chan KW, Cruickshank B. Determination of a locus of instantaneous centers of rotation of the lumbar disc by Moire fringes - a new technique. *Spine* 1984;9(4):409-413
- 122) Chasles M. Note sur les proprietes generales du systeme de deux corp semblables entreux. *Bull. Univ. deus Sciences* 1830;14:321
- 123) Adams LP. Biosterometrics in the study of the morphology of the lumbo-sacral spine. *Medical & Biological Engineering & Computing* 1988;383-388
- 124) Spiegelman JJ, Woo SLY. A rigid-body method for finding centers of rotation and angular displacements of planar joint motion. *Journal of Biomechanics* 1987;20(7):715-721
- 125) Woltring HJ. Estimation of the trajectory of the instantaneous centre of rotation in planar biokinematics. *Journal of Biomechanics* (acc. 90-2-3).
- 126) Pearcy MJ, Hindle RJ. New method for the non-invasive three-dimensional measurement of human back movement. *Clinical Biomechanics* 1989;4:73-79
- 127) Brown RH, Burstein AH, Nash CL, Schock CC. Spinal analysis using a three-dimensional radiographic technique. *Journal of Biomechanics* 1976;9:355-365
- 128) Stokes IAF, Wilder DG, Frymoyer JW, Pope MH. Assessment of patients with low-back pain by biplanar radiographic measurement of intervertebral motion. *Spine* 1981;6:233-240
- 129) Olsson TH, Selvik G, Willner S. Mobility in lumbosacral spine after fusion studied with the aid of roentgen stereophotogrammetry. *Clinical Orthopaedics and Related Research* 1977;129:181-190
- 130) Farfan H, Gracovetsky S. The nature of instability. *Spine* 1984;9:714-719
- 131) Wyke B. The neurology of low back pain. In: *The Lumbar Spine and Back Pain* (M Jayson ed.) 3rd Edition, 1987;56-100: Churchill Livingstone
- 132) Porter RW. *Management of Back Pain*. p122 1986; Churchill Livingstone

- 133) Howes RG and Isdale IC. The loose back: an unrecognised syndrome. *Rheumatol Phys Med* 1971;11:72
- 134) Hirsch C, Jonsson B, Lewin T. Low back symptoms in a Swedish female population. *Clinical Orthopaedics* 1969;63:171-176
- 135) Morgan FP, King I. Primary instability of lumbar vertebrae as a common cause of low back pain. *J Bone Joint Surg* 1957;39B:6-22
- 136) MacNab I. The traction spur - an indicator of segmental instability. *J Bone Joint Surg* 1971;52A:663
- 137) Nachemsen A. Lumbar spine instability; a critical update and symposium summary. *Spine* 1985;10(3):290-291
- 138) Penning L, Blickman JR. Instability in lumbar spondylolisthesis. A radiologic study of several concepts. *American Journal of Radiology* 1980;134:293-301
- 139) Pope MH, Panjabi M. Biomechanical definitions of spinal instability. *Spine* 1985;10(3):255-256
- 140) Bergmark A. Stability of the lumbar spine: a study in mechanical engineering. *Acta Orthopaedica Scandinavia (Suppl)* 1989;230(60)
- 141) Lucas DB, Bresler B. Stability of the ligamentous spine. Technical report serl 11, nr 40, 1961 Biomechanics Laboratory, University of California, Berkley and San Francisco
- 142) Panjabi MM, Goel VK, Takata K. Physiologic strains in the lumbar spinal ligaments. *Spine* 1982;7:196-201
- 143) Koeller W, Muelhaus S, Meier W, Hartmann F. Biomechanical properties of human intervertebral discs subjected to axial dynamic compression - influence of age and degeneration. *Journal of Biomechanics* 1986;19(10):807-816
- 144) Dupuis PR, Yong-Hing K, Cassidy JD & Kirkaldy-Willis WH. Radiologic diagnosis of degenerative lumbar spinal instability. *Spine* 1985;10(3):262-276
- 145) Miller JAA, Schultz AB, Warwick DN, Spencer DL. Mechanical properties of lumbar spine motion segments under large loads. *Journal of Biomechanics* 1986;19(1):79-84
- 146) Van Akkerveeken PF, O'Brien JP, Park WM. Experimentally induced hypermobility in the lumbar spine. A pathologic and radiologic study of the posterior ligament and annulus fibrosus. *Spine* 1979;4(3):236-241
- 147) Knutsson F. The instability associated with disc degeneration in the lumbar spine. *Acta Radiol* 1944;25:593-609

- 148) Lettin AWF. Diagnosis and treatment of lumbar instability. J Bone Joint Surg 1967;49B:520-529
- 149) Froning EC, Frohman B. Motion of the lumbosacral spine after laminectomy and spine fusion. J Bone Joint Surg 1968;50(A):897-918
- 150) Frymoyer JW, Hanley EN, Howe J, Kuhlmann Dm Matteru RE. A comparison of radiographic findings in fusion and non-fusion patients ten or more years following lumbar disc surgery. Spine 1979;4:435-439
- 151) Rolander SD. Motion of the lumbar spine with special reference to the stabilising effect of posterior fusion - an experimental study on autopsy specimens. Acta Orthopaedica Scandinavia 1966;Suppl 90
- 152) Goel VK, Clark RC, McGowan D, Goyal S. An in-vitro study of the kinematics of the normal, injured and stabilized cervical spine. Journal of Biomechanics 1984;17(5):363-376
- 153) White AA, Southwick WO, Panjabi MM. Clinical instability in the lower cervical spine. A review of past and current concepts. Spine 1976; 1(1):15-27
- 154) Dvorak J, Panjabi M, Gerber M, Wichmann W. CT-functional diagnostics of the rotatory instability of upper cervical spine. 1. An experimental study on cadavers. Spine 1987;12(3):197-205
- 155) Dvorak J, Hayek J, Zehnder R. CT-functional diagnostics of the rotatory instability of the upper cervical spine. Part 2. An evaluation on healthy adults and patients with suspected instability. Spine 1987;12(8):726-731
- 156) Lawrence JS. Disc degeneration: its frequency and relationship to symptoms. Ann Rheum Dis 1969;28:121
- 157) Smith A. Posterior displacement of the fifth lumbar vertebra. J Bone Joint Surg 1934;16A:877-888
- 158) Epstein JA, Epstein BS, Rosenthal A, Carras R, Lavine LS. Sciatica caused by nerve root entrapment in the lateral recess;the superior facet syndrome. Journal of Neurosurgery 1972;36:584-589
- 159) Fletcher CH. Backward displacement of fifth lumbar vertebra in degenerated disc disease. J Bone Joint Surg 1947;29:1019
- 160) Melamed A, Ansfield DJ. Posterior displacement of lumbar vertebrae (Classification and criteria for diagnosis of true retrodisplacement of lumbar vertebrae) Amer J Roentgenol 1947;58:307-328
- 161) Gillespie HW. Vertebral retroposition (reversed spondylolisthesis). Brit J Radiol 1951;74:193-197



- 162) Ben-Eliyahu DJ, Rutili MM, Przybysz R. Lateral recess syndrome: diagnosis and chiropractic management. *Journal of Manipulative and Physiological Therapeutics* 1983;6(1)25-31
- 163) Hagelstam L. Retroposition of lumbar vertebrae. *Acta Chir Scand Suppl* 1949;143
- 164) Mior SA, Cassidy JD. Lateral nerve entrapment: pathological clinical and manipulative considerations. *Journal of the Canadian Chiropractic Association* 1982;143
- 165) Ogston NG, King GJ, Gertzbein SD, Tile M, Kapasouri A, Rubenstein JD. Centrode patterns in the lumbar spine: baseline studies in normal subjects. *Spine* 1986;6:591-595
- 166) Feffer HL., Wiesel SW., Cuckler JM., Rothman RH. Degenerative spondylolisthesis: to fuse or not to fuse. *Spine* 1985;10(3):287-289
- 167) Mixter WJ, Barr JS. Rupture of the intervertebral disc with involvement of the spinal canal. *New England Journal of Medicine* 1934;211:210-5
- 168) Farfan H. The effects of torsion on the lumbar intervertebral joint; the role of torsion in the production of disc herniation. *J Bone Joint Surg* 1970;52A:468-453
- 169) Goel VK, Nishiyama K, Weinstein J, Liu YK. Mechanical properties of lumbar spinal motion segments as affected by partial disc removal. *Spine* 1986;11:1008-1012
- 170) Pearcy MJ, Bogduk N. Instantaneous axes of rotation of the lumbar intervertebral joints. *Spine* 1988;13(9):1033-1041
- 171) Breen AC. The measurement of the kinematics of the human spine using digital videofluoroscopy. Research report ME/89/2, Department of Mechanical Engineering, University of Southampton 1989
- 172) Shaffer WO, Spratt KF, Weinstein J, Lehmann TR, Goel V. The consistency and accuracy of roentgenograms for measuring sagittal translation in the lumbar vertebral motion segment: an experimental model. *Spine* 1990;15(8)741-750
- 173) Woolnough D. Kinematics of the human spine. Student Project, Department of Mechanical Engineering, University of Southampton 1988
- 174) Penning L. Normal movements of the cervical spine. *American Journal of Roentgenology* 1978;91:1036-1050
- 175) Jirout J. Notes on x-ray research into joint play in the cervical spine. *Manual Medicine* 1987;3:70-72
- 176) Jirout J. Dynamic radiological studies of the spine and their role in prevention of spinal disorders. *Manual Medicine* 1989;4:136-137

177) Gonzalez RC, Wintz P. Digital Image Processing 1977; Addison-Wesley Publishing Company

178) International Commission on Radiological Protection - Draft Recommendations of the Commission. Commission of the European Economic Communities: Brussels; February 1990 (consultative document)